

JAERI-Tech  
95-018



DESIGN STUDY ON A 1MeV, 12.5MW NEUTRAL BEAM  
INJECTOR MODULE FOR ITER

March 1995

Yoshikazu OKUMURA, Masaya HANADA  
Takashi INOUE, Koichi MAKI\*<sup>1</sup>  
Shuichi MAENO\*<sup>2</sup>, Kenji MIYAMOTO  
Yoshihiro OHARA, Kazuhiro WATANABE  
and Sergei ZIMIN\*<sup>3</sup>

日本原子力研究所  
Japan Atomic Energy Research Institute

本レポートは、日本原子力研究所が不定期に公刊している研究報告書です。  
入手の間合わせは、日本原子力研究所技術情報部情報資料課（〒319-11 茨城県那珂郡東海村）あて、お申し越してください。なお、このほかに財団法人原子力弘済会資料センター（〒319-11 茨城県那珂郡東海村日本原子力研究所内）で複写による実費頒布をおこなっております。

This report is issued irregularly.

Inquiries about availability of the reports should be addressed to Information Division, Department of Technical Information, Japan Atomic Energy Research Institute, Tokai-mura, Naka-gun, Ibaraki-ken 319-11, Japan.

© Japan Atomic Energy Research Institute, 1995

---

編集兼発行 日本原子力研究所  
印刷 日立高速印刷株式会社

Design Study on a 1MeV, 12.5MW Neutral Beam Injector Module  
for ITER

Yoshikazu OKUMURA, Masaya HANADA<sup>+</sup>, Takashi INOUE, Koichi MAKI\*<sup>1</sup>  
Shuichi MAENO\*<sup>2</sup>, Kenji MIYAMOTO, Yoshihiro OHARA  
Kazuhiro WATANABE and Sergei ZIMIN\*<sup>3</sup>

Department of Fusion Engineering Research  
Naka Fusion Research Establishment  
Japan Atomic Energy Research Institute  
Naka-machi, Naka-gun, Ibaraki-ken

(Received February 6, 1995)

A high energy neutral beam injector has been designed for the International Thermo-nuclear Experimental Reactor(ITER). Two types of designs are proposed; a short beamline option and a long beamline option. The short beamline option is characterized by a very short neutralizer, which makes it possible to integrate all the beamline components within the cryostat of ITER. The long beamline option has a conventional layout, where the beamline is installed outside the cryostat. In both cases, the system is more compact and more reactor-relevant than the ITER-CDA(Conceptual Design Activity)design, since the present design is based on the recent progress on the negative ion beam development.

In the design, 25A D-ion beam is produced by a cesium-seeded volume negative ion source and accelerated to 1MeV by a multi-stage electrostatic accelerator. The beam is neutralized in a gas cell and

---

<sup>+</sup> Department of ITER Project

\*1 Energy Research Laboratory, Hitachi, Ltd.

\*2 Nissin Electric Co. Ltd.

\*3 Research Fellow

12.5MW(1MeV, 12.5A)neutral beam is injected into each injection port. Using 4 NBI modules and 4 ports, 50MW is to be injected into the plasma in ITER.

A special emphasis is laid on the radiation shielding and the radiation effects in the beamline components, which was considered to be a serious problem in applying a neutral beam system for ITER. We found that the irradiation dose rate in the beamline components including the ion source/accelerator can be suppressed to a moderate value and no serious damage on these components is expected.

Keywords : ITER, EDA, Neutral Beam, NBI, Negative Ion Source, Accelerator, Neutralizer, Neurons, Neutron Shielding, Radiation Effect

国際熱核融合実験炉 (ITER) 用 1MeV, 12.5MW 中性粒子入射装置の設計検討

日本原子力研究所那珂研究所核融合工学部

奥村 義和・花田磨砂也\*・井上多加志・真木 紘一\*<sup>1</sup>

前野 修一\*<sup>2</sup>・宮本 賢治・小原 祥裕・渡辺 和弘

Sergei ZIMIN\*<sup>3</sup>

(1995年2月6日受理)

国際熱核融合実験炉 (ITER) の工学設計 (EDA) の一環として、負イオンを用いた高エネルギー中性粒子入射装置の設計検討を行った。ビームライン長の異なる2種類の設計概念、即ち、極めて短い中性化セルを持ちITERのクライオスタット内に全てのビームライン機器を設置した短ビームライン案と、細いビームラインをクライオスタット外においた長ビームライン案を考案し、検討した。いずれも、最近の負イオン源開発における成果を取り入れ、ITER-CDAの設計と比べて大幅なコンパクト化を図るとともに、炉との整合性に優れた設計となっている。

本設計においては、セシウム添加体積生成型負イオン源を用いて25Aの重水素負イオンビームを発生し、多段静電加速器により1MeVに加速する。加速されたビームはガスセルにより中性化され、12.5MWの中性粒子ビームが入射ポートから入射される。ITERでは4モジュールを用いて、4ポートから50MWを入射する。

ITERにNBIを採用する際に考慮しなければならない課題として、炉からの中性子の遮蔽と、放射化による機器の損傷がある。本設計では、特にそれらについても検討を行い、負イオン源や加速器等のビームライン機器の照射線量を損傷を起こさない程度に低くできることを明らかにした。

---

那珂研究所：〒311-01 茨城県那珂郡那珂町大字向山801-1

+ ITER 開発室

\*1 日立製作所エネルギー研究所

\*2 日新電機(株)

\*3 リサーチフェロー

## Contents

1. Introduction	1
2. Outline of the System Design	3
2.1 Requirements from ITER	3
2.2 Design Concept	3
2.3 System Overview	7
2.4 Gas Flow and Power Flow	10
3. Design Studies on Critical Components	23
3.1 Ion Source/Accelerator	23
3.2 Estimation of Cs Consumption	33
3.3 Estimation of Tungsten Filament Lifetime	34
3.4 Large Bore Insulator	35
3.5 Mechanical Strength against the Pressure Difference	37
3.6 Beam Steering System	42
3.7 Neutralizer	44
3.8 Magnetic Shield	48
3.9 Ion Deflector	54
3.10 Ion Dump and Calorimeter	61
3.11 Cryopump	63
3.12 Double Seal Gate Valve	65
3.13 Fast Shutter	66
3.14 Bellows	68
3.15 High Voltage Power Supply	70
3.16 Surge Blocker	70
3.17 Maintenance	74
3.18 Gas Handling System	80
4. Neutronics	83
4.1 Modeling of Computation	83
4.2 Results of Neutronics Calculation	84
4.3 Nuclear Heating in TFC and Cryopump	84
4.4 Radiation in the Accelerator Insulator	84
4.5 Radiation Effect of the Permanent Magnet in the Ion Source	85
4.6 Activation of the Insulating Gas	86
5. Conclusion and Necessary Future R&Ds	103
Acknowledgment	104

## 目 次

1. はじめに .....	1
2. 設計の概要 .....	3
2.1 ITERからの要求 .....	3
2.2 設計概念 .....	3
2.3 システム概要 .....	7
2.4 ガスフロー, パワーフロー .....	10
3. 要素機器の設計検討 .....	23
3.1 イオン源/加速器 .....	23
3.2 セシウム消費量の評価 .....	23
3.3 タングステンフィラメントの寿命評価 .....	34
3.4 大口径絶縁管 .....	35
3.5 圧力差に対する機械的強度 .....	37
3.6 ビーム軸偏向系 .....	42
3.7 中性化セル .....	44
3.8 磁気シールド .....	48
3.9 イオン偏向器 .....	54
3.10 イオンダンプ, カロリメータ .....	61
3.11 クライオポンプ .....	63
3.12 2重シールゲート弁 .....	65
3.13 高速シャッター .....	66
3.14 ベローズ .....	68
3.15 高電圧電源 .....	70
3.16 サージブロッカー .....	70
3.17 保守 .....	74
3.18 ガス循環系 .....	80
4. 中性子遮蔽, 放射化 .....	83
4.1 中性子計算モデル .....	83
4.2 中性子計算結果 .....	84
4.3 TFCとクライオポンプの放射線効果 .....	84
4.4 加速器絶縁管の放射線効果 .....	84
4.5 イオン源の永久磁石の放射線効果 .....	85
4.6 絶縁ガスの放射化 .....	86
5. 結論, 及び今後必要な研究開発 .....	103
謝辞 .....	104

## 1. Introduction

Steady state operation of the tokamak type fusion reactors is one of the most important issues in the research and development of the fusion reactors, and non-inductive current drive is a definitely important R&D item in realizing the steady state operation. In JT-60, a 500keV, 10MW negative-ion-based NBI system is under construction, and experiments on neutral beam current drive in high density plasmas will be started in 1996 [1]. This project will give both a physics and an engineering base to the ITER project as an intermediate step, and also give a guiding principle in realizing the steady state tokamak reactor [2].

On the other hand, the ITER machine is requested to aim at demonstrating steady state operation using non-inductive current drive in reactor-relevant plasmas according to the ITER Special Working Group 1 Review Report [3]. Unfortunately, however, neutral beam current drive has not been assessed sufficiently so far within ITER though it is one of the most promising heating and current drive methods. In the meantime, development of high power negative ion sources and accelerators has progressed particularly at JAERI and production of high energy and convergent negative ion beams has become realistic. This leads to a possibility to make the beamline more compact and more reactor-relevant. On these backgrounds, a design guide line has been presented in the ITER Outline Design Report for the TAC-4 Meeting [4]. The present design has been made following the concept shown in the Report.

Two beamline design options are studied, one is a short beamline option and the other is a long beamline option. In the short beamline option, the beamline is mounted inside or with the cryostat and the ion source/accelerator outside the cryostat is connected to the beamline through a double gate valve. In the long beamline option, the entire beamline is placed outside the cryostat and can be isolated from the reactor through a double gate valve. Merits and demerits of each option are assessed primarily from maintenance, magnetic shielding and neutron shielding point of view, and the long beamline option is recommended for the ITER neutral beam system.

In the long beamline option, two different designs are studied; the long beamline option and the long beamline option II. The differences between the two designs are the beamline length and the required pumping speed. In the long beamline option, the gas flow rate is minimized by assuming a low source operating pressure and utilizing a long neutralizer, while the beamline length is minimized in the beamline option II at the expense of gas flow rate or the required pumping speed.



In the present report, an outline of these three system designs, i.e. the short beam line option, the long beamline option, and the long beamline option II, is presented in the following section. In section 3, design studies on critical components in the neutral beam injection system are presented. A special emphasis is laid on the radiation shielding and the radiation effects in the beamline components, about which the ITER- JCT (Joint Central Team) expressed a concern in applying a neutral beam system for ITER. Studies on the neutronics and the evaluation of radiation effects are shown in Section 4. Finally, necessary R&Ds is to be discussed together with a conclusion.

## References

- [1] M. Kuriyama, et al.; 5th Int. Toki Conf. on Plasma Physics and Controlled Nuclear Fusion, Nov. 16-19, Toki, Japan (1993).
- [2] Y. Seki, M. Kikuchi, et al.; 13th IAEA Conf. on Plasma Physics and Controlled Nuclear Fusion Research, Washington D.C. U.S.A (1990) IAEA-CN-53 / G-1-2.
- [3] ITER Special Working Group 1; SWG-1 Review Report, October (1992).
- [4] ITER Joint Central Team, ITER Outline Design Report, presented for the 4th Meeting of the Technical Advisory Committee, San Diego Joint Work Site, 10-12 January (1994).

## 2. Outline of the System Design

### 2.1 Requirements from ITER

The following specifications are chosen for the present design studies;

Neutral power to the plasma	:50 MW
Beam energy	:1 MeV
Ion Species	:D <sup>-</sup>
Number of ports	:4
Number of beamlines	:4, one per port
Number of ion sources	:4, one per beamline
Injection power per port	:12.5 MW

### 2.2 Design Concept

#### Background

In the past couple of years, several important improvements have been made in negative ion source development at JAERI. Among them, source operating pressure was reduced extremely with keeping a high negative ion current density [1]. The lowest operating pressure in a 1.2 m large negative ion source [2] was 0.03 Pa at a current density of 8 mA/cm<sup>2</sup>, and that in the negative ion source used in US-Japan collaborative experiment was 0.13 Pa at a current density of 10 mA/cm<sup>2</sup>. These pressures are one or two order lower than the pressures assumed in the past NB system designs such as ITER-CDA. In addition, beam focusing technology has been developed in the US-Japan collaborative experiments [3], where multiple beamlets are focused into a single accelerating channel. This makes it possible to use a narrow neutralizer that has low gas conductance. Combination of the low gas pressure and the narrow neutralizer reduces the gas flow rate for producing and neutralizing the negative ions. It results in a low vacuum pumping speed and a short neutralizer cell, which makes the beamline compact.

Using a multi-stage electrostatic accelerator, we have succeeded to accelerate negative ions up to an energy of 400 keV with a good beam optics; i.e. beamlet divergence angle of less than 6 mrad at 400 keV, 13 mA/cm<sup>2</sup> [4]. At an optimum condition, minimum beam divergence of 1.5 mrad was also obtained. It will be possible to minimize the beam

divergence to less than 2-3 mrad, which enables us to design the injection port smaller than the past NB system design.

A large negative ion source has been developed for the JT-60, negative-ion-based NB injector [5]. The source, whose dimensions are 2 m in diameter and 1.7 m in height, is designed to produce 500 keV, 22 A (11 MW)  $D^-$  ion beams for a pulse duration of 10 s [6]. These specifications are ITER relevant, especially in the  $D^-$  ion beam current and beam power. A high current (10 A) negative ion beam production was demonstrated at a current density of  $37 \text{ mA/cm}^2$  [7]. A negative ion source producing  $>20 \text{ A } D^-$  ion beam is, therefore, within a scope of present development.

These experimental achievements enable us to make a new NB system design, which fits the ITER-EDA requirements.

### **Size of the NB system**

In the ITER-CDA design, the NB system has 9 beamlines. Three ports are used for the 9 beamlines and the length of each beamline is more than 20 m long. This design requires a significant space outside the cryostat, resulting in difficulties in  $T_2$  confinement and the layout of NB system. In the present design, we tried to minimize the number of beamlines and the beamline length to improve the space utility, to fulfill the safety requirement ( $T_2$  confinement), and to make the maintenance easy.

From a view point of space utility, one ion source per one beamline is preferable. Although this increases the beam current per ion source, a large negative ion source producing  $>20 \text{ A } D^-$  ion beams can be realized from a small extension of the JT-60 negative ion source.

### **Beam Energy**

The beam energy should be determined from viewpoints of physics and engineering. From an engineering point of view, 1 MeV is considered to be the most suitable beam energy. If a relatively low energy were chosen for the same power, the system would need either bigger ion sources or sources that provide a higher  $D^-$  current density than a higher energy system. On the other hand, the use of very high energies needs a significant step in accelerator and power supply technologies. The beam energy used for the negative-ion-based NBI for the JT-60, is 500 keV, which is to be operational by the end of

1996. Negative ion acceleration of up to 400 keV has already been demonstrated at JAERI. The energy of 1 MeV is, therefore, a reasonable step from the present technology of ion source/accelerator and power supplies.

### Ion Source

The specifications of the negative ion source are based on the values that have already achieved experimentally at JAERI. The source type is a cesium-seeded multicusp volume source, which can produce a high current negative ion beam at a low operating pressure. In addition, this source can produce a convergent negative ion beam because of a low negative ion temperature.

There was a strong argument that the cesium would be condensed on surfaces of the insulators in the accelerator, and causes frequent high voltage breakdowns. Another argument was that a large amount of cesium would be injected into the torus as a high-Z impurity. To answer these questions, we developed a cesium-seeded multicusp volume source that can be operated continuously. We found that the consumption rate of cesium is extremely small. Once 100 mg cesium was seeded, the source was operated for a pulse length of 24 hours without additional cesium seeding at 50 keV, 0.3 A (8 mA/cm<sup>2</sup>) [8]. The cesium consumption rate was so small that we had no problem associated with cesium. We measured impurity content in the beam to find that there is no metal impurity detectable [9]. We also operated the cesium-seeded multicusp volume source at the beam energy of 400 keV without any breakdown problems. By these experimental demonstration, we are confident in using this source type for NB system for ITER.

### Accelerator

We propose a multiple stage electrostatic accelerator, which can produce a convergent ion beam with a high electrical efficiency. One of the advantages of the multi-stage acceleration is that the free electrons produced by the stripping of the negative ions are disposed in each stage before fully accelerated. This improves the electrical efficiency, and at the same time, reduces the heat loading dissipated in the accelerator grids. Another advantage is that the negative ion beams can be converged by the electrostatic lenses between the stages.

We are operating a three stage electrostatic accelerator successfully for the 400 keV H<sup>-</sup> ion beam acceleration [4]. Same accelerator system is to be used in the 500 keV D<sup>-</sup> ion source in the JT-60, NB system. Though it is difficult to propose a best accelerator for the

ITER at present, we apply a five stage electrostatic accelerator as the first option.

Disadvantage of the multi-stage accelerator is that the gas pressure in the accelerator gap is higher than that in a single-stage accelerator because of the low conductance of the grids. This results in a large amount of stripping loss of the negative ions, if the source operating pressure is high. However, since the source pressure is low in our negative ion sources, this is not a serious problem anymore.

### **Neutralizer**

A gas neutralizer, giving a 60 % neutralization efficiency, is adopted in the present design. A plasma neutralizer is more attractive for the future design. The neutralization efficiency of more than 80 % is expected in the plasma neutralizer, which improve the overall system efficiency. In addition, higher neutralization efficiency decreases the heat loading and the gas loading in the beam dump, which makes the system more compact. Although experimental data base is not sufficient to adopt in the present design, the plasma neutralizer is worthwhile to be developed for future upgrade of the design.

## 2.3 System Overview

In the present design studies, two types of the beamline are proposed; one is a "short beamline" option and the other is a "long beamline" option.

The short beamline option is characterized by a very short neutralizer, which makes it possible to integrate the beamlines within the cryostat. Only the ion source and the accelerator are placed outside the cryostat.

The long beamline option has a conventional layout; entire beamline components are placed outside the cryostat and they are connected with the tokamak through a narrow duct and a double seal gate valve.

In both design options, four beamline modules are installed on four injection ports.

### Short Beamline Option

A side view of the beamline module is shown in Fig. 2-1 for the short beamline design. The major beamline components are a negative ion source/accelerator, a steering mechanism, a source disconnecting valve (or a double seal gate valve), a gas neutralizer, an ion deflector, ion beam dumps, a fast shutter, and vacuum pumps. All components except for the ion source/accelerator are installed in a vacuum vessel whose dimensions are approximately 4 m in inner diameter and 5 m in length. The vacuum vessel is made of mild steel, and serves as an inner magnetic shield. The region of the ion source and the neutralizer is covered with an outer magnetic shield.

The ion source/accelerator produces 1 MeV, 25 A negative deuterium ion beam. In the gas neutralizer, which consists of 22 narrow cylinders of 8 cm in diameter and 2 m in length, about 60 % of the ion beam is converted to neutrals by the collisions with the deuterium gas molecules. The residual ions are deflected by the ion deflector and in the ion dump. Neutral beams of about 12.8 A, equivalent current, are injected to a plasma through the injection port.

In this design option, multiple beamlets extracted from the negative ion source are focused into large bore accelerating channels in the accelerator. The accelerator has 22 accelerating channels, each accelerating 1.1 A  $D^-$  ion beam. The ion beams accelerated in these channels are injected into the 22 cylinders of the neutralizer. The conductance of the neutralizer is small compared with a conventional neutralizer. This saves the gas

flow rate into the neutralizer and makes it possible to shorten the beamline length.

No gate valve can be installed between the reactor vessel and the beamline because of the limited space. In addition, a calorimeter for measuring the neutral beam power is eliminated in this design option.

Fig. 2-2 shows the layout of the four beamline modules for the short beamline option.

### Long Beamline Option

A side view of the beamline module is shown in Fig. 2-3 for the long beamline design. The beamline module consists of an ion source/accelerator, a steering mechanism, a double seal gate valve I, a gas neutralizer, an ion deflector, beam dumps, a calorimeter, a double seal gate valve II, and a neutron shutter. The size of the beamline is in 4 m in inner diameter and 10 m in length. All the beamline components are placed outside the cryostat and the beamline is connected with the reactor vessel through a narrow duct. Hence all the beamline modules are isolated from the reactor vessel completely by closing the neutron shutter and the double seal gate valve II.

The negative ions are not merged in this design option; the multiple beamlets extracted from the negative ion source are accelerated individually in a multi-aperture accelerator. This type of acceleration has been tested at JAERI at the energies up to 400 keV. The experiments demonstrated that the accelerated beam divergence is extremely small; less than 1.5 mrad at the best condition. We concluded that it will be possible to achieve a beam divergence of less than 3 mrad, which makes it possible to inject all beamlets through a narrow injection port. Dimensions of 0.4 m x 0.6 m are enough for the injection port to inject 12.5 MW neutral beam power.

The overall size of the neutralizer is 0.45 m in width, 1.2 m in height and 5 m in length. The neutralizer is divided into 5 sections by vertical plates to reduce the conductance and to save the gas flow rate into the neutralizer.

Figure 2-4 shows a plain view of the ITER and the four beamline modules.

### Long Beamline Option II

Although the design concept is the same as the long beamline option, the beamline length is minimized in the beamline option II. This is because the space required for the

NBI system is limited in the ITER and there is not enough room for the long beamline option. In order to minimize the total length, the neutralizer is shortened to 3m. At the same time, the operating gas pressure in the negative ion source is increased to 0.2 Pa to allow adopting various types of negative ion sources. These modifications result in increasing the pumping speed, but the pumping speed required is still less than a reasonable value.

Figures 2-5 and 2-6 show a side view and plane view of the long beamline option II.

### Merit and Demerit in Short and Long Design Options

The merits of the short beamline option are as follows;

- 1) All the beamline components are installed inside the cryostat, so that the tritium boundary is limited near the cryostat.
- 2) Neutron fluence at the ion source/accelerator can be reduced considerably because the neutralizer acts as a neutron shield.
- 3) Required gas flow rate is small, resulting in a low pumping speed of the cryopumps.

There are some demerits in this design option;

- 1) Maintenance of beamline components is difficult. They should be regarded as in-vessel components.
- 2) Upgrade of the beamline (e.g. employing plasma neutralizer, which enhances the system efficiency from 40 % to 60 %) is impossible because of the limited space and hard accessibility inside the cryostat.
- 3) Additional R&D is required for the merged beam acceleration
- 4) Magnetic shielding is more difficult than the long beamline option.

On the other hand, the long beamline option has following merits;

- 1) Maintenance of the beamline components is easy.
- 2) Upgrade of the beamline is easy. Combination of employing the plasma neutralizer and upgrade of the ion source/accelerator will make it possible to inject 100 MW neutral beams.
- 3) The NB system can be isolated completely from the reactor by closing the neutron shutter and the double seal gate valve.
- 4) The accelerator can be developed with an extension of the present technologies.

The demerits of the long beamline option are as follows;

- 1) The beamline is long and tritium boundary is extended outside the cryostat.
- 2) The neutron fluence is higher than the short beamline option because of the large bore neutralizer cell



Final choice of the beamline design should be done by considering these merits and demerits. From an engineering point of view, we consider the long beamline option is superior to the short beamline option. Although the short beamline option has a big advantage that all the beamline components are installed in the cryostat, the demerits on the maintenance and the upgrade seems to be more severe than the demerits of the long beamline option. In the long beamline option, the entire NB system can be isolated completely by closing the neutron shutter so that the remote maintenance is easy as described in 3.9. Although the neutron fluence is higher in the long beamline option than the short beamline option, the radiation dose rate is far below the critical value inducing the damages on the beamline components, as described in Chapter 4.

## 2.4 Gas Flow and Power Flow

Figures 2-7, 2-8 and 2-9 show diagrams of the gas flow for the short beamline option, the long beamline option and long beamline option II, respectively. Gas pressure distribution along the source and the beamline is also shown in the same figures.

In the short beamline option,  $D_2$  gas of  $0.6 \text{ Pa}\cdot\text{m}^3/\text{s}$  is fed to the ion source to keep the operating pressure at  $0.1 \text{ Pa}$ . The stripping loss of the negative ions in the accelerator ( $200\text{keV} - 1\text{MeV}$ ) is estimated to be  $4.5 \%$  when the pressure at the exit of the accelerator being kept at  $0.02 \text{ Pa}$  using a cryo pump with an effective pumping speed of  $137 \text{ m}^3/\text{s}$ .  $D_2$  gas of  $3.64 \text{ Pa}\cdot\text{m}^3/\text{s}$  is fed to the neutralizer to keep the peak gas pressure in the neutralizer at  $0.48 \text{ Pa}$ .

The gas line density from the exit of the accelerator to the exit of the neutralizer is  $1.2 \times 10^{16} \text{ molecules/cm}^2$ , which gives the highest neutralization efficiency of  $60 \%$ .

Out of the input gas,  $1.2 \text{ Pa}\cdot\text{m}^3/\text{s}$  is going out to the beam dump region. Another  $0.19 \text{ Pa}\cdot\text{m}^3/\text{s}$  comes from the beamdump in beam dump region, where a cryopump of an effective pumping speed of  $685 \text{ m}^3/\text{s}$  is installed to keep the pressure at  $0.002 \text{ Pa}$ .

Re-ionization loss in the beam drift duct is estimated to be  $4.7 \%$ . Assuming the geometrical efficiency is about  $90 \%$ , which is achievable at a beam divergence of an order of  $10 \text{ mrad}$ , the neutral beam power to a plasma is;

$$1 \text{ MeV} \times 25 \text{ A} \times 0.9 \times 0.6 \times 0.95 = 12.8 \text{ MW}$$

- 0.9 : Geometrical Efficiency
- 0.6 : Neutralization Efficiency
- 0.95: Re-Ionization Efficiency

The gas flow diagram of the long beamline option is shown in Fig. 2-8, where the peak gas pressure in the neutralizer is 0.19 Pa and the required pumping speeds are 554 m<sup>3</sup>/s for the exit of the accelerator and 1425 m<sup>3</sup>/s for the beam dump region. The system efficiency in the long beamline option is the same as that of the short beamline option.

The stripping loss of negative ions in the extractor and the accelerator is shown in Fig. 2-10 as a function of the distance from the extraction surface for various operating pressure. It would be necessary to operate the source at the pressure lower than 0.2 Pa, otherwise the power loss in the accelerator becomes large, resulting in a low system efficiency and severe heat loadings in the accelerator grids.

Figure 2-11 shows a power flow diagram of ITER NB System. Total electrical power to the ion source/accelerator is 27 MW per module, whereas the injected neutral beam power is 12.8 MW. Therefore, the total power efficiency is 0.47.

## References

- [1] Y. Okumura et al.; "Reduction of the Operating Gas Pressure in a Cesium-Seeded Large Multicusp H<sup>-</sup> Ion Source", Proc. 4th European Workshop on the Production and Application of Light Negative Ions, Belfast, 35-40 (1991)
- [2] M. Hanada et al., Rev. Sci. Instrum. 63, 2699-2701 (1992)
- [3] Inoue et al.; "Merging Beam Experiment of Intense Negative Ions for Advanced Compact Neutral Beam Injectors", Proc. 15th Symp. on Fusion Engineering, Hyannis, MA, USA (1993)
- [4] K. Watanabe et al.;
- [5] M. Kuriyama et al.; "High Energy Negative Ion Based NBI System for JT-60U", 5th International Toki Conference on Plasma Physics and Controlled Nuclear Fusion, Toki, (1993)
- [6] Y. Okumura et al.; "Development of a Large D<sup>-</sup> Ion Source for the JT-60U Negative-Ion-Based Neutral Beam Injector", Proc. 15th Symp. on Fusion Engineering, Hyannis, MA, USA (1993)
- [7] Y. Okumura et al.; "A Ten Ampere Negative Ion Source for High Energy Neutral Beam Injector", Proc. 16th Symp. on Fusion Technology, London, 1026-1030 (1990)
- [8] Y. Okumura et al.; Rev. Sci. Instrum. 63, 2708-2710 (1992)
- [9] Y. Okumura et al.; JAERI-M 89-090 (1989)

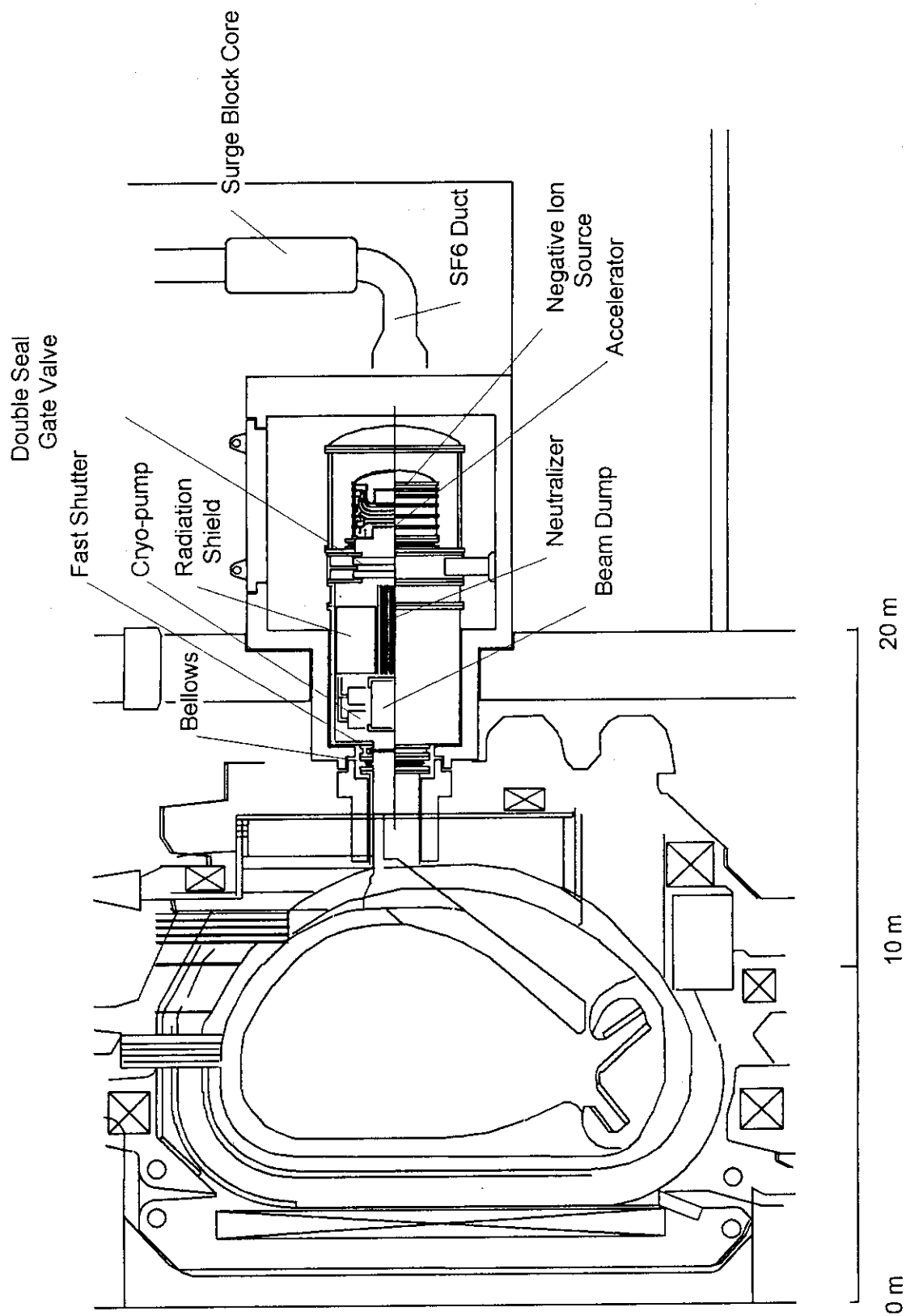


Fig.2-1 Side view of the beamline module (Short Beamline Option)

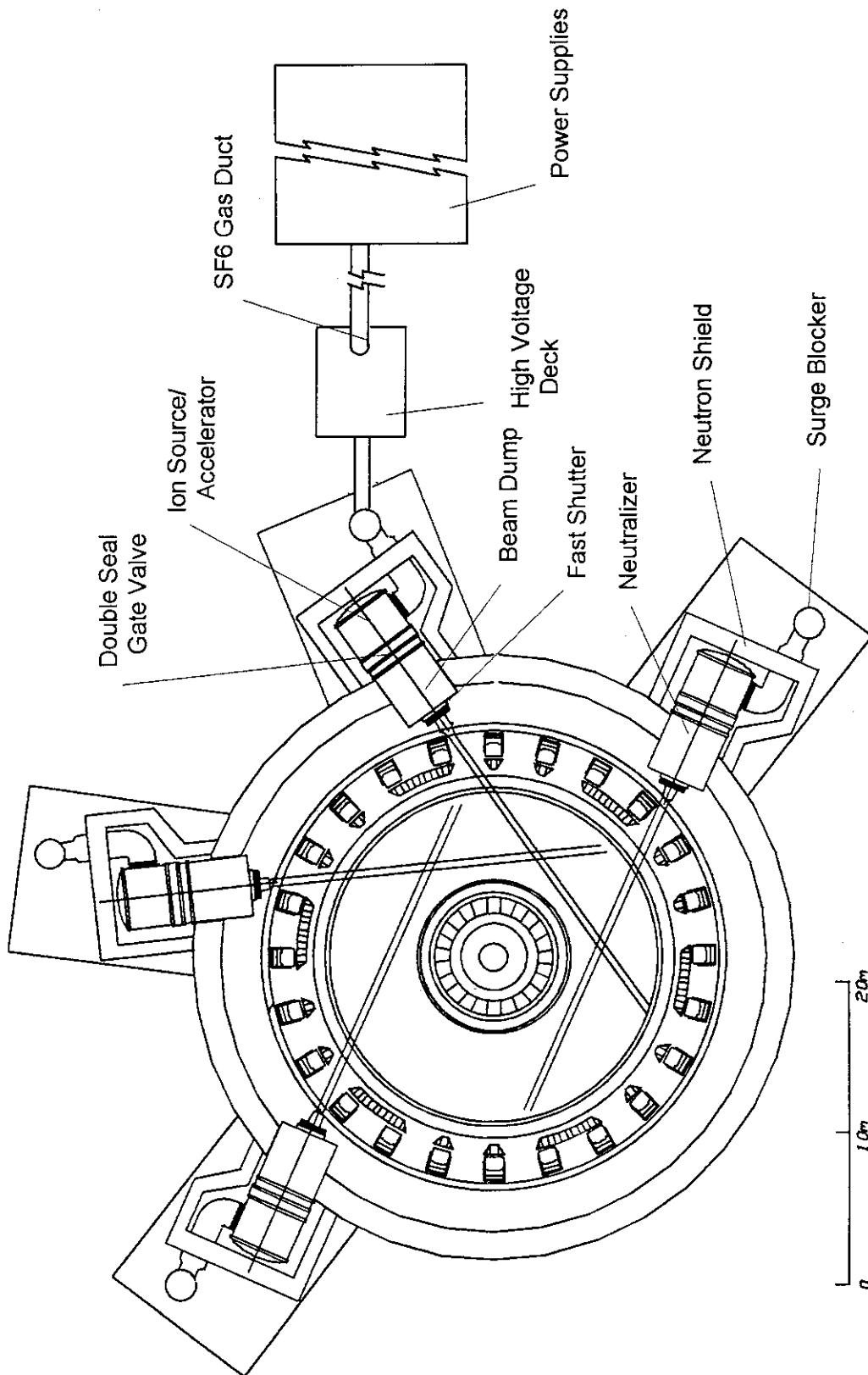


Fig.2-2 Layout of the four beamline modules (Short Beamline Option)

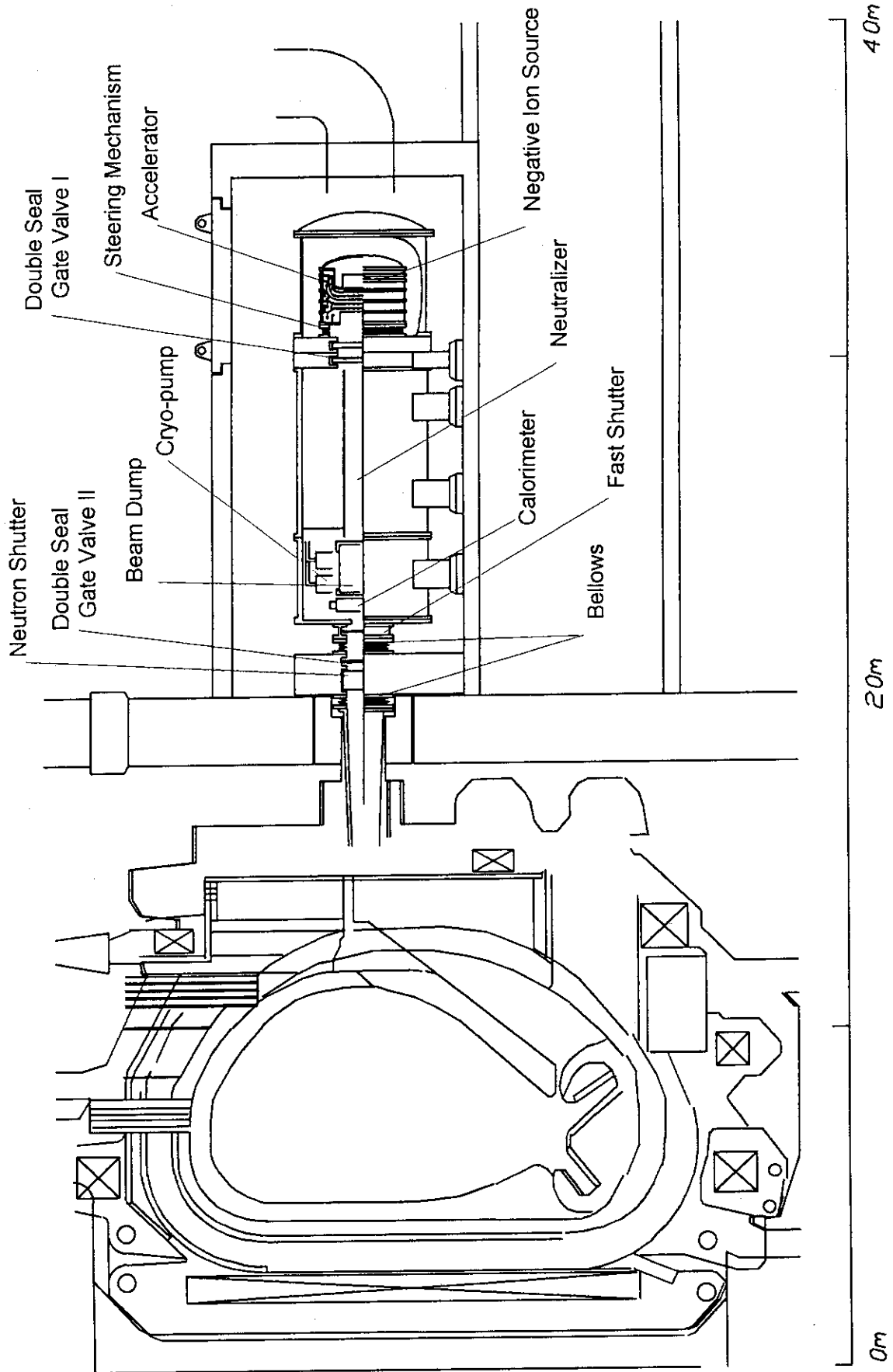


Fig.2-3 Side view of the beamline module (Long Beamline Option)

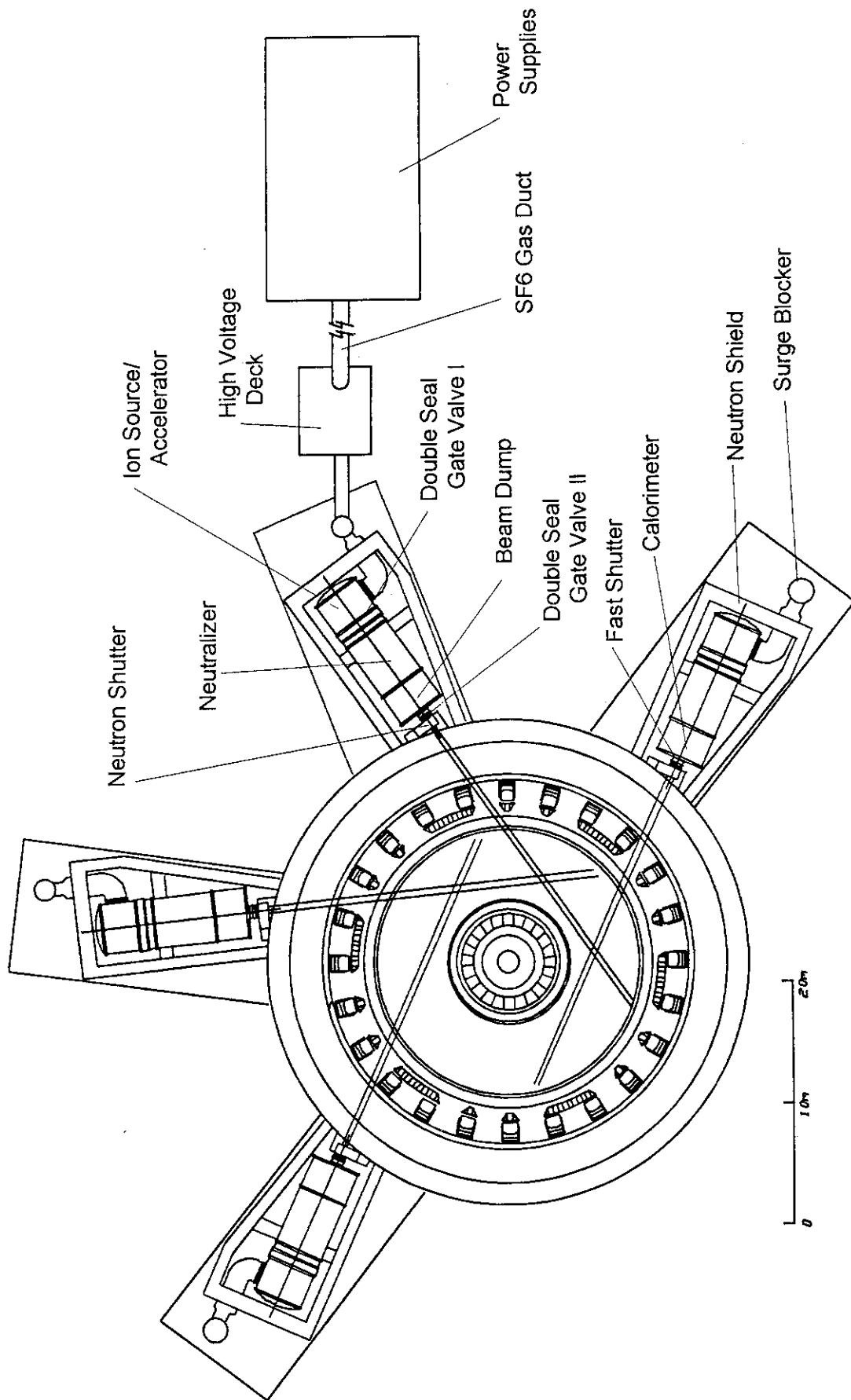


Fig.2-4 Layout of the four beamline modules (Long Beamline Option)

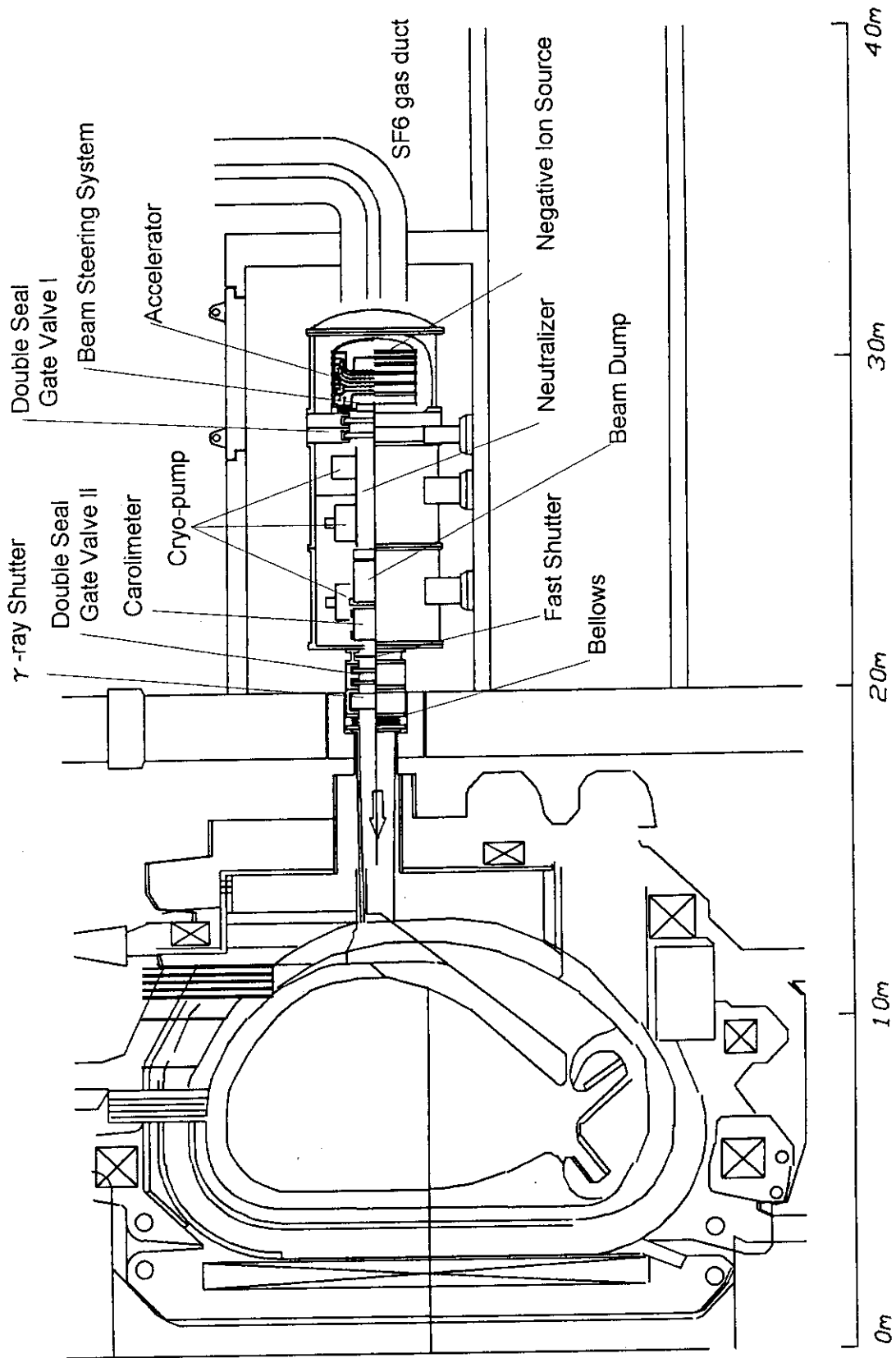


Fig.2-5 Side view of the beamline module (Long Beamline Option II)

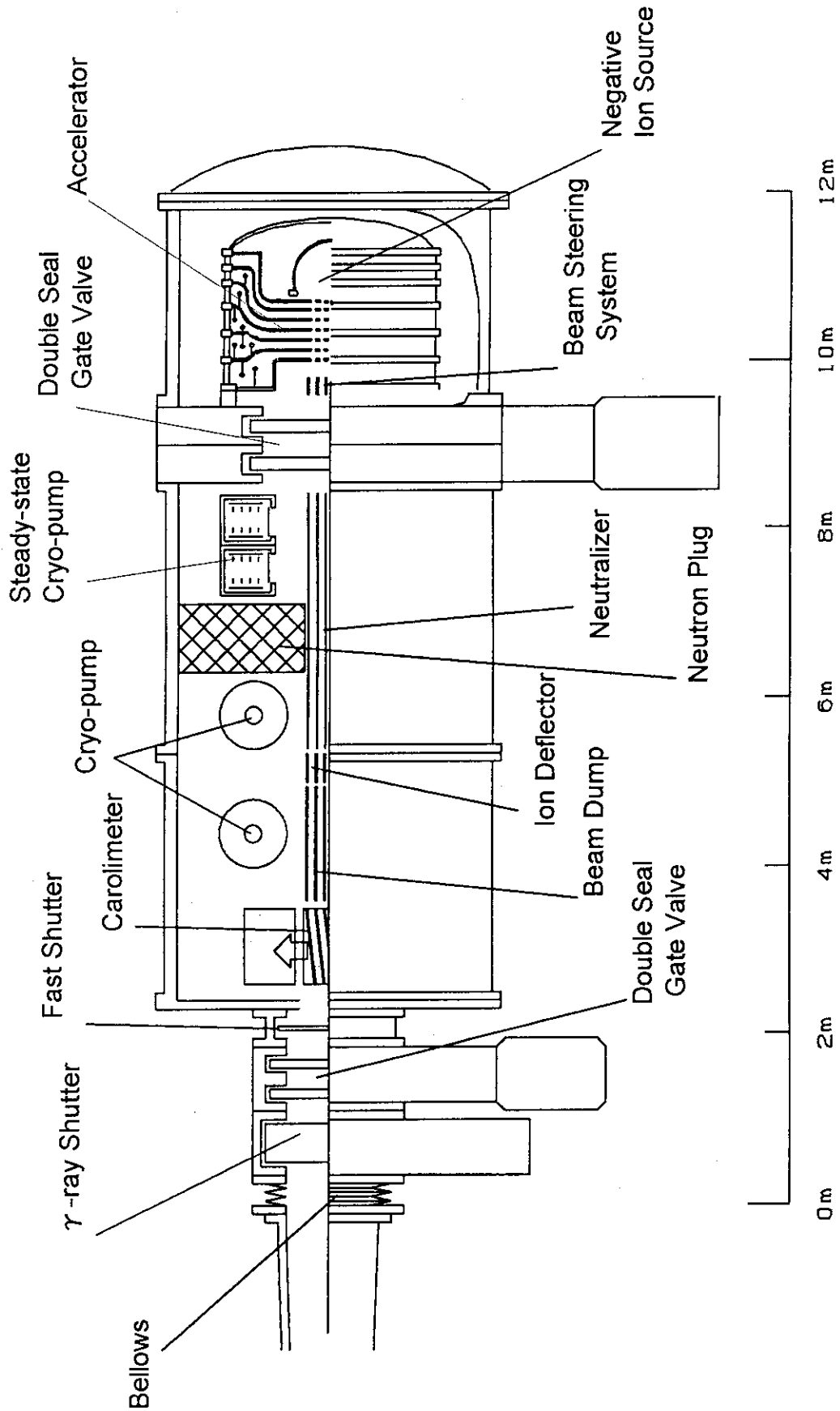


Fig.2-6 Plain view of the beamline module (Long Beamline Option II)



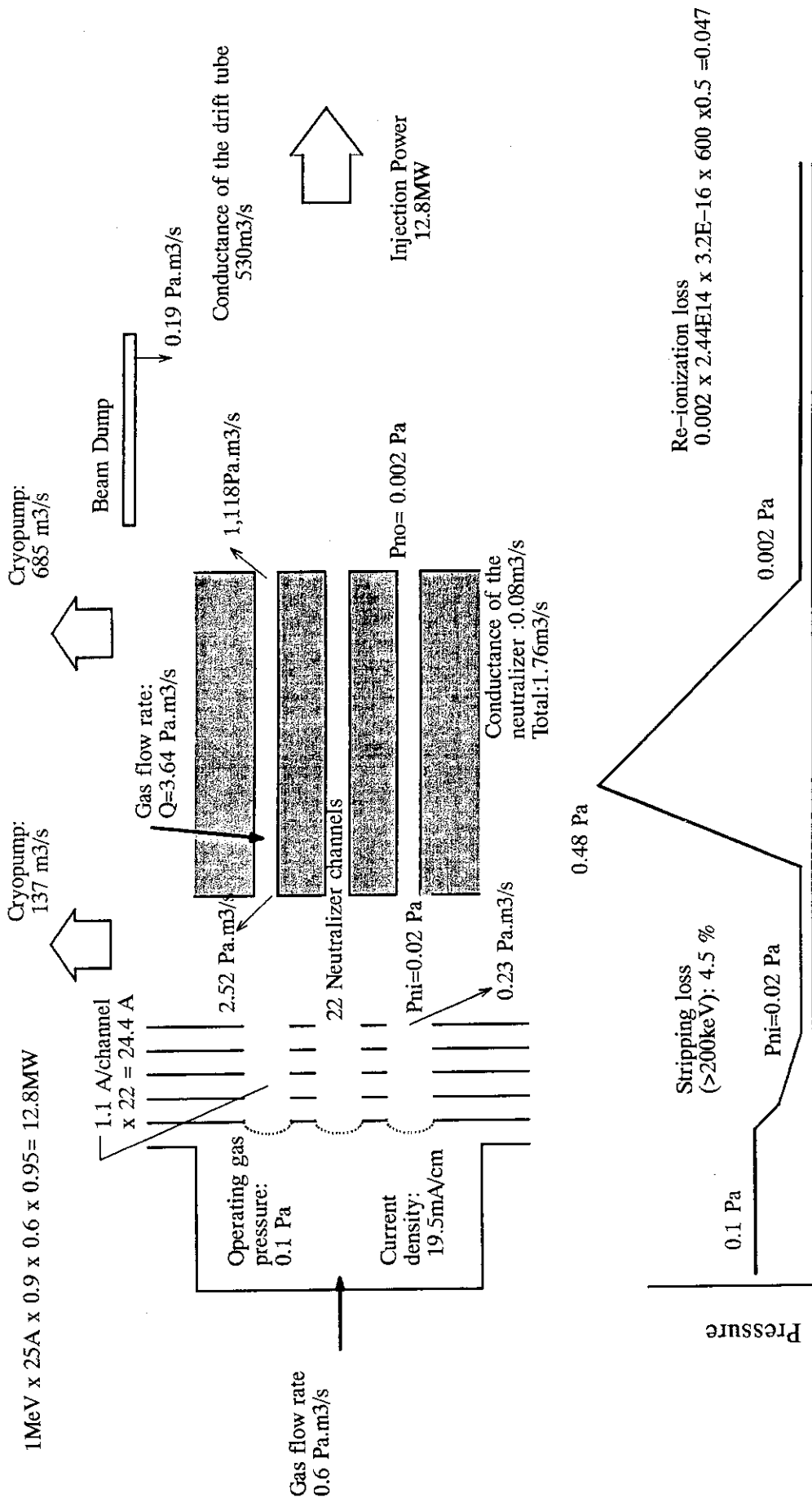


Fig.2-7 Gas flow diagram (Short Beamline Option)

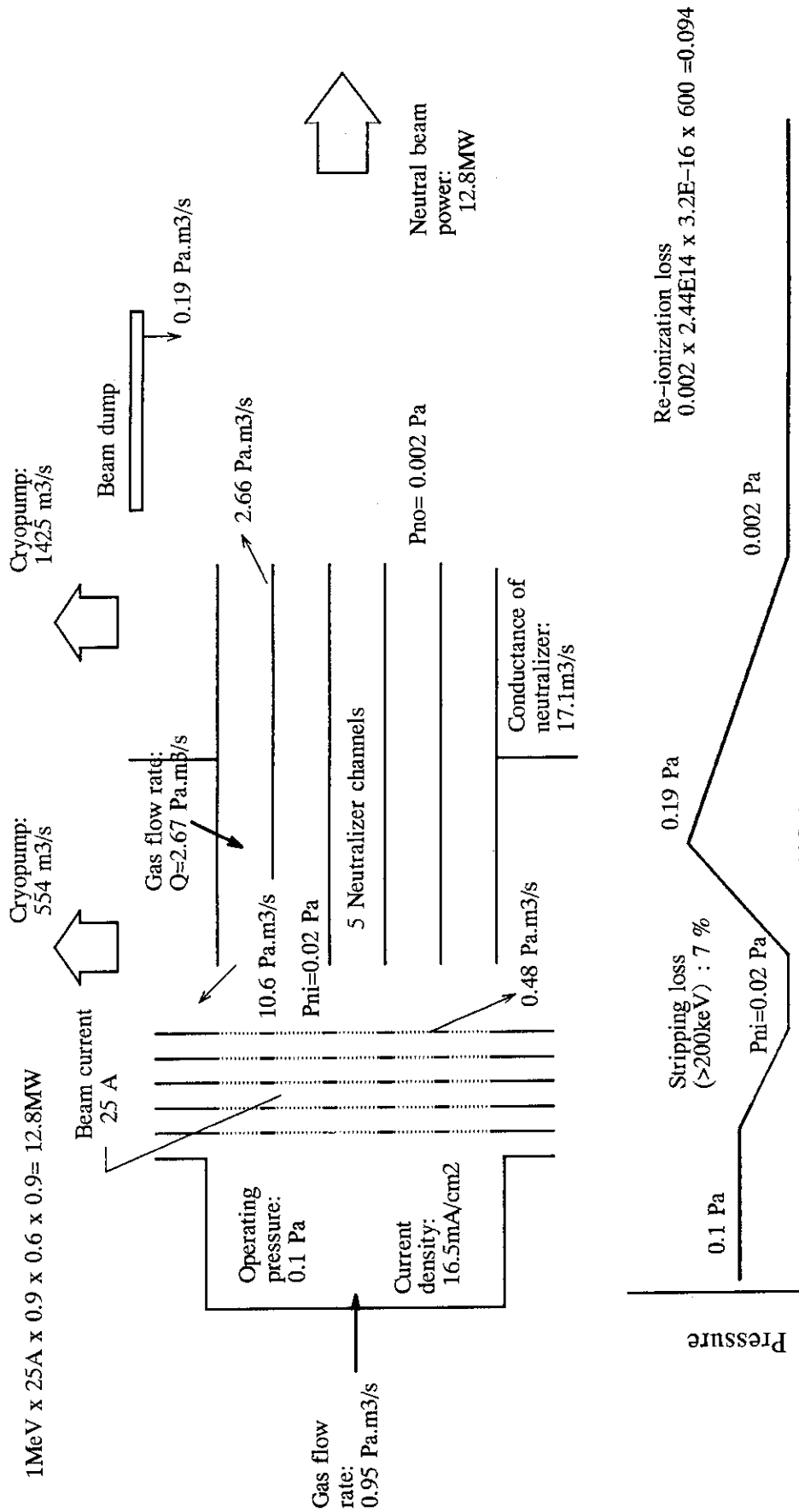


Fig.2-8 Gas flow diagram (Long Beamline Option)

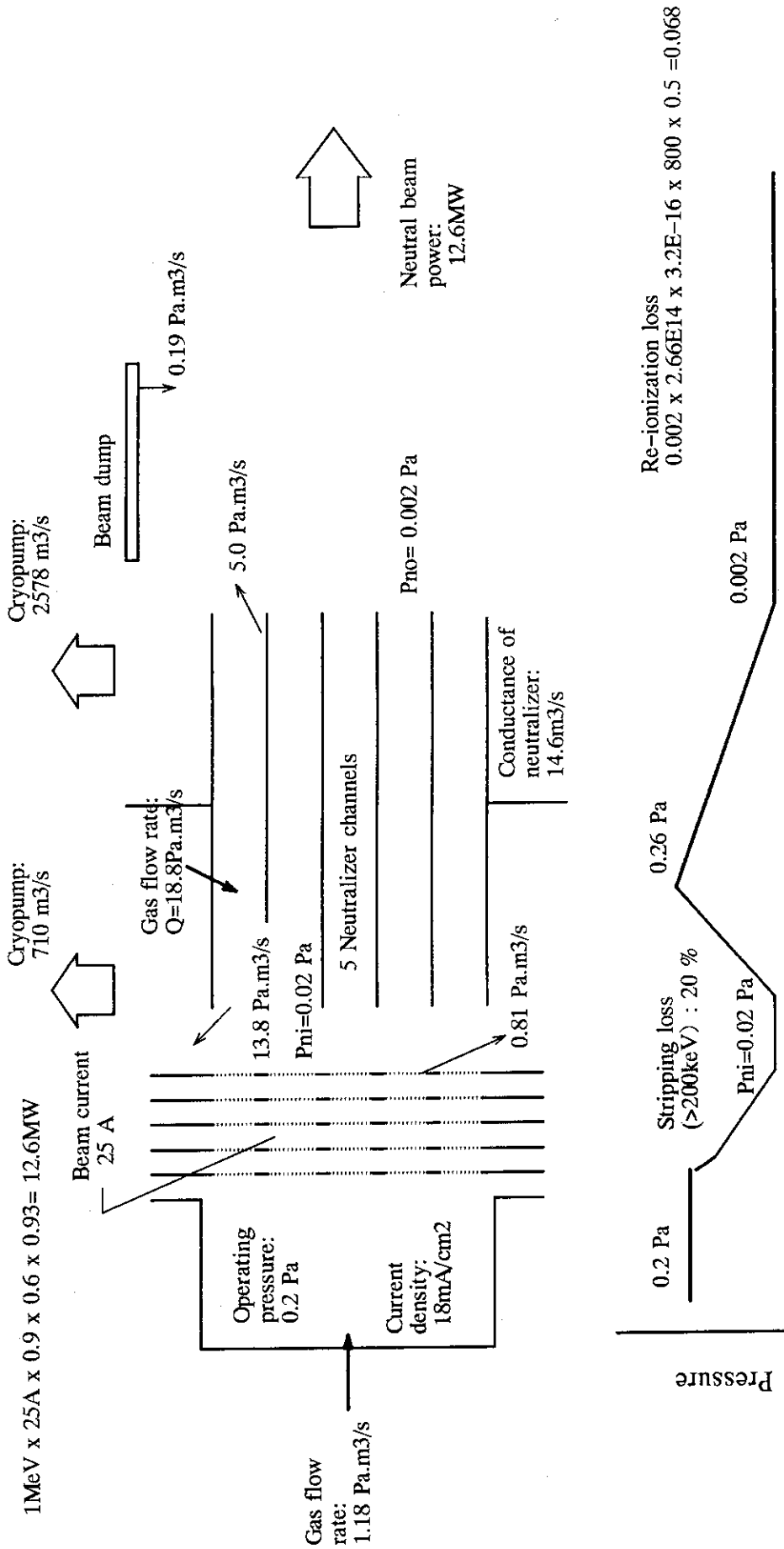


Fig.2-9 Gas flow diagram (Long Beamline Option II)

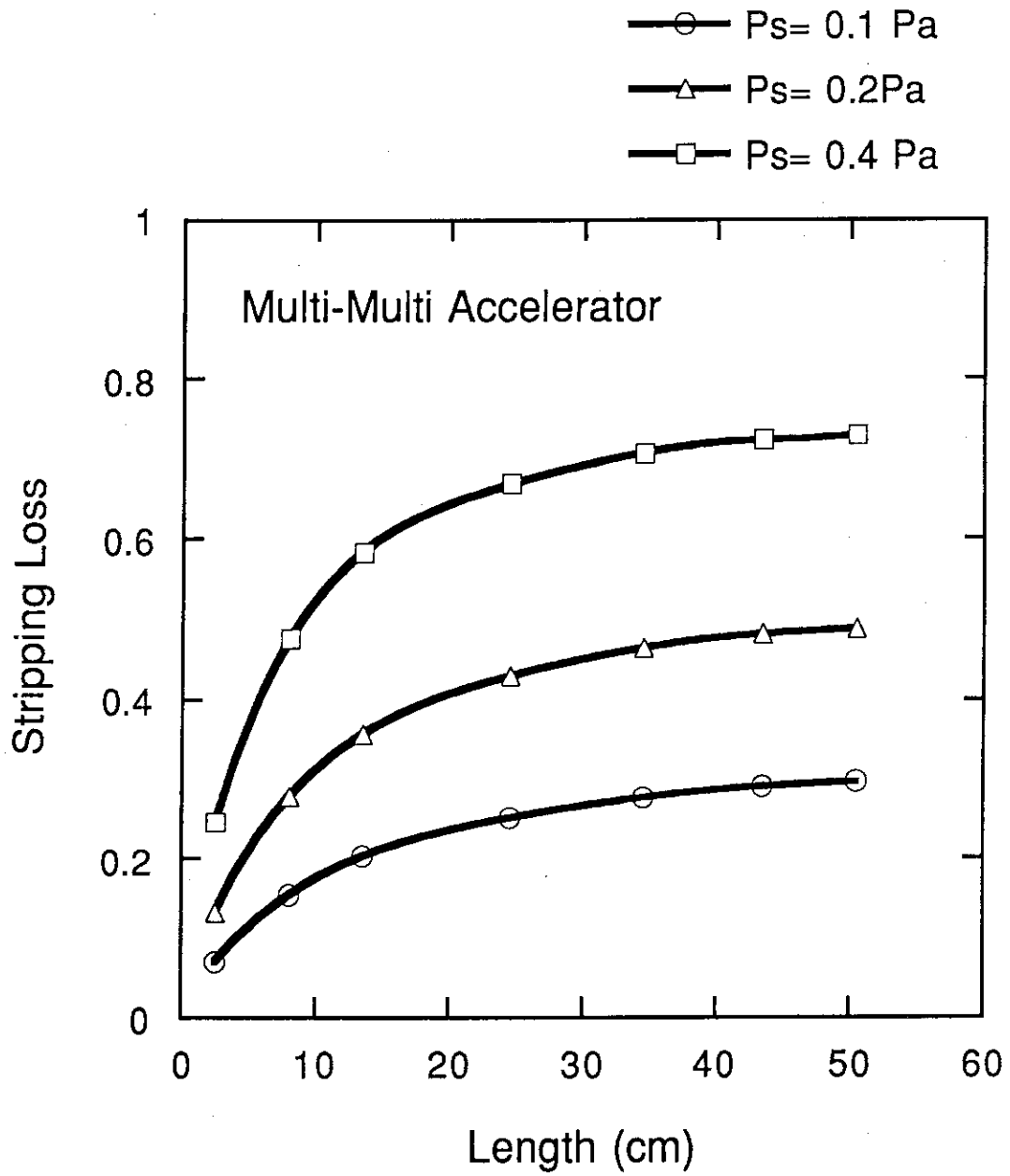


Fig.2-10 Stripping loss of negative ions in the extractor accelerator

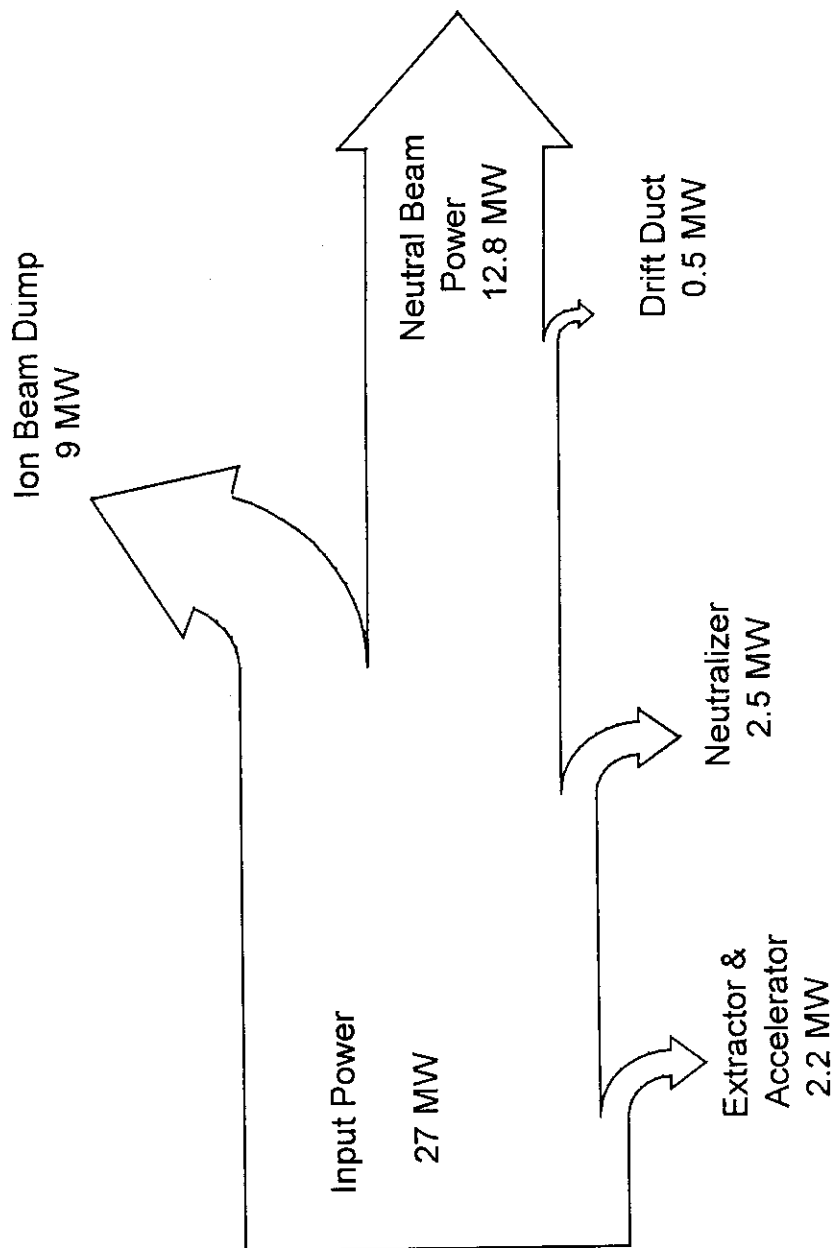


Fig.2-11 PowerFLOW diagram of ITER-NBI using a gas neutralizer cell

### 3. Design Studies on Critical Components

#### 3.1 Ion Source/Accelerator

A cross-sectional view of the ion source/accelerator is shown in Fig. 3-1. It consists of a plasma generator, an extractor, an accelerator, and a high voltage insulator column.

The  $D^-$  ions are produced in the cesium seeded multicusp plasma generator with a uniform  $D^-$  density over an extraction area of 44 cm x 126 cm for the short beamline option. This size is almost the same as that of the JT-60U source, which has an extraction area of 45 cm x 110 cm. We assume a small improvement in the current density and the source operating pressure; the current density is 20 mA/cm<sup>2</sup> and the pressure is 0.1 Pa for the short beamline design, while the design values in the JT-60U source are 13 mA/cm<sup>2</sup> and 0.3 Pa, respectively. We think this improvement can be achieved in the R&D during the EDA period, because we have already achieved the current density of 37 mA/cm<sup>2</sup> over the area of 40 cm x 15 cm for  $H^-$  ions in our 10 A negative ion source [1] and the pressure of 0.03 Pa at the current density of 8 mA/cm<sup>2</sup> over the area of 120 cm x 12 cm [2].

The extractor consists of three grids, called a plasma, an extraction and an electron suppression grid. The  $D^-$  ions are extracted from a multi-aperture grid and pre-accelerated, while the electrons extracted with the ions are deflected magnetically and removed from the beam. In the short beamline option, there are 22 extraction segments. In each segment, 76 beamlets extracted from the area of 14 cm in diameter are focused and merged into a single beam in the accelerator.

The  $D^-$  ions are accelerated to 1 MeV in the 5-stage electrostatic accelerator; in each stage,  $D^-$  ion beams are accelerated by 200 keV. The electric field is increased step by step to the downstream so that the beam is converged by the electrostatic lens between the stages. Free electrons are produced by the stripping, ionization and secondary electron emission in the accelerator gaps. To prevent these electrons from being accelerated to a high energy, magnetic field produced by permanent magnets inserted in the grid will be used.

In the short beamline option, multi-beamlets from the extractor are merged and accelerated through a large aperture accelerator (Multi-Single Type) to form a convergent ion beam whose diameter is less than 5 cm. In the long beamline option, each beamlet is accelerated individually by multi-aperture accelerator (Multi-Multi Type). A conceptual illustration of these types of accelerator is shown in Fig. 3-2. Figures 3.3, 3-4 and 3-5

show the layout of the extraction segments in the short beamline option, the long beamline option, and the long beamline option II, respectively. Figure 3-6 shows an example of the beam trajectory in the Multi-Multi Type electrostatic accelerator. The negative ions are accelerated up to 1 MeV with a good beam optics.

The insulator column is made of alumina ceramics, colona shields and flanges. The inner diameter of the insulator is 2.4 m, which can be fabricated by a small extension of the present technology of making a big alumina ceramics in a Japanese company. The major specifications of the ion source/ accelerator are listed in Table 3-1.

Figure 3-7 shows a concept of connection/disconnection of electric power cables and water pipes in large diameter SF<sub>6</sub> gas duct connected to the ion source/accelerator.

[1] Y.Okumura et al., Proc 16th Symp. on Fusion Technology, London, 1026-1030 (1990)

[2] M. Hanada et al., Rev. Sci. Instrum. 63, 2699-2701 (1992)

Table 3-1 Basic Specifications of the Ion Source/Accelerator

Beam Energy	:1 MeV
Beam Current	:25 A
Beam Species	:D <sup>-</sup>
Operating Source Pressure	:0.1 Pa (Short BL, Long BL) :0.2 Pa (Long BL II)
Current Density	:20 mA/cm <sup>2</sup> (Short BL) :16 mA/cm <sup>2</sup> (Long BL) :18 mA/cm <sup>2</sup> (Long BL II)
Extraction area	:44 cm x 126 cm (Short BL) :52 cm x 120 cm (Long BL) :45 cm x 142 cm (Long BL II)
Ion Source Type	:Magnetically Filtered Cs-seeded Multicusp
Extractor Type	:Extraction/ Electron Suppression System
Accelerator Type	:Electrostatic, 5 stages :Multi-Single Type (Short BL) :Multi-Multi Type (Long BL, Long BL II)
Beam Divergence	:5 mrad (Short BL) :< 3mrad (Long BL, Long BL II)
Gas Input	:0.6 Pa.m <sup>3</sup> /s (Short BL) :0.95 Pa.m <sup>3</sup> /s (Long BL) :1.18 Pa.m <sup>3</sup> /s (Long BL II)
Power Input	:250 kW (Plasma Generator) :800 kW (Extractor) :28 MW (Accelerator)
Dimensions	:2.5 m in outer diameter :2.2 m in height
Weight	:25 ton



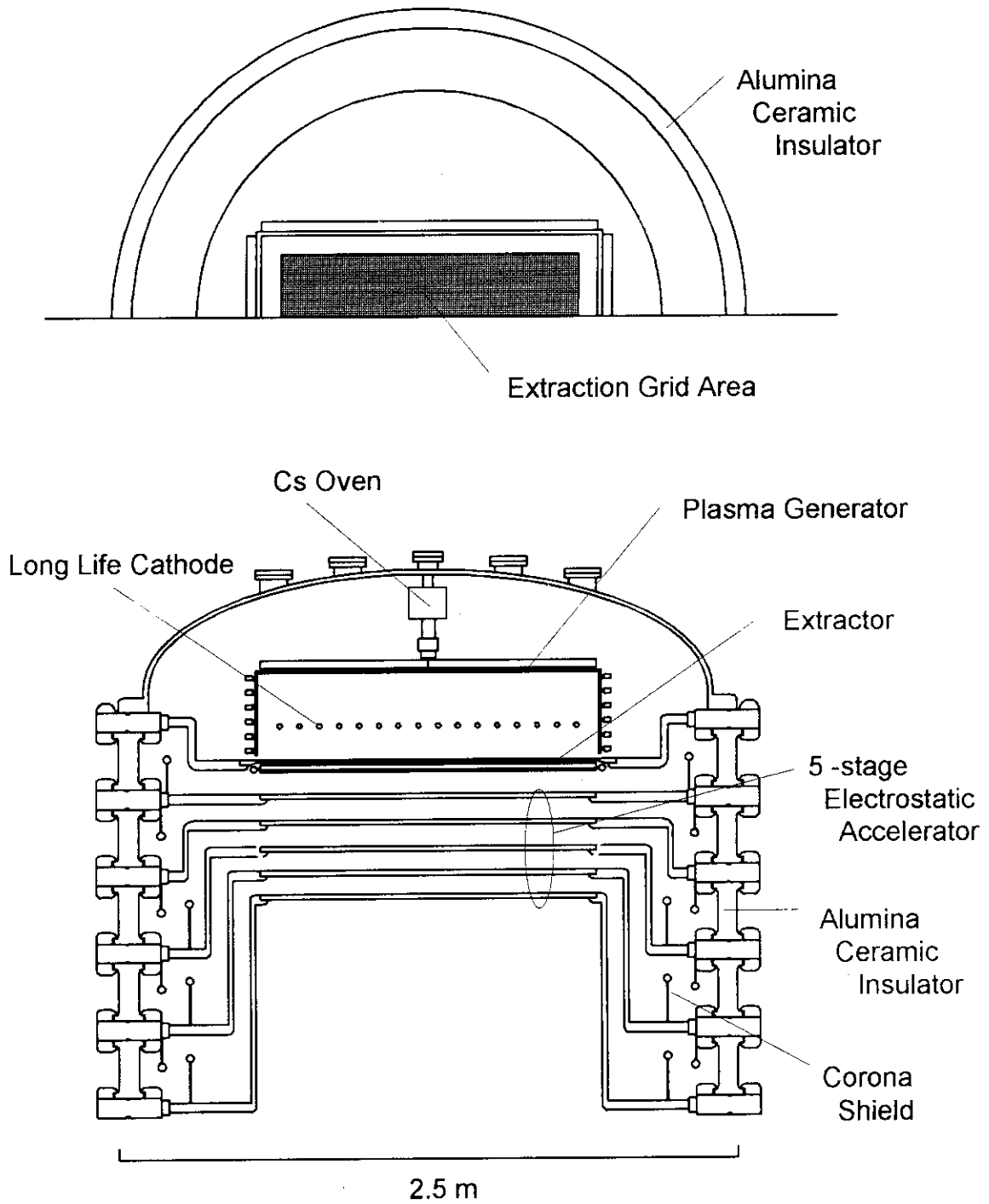


Fig.3-1 Negative Ion Source Accelerator

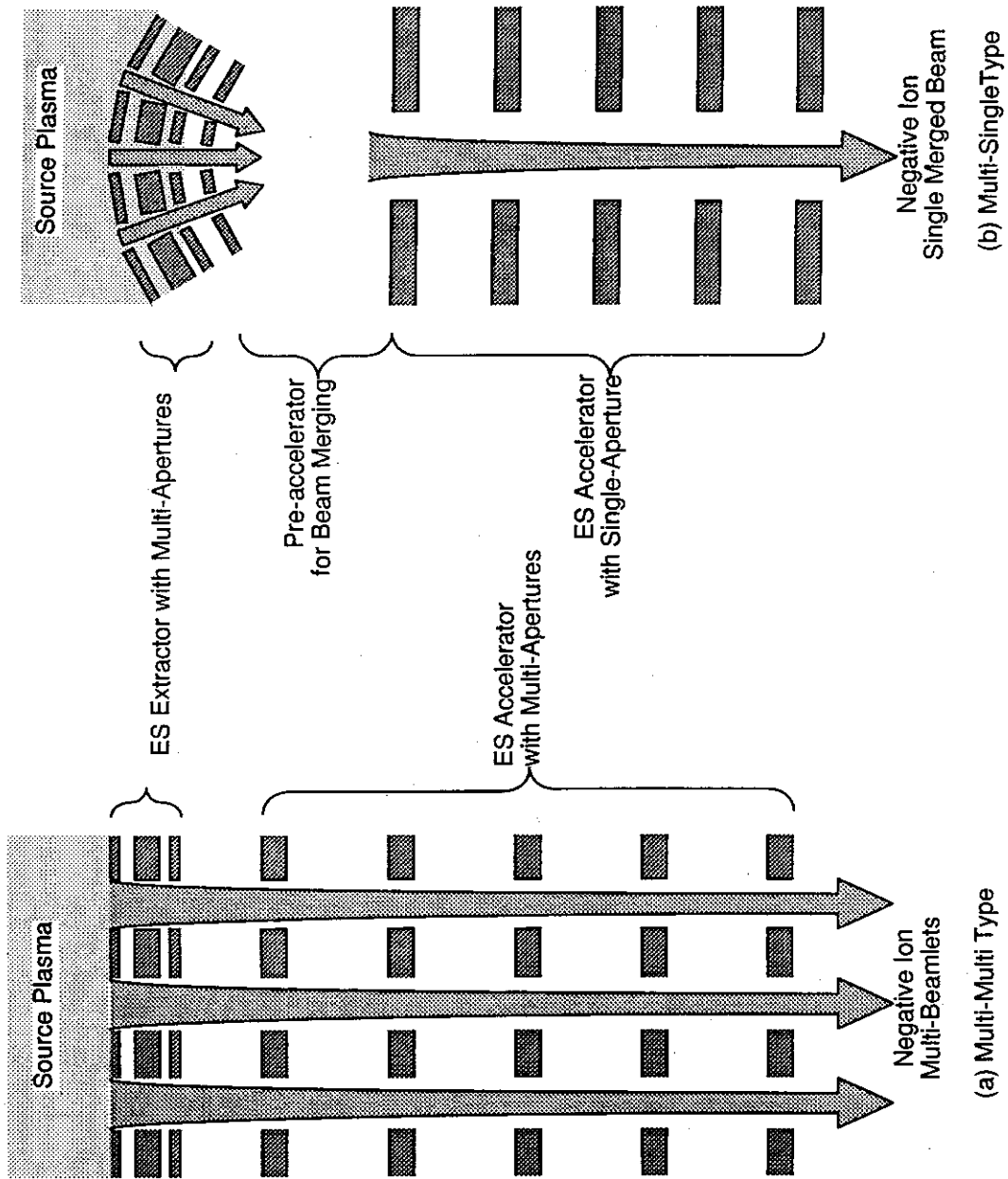


Fig.3-2 A conceptual illustration of (a) Multi Type

and (b) Multi-Single Type electrostatic accelerator

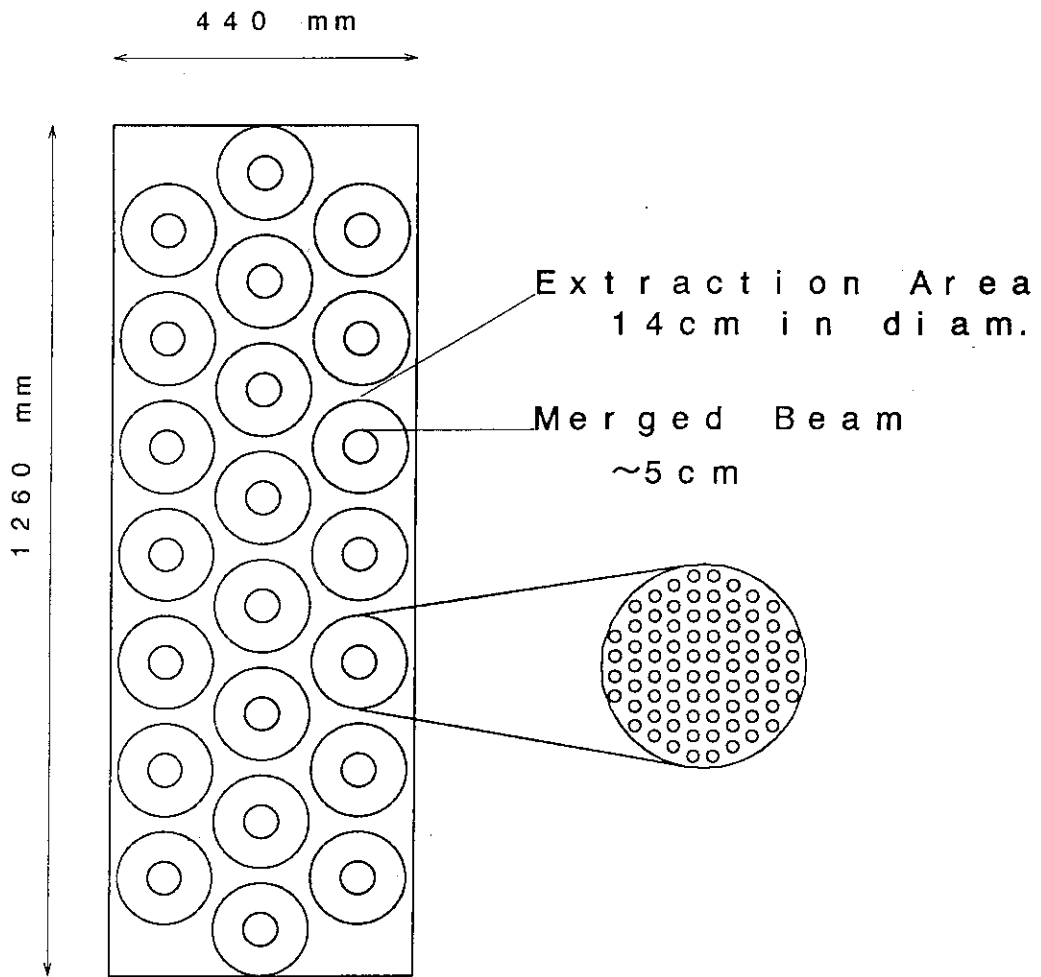


Fig.3-3 Layout of the extraction segments (Short Beamline Option)

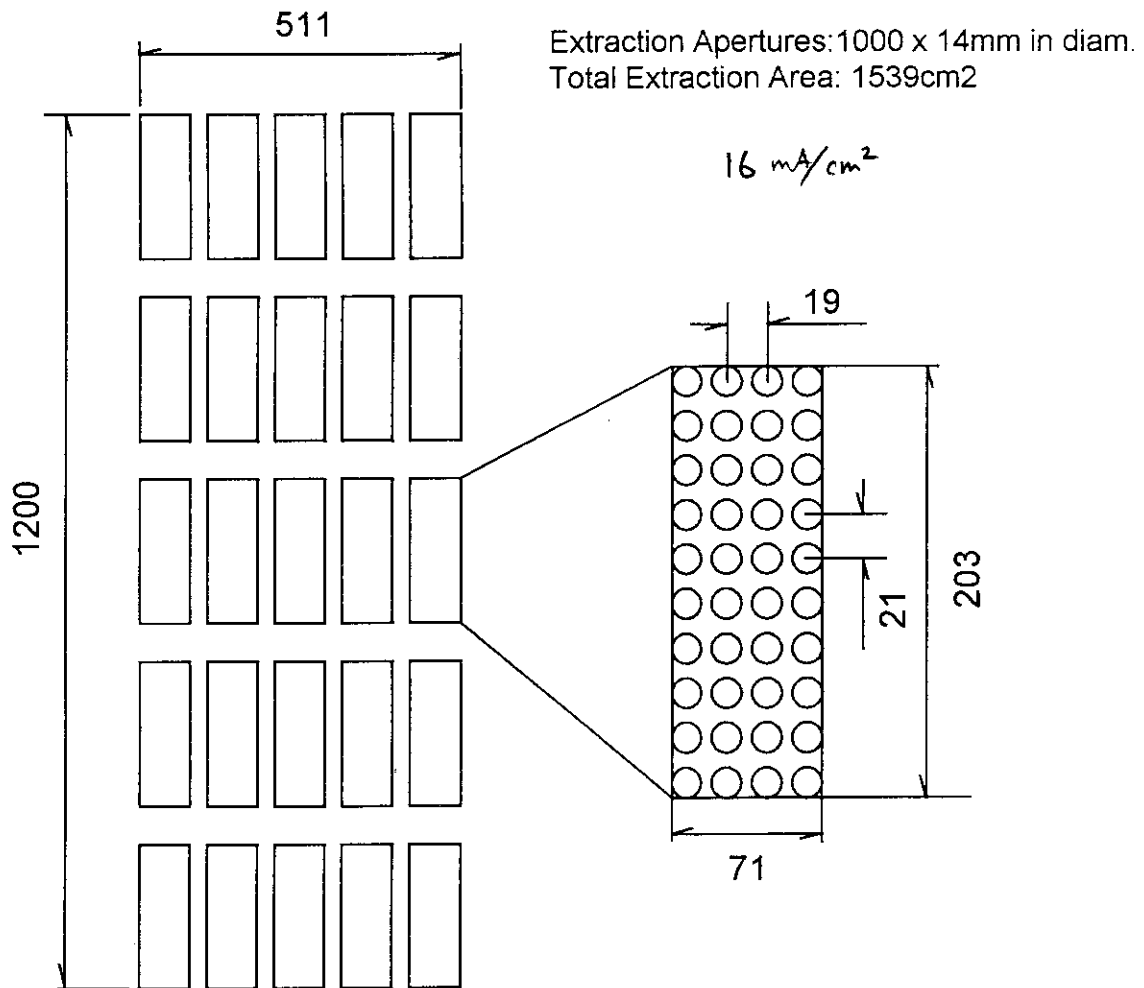


Fig.3-4 Layout of the extraction apertures (Long Beamline Option)

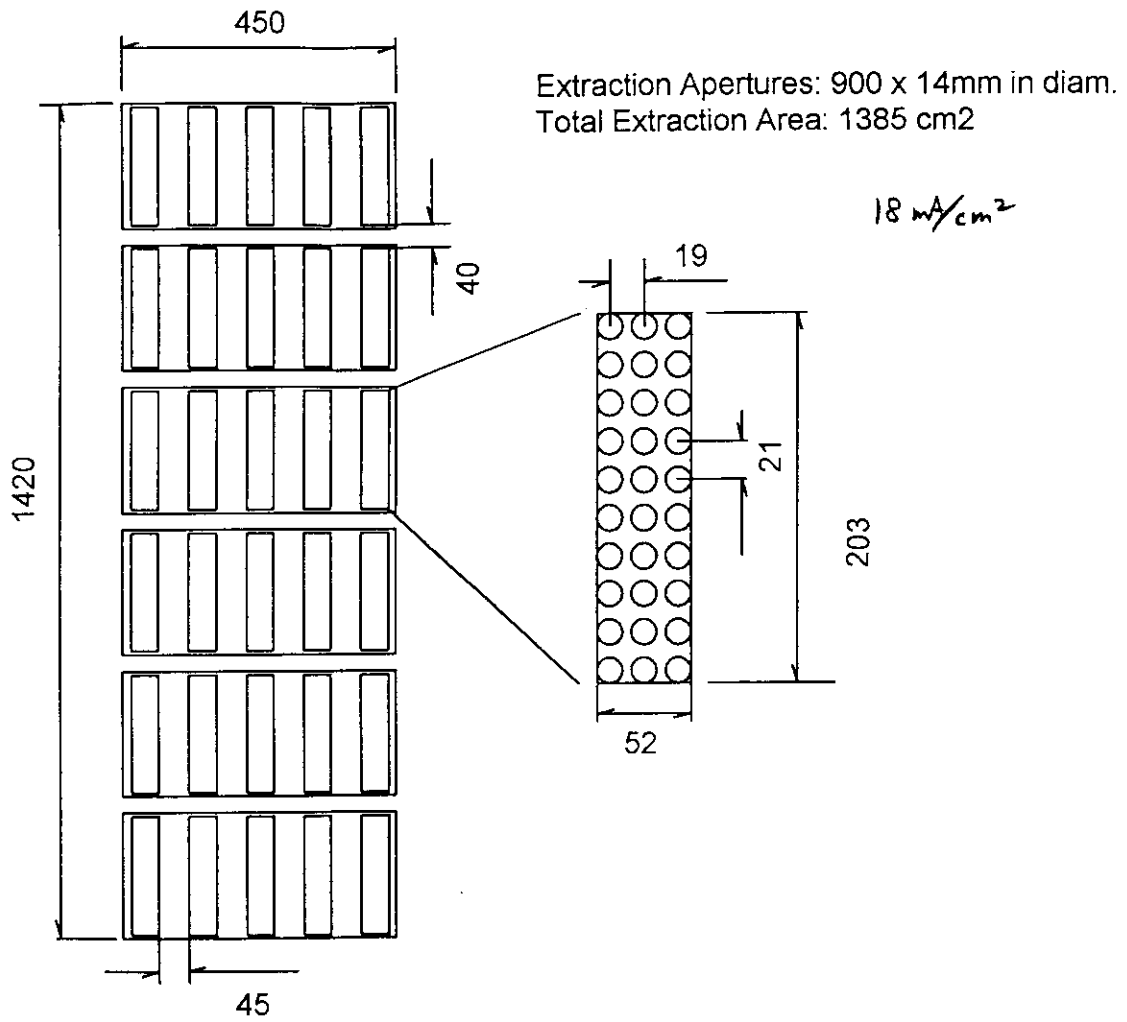


Fig.3-5 Layout of the extraction apertures (Long Beamline Option II)

\*MEV VACC=1000KV VEXT= 7.5KV 26. MA/CM2 H- GAP 100/90/80/70/60

Current Density = 2.6000E+01(mA/cm2)  
 Total Current = 3.8540E-02(A)  
 Perveance = 3.8111E-11(A/V\*\*1.5)  
 Minimum Potential = 0.0000E+00(V) AT Z = 5.4068E-01(m)  
 Divergence (RMS) = 1.8282E-01(Deg)  
 Electron Temperature = 0.0000E+00(eV)  
 Ion Temperature = 0.0000E+00(eV)

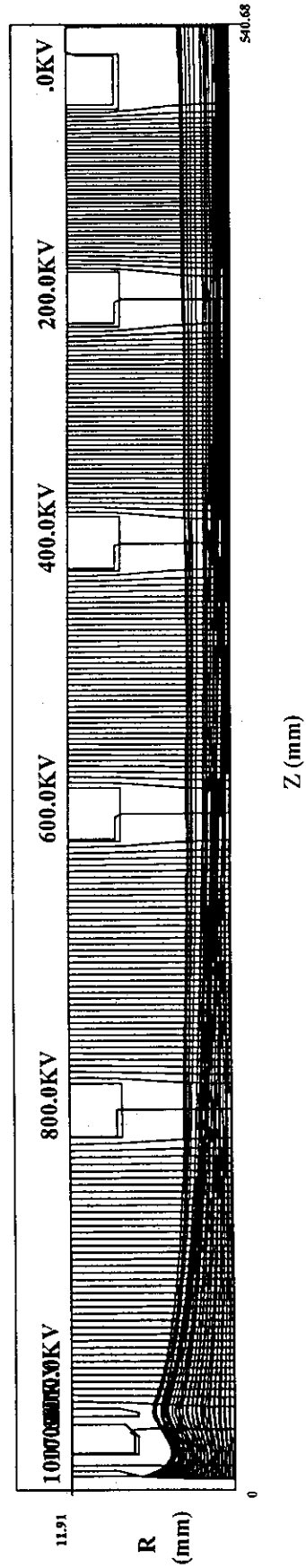


Fig.3-6 An example of the computation of the beam trajectory in acceleration up to 1MeV

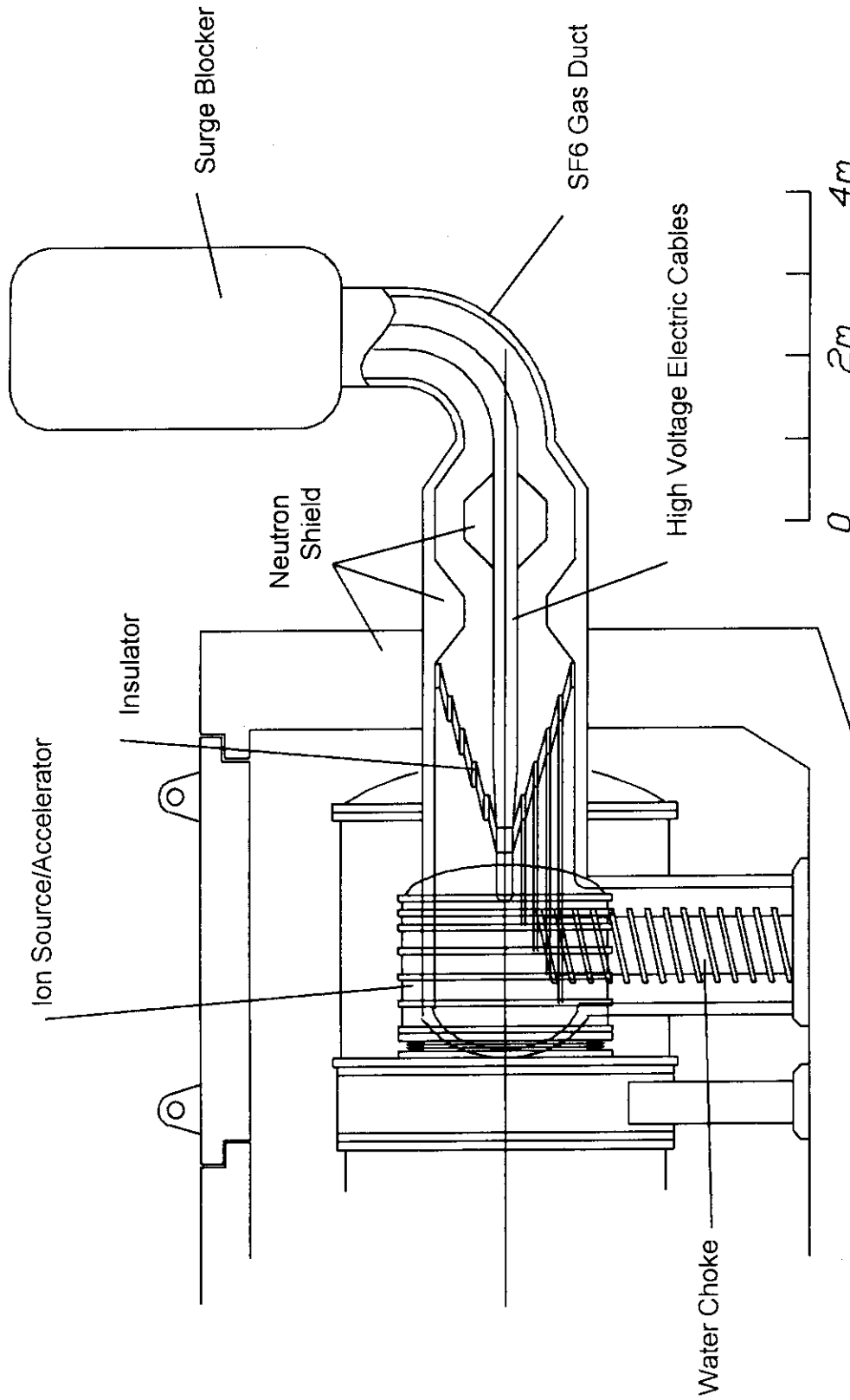


Fig.3-7 A concept of connection/disconnection of electric power cables and water pipes

### 3.2 Estimation of Cs Consumption

The cesium consumption rate is estimated using the experimental results on JAERI Long Pulse H- ion source [1], which was operated continuously with a pulse duration of 24 hours.

In the measurement of mass spectrum [2] in the JAERI Long Pulse Source, the extracted Cs<sup>+</sup> ion current was about 1% of hydrogen ion current. This means that the partial density of Cs<sup>+</sup> ions in the plasma is about 8% of hydrogen ions. Since the plasma density is the order of 10<sup>12</sup> cm<sup>-3</sup>, the Cs<sup>+</sup> density in the plasma is estimated 10<sup>11</sup> cm<sup>-3</sup>. As the ionization degree of Cs in the source plasma is 98 % [3], the neutral gas density of Cs would be 2x10<sup>9</sup> cm<sup>-3</sup>, or 6 x 10<sup>-8</sup> Torr in partial pressure.

Hence the Cs flow rate Q in the JAERI Long Pulse Source is;

$$\begin{aligned} Q &= 6 \times 10^{-8} \times 62.5 / (133)^{0.5} \times 38 \\ &= 8.2 \times 10^{-6} \text{ Torr l/s} \end{aligned}$$

The amount of Cs required for 24 hour operation for the source is calculated;

$$\begin{aligned} S &= 8.2 \times 10^{-6} \text{ Torr l/s} \times 3600 \times 24 = 0.7 \text{ Torr l} \\ &\text{or } 5.5 \text{ mg.} \end{aligned}$$

This agrees well with the experimental result, where <50 mg of Cs was enough to operate the source for 24 hours without additional Cs, at 50keV, 0.3A.

In the ITER ion source, the conductance of the plasma grid is 7511 l/s for the Long Beamline Option II (900 apertures of 14mm in diam.). The Cs gas flow rate is 3 x 10<sup>-4</sup> Torr.l/s. Therefore, the Cs consumption rate is estimated to be 2.3 x 10<sup>-3</sup> g/shot and 2.3 g for 1000 shots of 1000s operation.

A large amount of Cs can be confined inside the plasma generator by using a cold trap system. This can save Cs consumption. Regeneration of Cs can be controlled by a heater.

[1] Y.Okumura et al., Rev. Sci. Instrum. 63 (1992) p.2708

[2] Y.Okumura et al., Proc. 13th Symp. on ISIAT '90,(1990) p.149-152

[3] Y.Ohara et al., JAERI-M 91-052, 1991



### 3.3 Estimation of Tungsten Filament Lifetime

The present design utilizes tungsten filaments as a hot cathode, though long life cathode or RF plasma generation will be required for longer pulse operation of the NBI system. The life time of the tungsten filament is estimated by assuming that the the life time is determined by both the evaporation and the sputtering effects.

#### Evaporation effect

Arc current	:3.2 kA
Filament size	:1.8mm in diam. x 200 mm x 50 pieces
Emission current density	:5.66 A/cm <sup>2</sup>
Filament temperature	:2840 K
Evaporation rate	:1.49 x 10 <sup>-6</sup> (kg.m <sup>-2</sup> .s <sup>-1</sup> )

#### Sputtering effect

Plasma density	:1 x 10 <sup>13</sup> cm <sup>-3</sup>
O ion	:1%
W ion	:0.1 %
Sputtering yeild	: O ion ... 3.469 x 10 <sup>-4</sup> (kg/m <sup>3</sup> s) Wion ... 5.497 x 10 <sup>-6</sup> (kg/m <sup>3</sup> s)
Temperature factor	:x10 at 2840 K
Total sputtering rate at 2840K	:3.524 x 10 <sup>-3</sup> (kg/m <sup>3</sup> s)

Assuming the filament should be replaced when the diameter decreases to 85 % of the original value, the filament lifetime under the ITER condition is estimated to be 640,000s or 640 shots of 1000s pulses.

### 3.4 Large Bore Insulator

The insulator column is composed of 5 stages of large bore insulators. Dimensions of each insulator are 2.4 m in inner diameter and 24 cm in height. The insulators are connected with flanges by metal O-rings to seal the vacuum. As the insulator column is immersed in pressurized gas for high voltage insulation, it is designed to sustain the outside pressure of up to 2 MPa. In addition, the insulator column withstands the inside pressure of 2 MPa at the accident of ITER.

A large bore insulator, whose inner diameter is 1.8 m, is being used in the JT-60U negative ion source as a 500 keV insulator column. A larger insulator, 2.4 m in inner diameter and 21 cm in height, was developed at JAERI and tested at 160 kV, 10 min. Although the size of these insulators are ITER relevant, they are made of FRP (Fiber Reinforced Plastic), which might be difficult to be used in ITER because of the radiation of neutron and  $\gamma$ -ray.

An alumina ceramic insulator has enough durability against the radiation as described in 4.4. Electrical and mechanical characteristics are better than the FRP insulators. At present, however, the maximum size of the alumina ceramic is 70 cm in diameter and 30 cm in height, which is used in the 400 keV negative ion source developed at JAERI.

Engineers in a Japanese company, Kyocera Co. LTD., have studied on the feasibility of a large bore insulator. They concluded that it is possible to fabricate a 2.4 m diam. alumina ceramic insulator with a small extension of present technologies. The specifications of the alumina ceramic insulator proposed are listed in Table 3-2. They estimate the time required to develop the technology and to fabricate the 2.4 m insulator is two years.

There are three processes in fabricating the alumina ceramic; i.e. forming, sintering (firing), and grinding. Out of these processes, most critical process is the forming process. It is difficult to form a large alumina uniformly without void inside. Although cold isostatic press method is widely used to form a large alumina, the pressing machine becomes very big and very expensive for the 2.4 m insulator. In addition, transportation of the formed alumina is difficult in case of the 2.4 m insulator. To overcome these problems, a newly developed forming method or an improved slip casting method is proposed, where the forming is performed inside the furnace for sintering and no expensive forming machine is needed.

Table 3-2 Specifications of Large Bore Insulator

Size	:2.4 m in inner diameter
	:2.55 m in outer diameter
	:24 cm in height
Material	:99 % Al <sub>2</sub> O <sub>3</sub>
Sintering Temperature	:1700 °C
Forming Method	:Improved slip casting

### 3.5 Mechanical Strength against the Pressure Difference

Some components of the ion source/accelerator, i.e. a ceramic insulator and a formed head for the ion source are considered to be weak against the pressure difference through the vacuum interface in the ITER NB system. Therefore, their structure and material should be designed carefully. The outside of the ion source is always pressurized by  $C_2F_6$  gas of 0.7 MPa or  $CO_2$  gas of 2.0 MPa. In the normal operation, the inside is vacuum. Therefore, the pressure difference is 0.7 MPa or 2.0 MPa, by which the components are subjected to the compression force. In the accident, however, the components are subjected to the tension force since the inside of the ion source would be pressurized at 2.0 MPa as shown in Fig. 3-8. The mechanical stress caused by the pressure difference was calculated in both cases to determine the structure of each component.

#### Ceramic Insulator

When the inside pressure is  $P_1$  and outside pressure is  $P_2$ , the maximum stress of the shell (ceramic insulator) is in circumferential direction, and its value is

$$\sigma = \frac{r (P_1 - P_2)}{t} \quad \dots\dots\dots (1)$$

Here, 'r' is the inner radius of the ceramic insulator, 't' is the thickness.

The inner radius is 1200 mm from the view point of the electrical insulation. As the ceramic insulator, the material of  $Al_2O_3$  with purity of more than 99 % is chosen from the view point of the electrical and mechanical characteristics. The permissible mechanical strengthes of this material are 250 MPa for the tension force, and 2500 MPa for the compression force. Since the ceramic insulator is weak against the tension force, the thickness is detemined only by estimating tension stress in the accident, whose pressure difference is 1.3 MPa. Taking the safety factor of 8, the thickness is estimated to be 5 cm. Using this insulator with thickness of 5 cm, the sufficient mechanical strength is attained also in the normal operation as shown in Table 3-3.

#### Formed Head of the Ion Source

As shown in Fig. 3-9, the formed head of the ion source is strong against the inner pressure, but weak against the outer pressure. Therefore, the structure should be determined only by estimating the compression force. When the stress of the formed head is given by the equation of

$$\sigma = \frac{(WR + 0.2 t)(P1 - P2)}{2 \eta t} \quad \dots\dots (2)$$

$$W = 1/4 (3 + (R/r)^{1/2})$$

where, W : geometry coefficient  
 R : major radius  
 r : minor radius  
 t : thickness  
 $\eta$  : welding coefficient

This equation is valid only for the tension force. To apply this equation to the compression force, the pressure difference should be calibrated. The calibrated pressure difference is larger approximately by a factor 2 than the actual pressure difference. Hence, the calibrated pressure differences are 1.4 MPa in the C<sub>2</sub>F<sub>6</sub> gas, and 4 MPa in CO<sub>2</sub> gas.

The major radius is 1200 mm, which is determined by the size of the ion source. The minor radius is generally 1/10 of the major radius, i.e. 120 mm, hence the geometrical coefficient is 1.54. The welding coefficient is 0.55, derived from JIS (Japan Industrial Standard). The permissible mechanical strength of stainless steel is 130 MPa, including a safety factor of 3. Substituting these values into eq. (2), the required thickness is evaluated to be 35 mm in the C<sub>2</sub>F<sub>6</sub> gas, and to be 90 mm in the CO<sub>2</sub> gas.

Table 3-3 Mechanical stress of the alumina ceramic with 50mm thickness

Outside pressure Inside pressure	C2F6 P2=0.7MPa	CO2 P2=2MPa
NORMAL OPERATION P1= 0 MPa	-17 MPa	-48 MPa
ACCIDENT P1=2MPa	31 MPa	0 MPa

\*) The minus symbol shows the compression force.

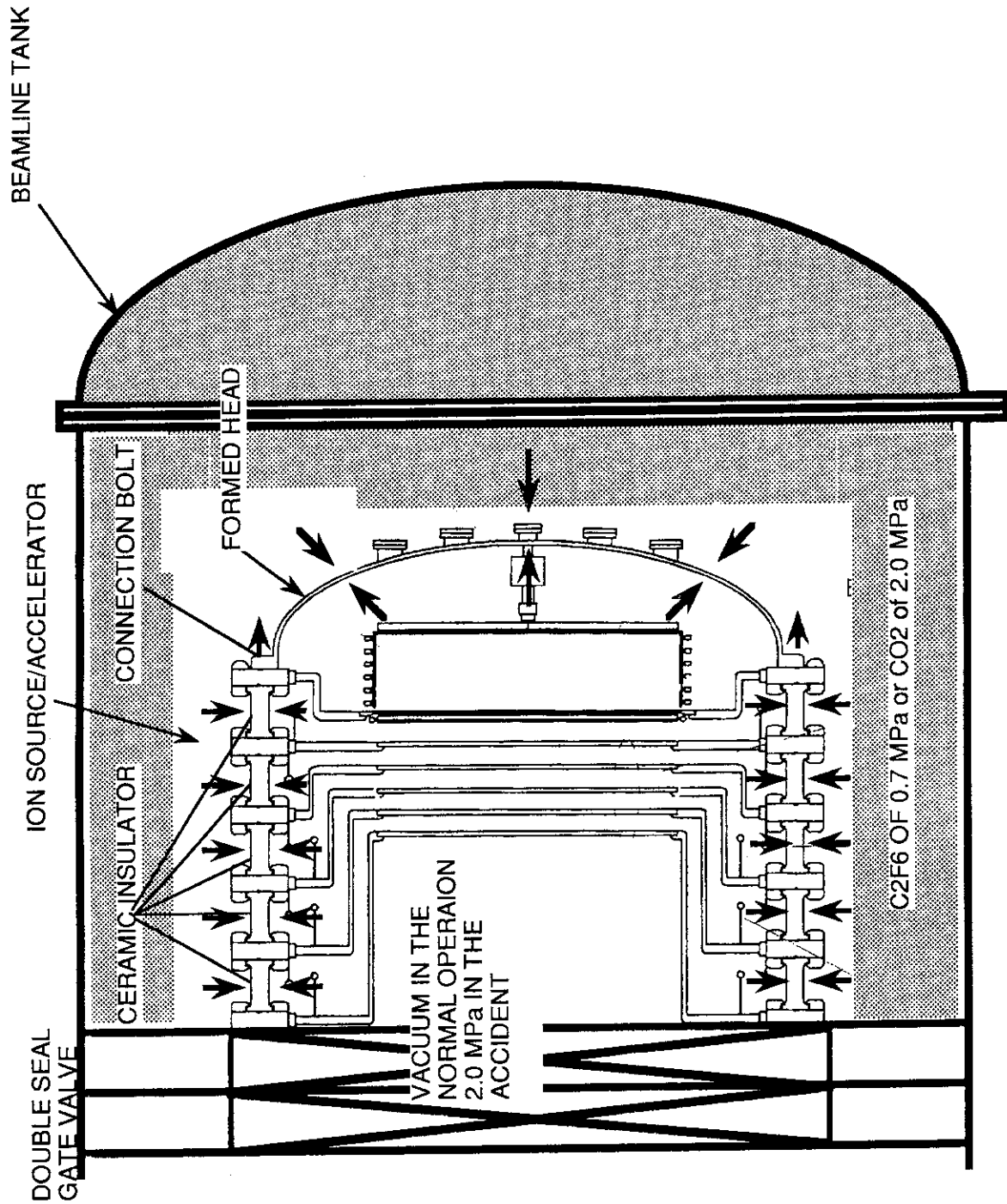


Fig.3-8 Pressure exposed to the ion source

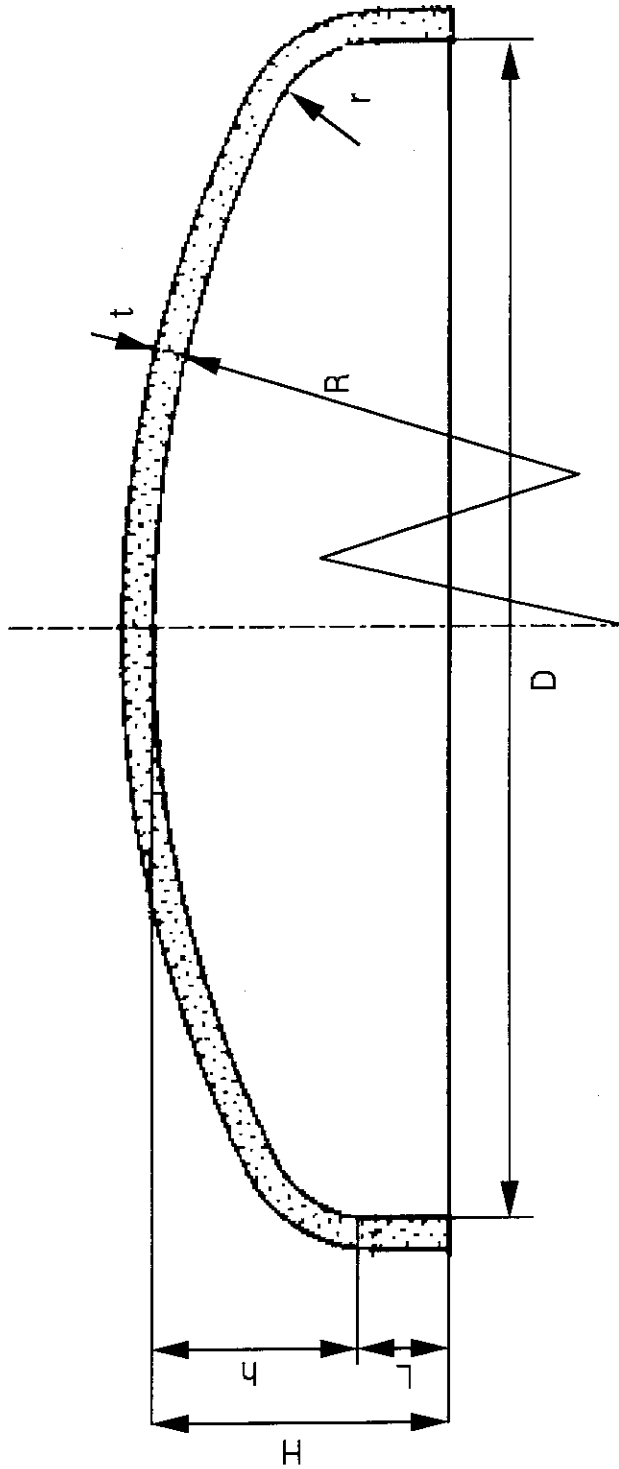


Fig.3-9 Geometry of the formed head



## 3.6 Beam Steering System

### Functions

The function of the beam steering system is to adjust the beam steering angle horizontally so as to transport the beam through the sub-divided neutralizer and beam dump, whose acceptances in the horizontal direction are very severe. Vertical steering will be made by tilting the grid segments of the extractor/accelerator.

### Requirements

Steering Angle :  $\pm 10\text{mrad}$

Adjustment : 1D independent Steering for each set of beamlets

### Design

Figure 3-10 shows a schematic of the beam steering system. An electrostatic deflector coupled with the accelerator can be utilized for the beam steering. Assuming that the distance between the electrode  $d=6\text{cm}$ , length of the electrode  $l=20\text{cm}$ , only  $\pm 3\text{ kV}$  is enough to deflect a 1 MeV D- beam by  $\pm 10\text{ mrad}$ .

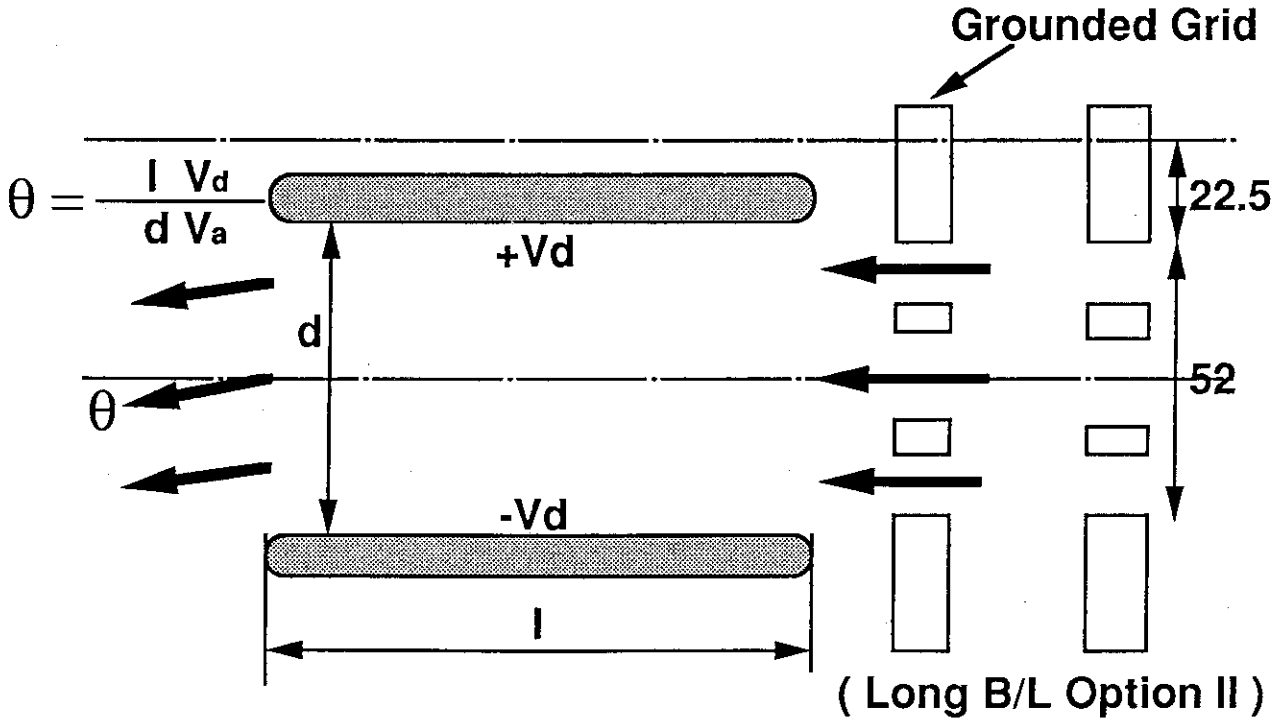


Fig.3-10 A schematic of beam steering system

### 3.7 Neutralizer

Two types of neutralizers are designed corresponding to the two design options; one is a multi-cylinder neutralizer for the short beamline option and the other is a multi-slot neutralizer for the long beamline option.

In the short beamline option, the neutralizer consists of 22 cylindrical channels in a neutron shield as shown in Fig. 3-11. The neutron shield is an iron block, which serves as an inner magnetic shield. The dimensions of the cylinder are 8 cm in diameter and 2 m in length, which are big enough for the merged negative ion beam. The conductance is small compared with a conventional neutralizer with a big bore. This can save the gas flow rate flowing into the neutralizer. The conductance is 0.08 m<sup>3</sup>/s per 1 cell, and 1.76 m<sup>3</sup>/s in total. The accelerated D<sup>-</sup> ions are neutralized by the collision with residual D<sub>2</sub> molecules. At a beam energy of 1 MeV, the optimum line density is 1.2 x 10<sup>16</sup> molecules/cm<sup>2</sup>, giving neutralization efficiency of 60 %. The required gas flow rate in the neutralizer is 3.64 Pa m<sup>3</sup>/s. A gas pressure at the entrance of the neutralizer is kept to be 0.02 Pa to reduce the stripping loss of D<sup>-</sup> ions in the accelerator below 4.5 %. On the other hand, the gas pressure at the exit of the neutralizer is 0.002 Pa. The re-ionization loss in the beam drift duct is estimated to be 4.7 %.

In the long beamline option, the neutralizer has five slot channels as shown in Fig. 3-12. An overall size of the neutralizer is 0.45m x 1.2m x 5 m. The conductance is 3.42 m<sup>3</sup>/s per channel, and 17.1 m<sup>3</sup> / s in total. The required gas flow rate in the neutralizer is estimated to be 13.35 Pa m<sup>3</sup>/s.

Figure 3-13 shows the neutralizer in the long beamline option II. The length is 3m, and the conductance is 14.6 m<sup>3</sup>/s. The gas flow rate of 18.8 Pa.m<sup>3</sup>/s is required to keep the line density, 1.2 x 10<sup>16</sup> molecules/cm<sup>2</sup>.

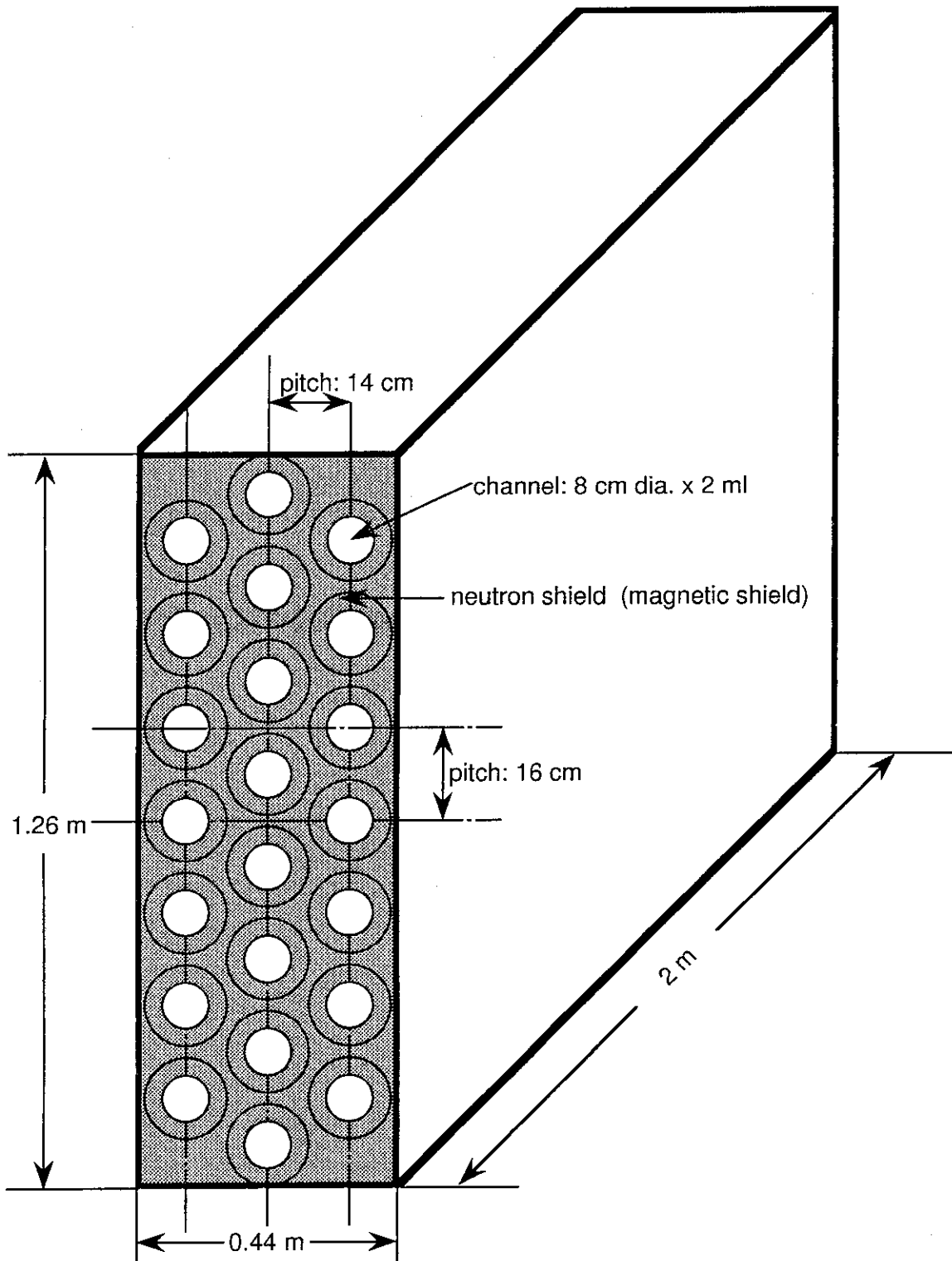


Fig.3-11 An illustration of the neutralizer  
(Short Beamline Option)

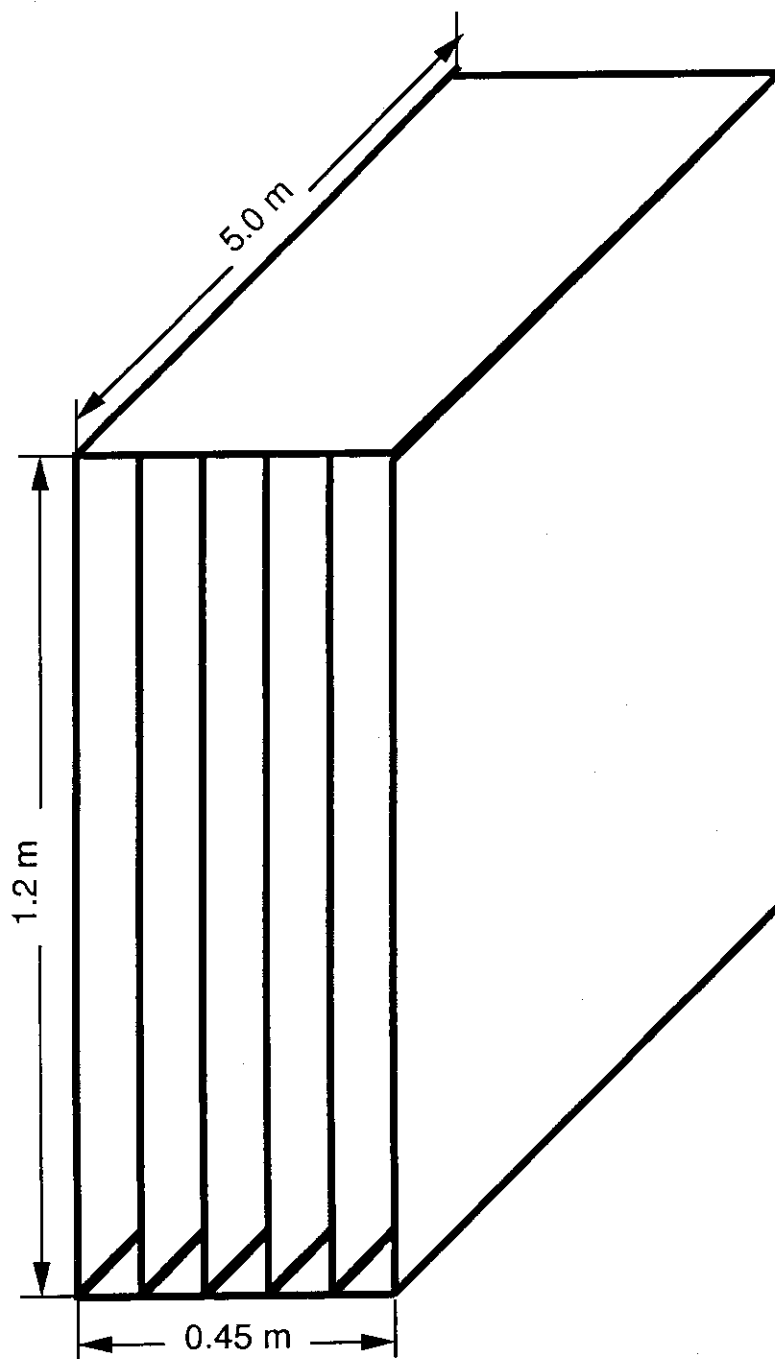


Fig.3-12 An illustration of the neutralizer  
(Long Beamline Option)

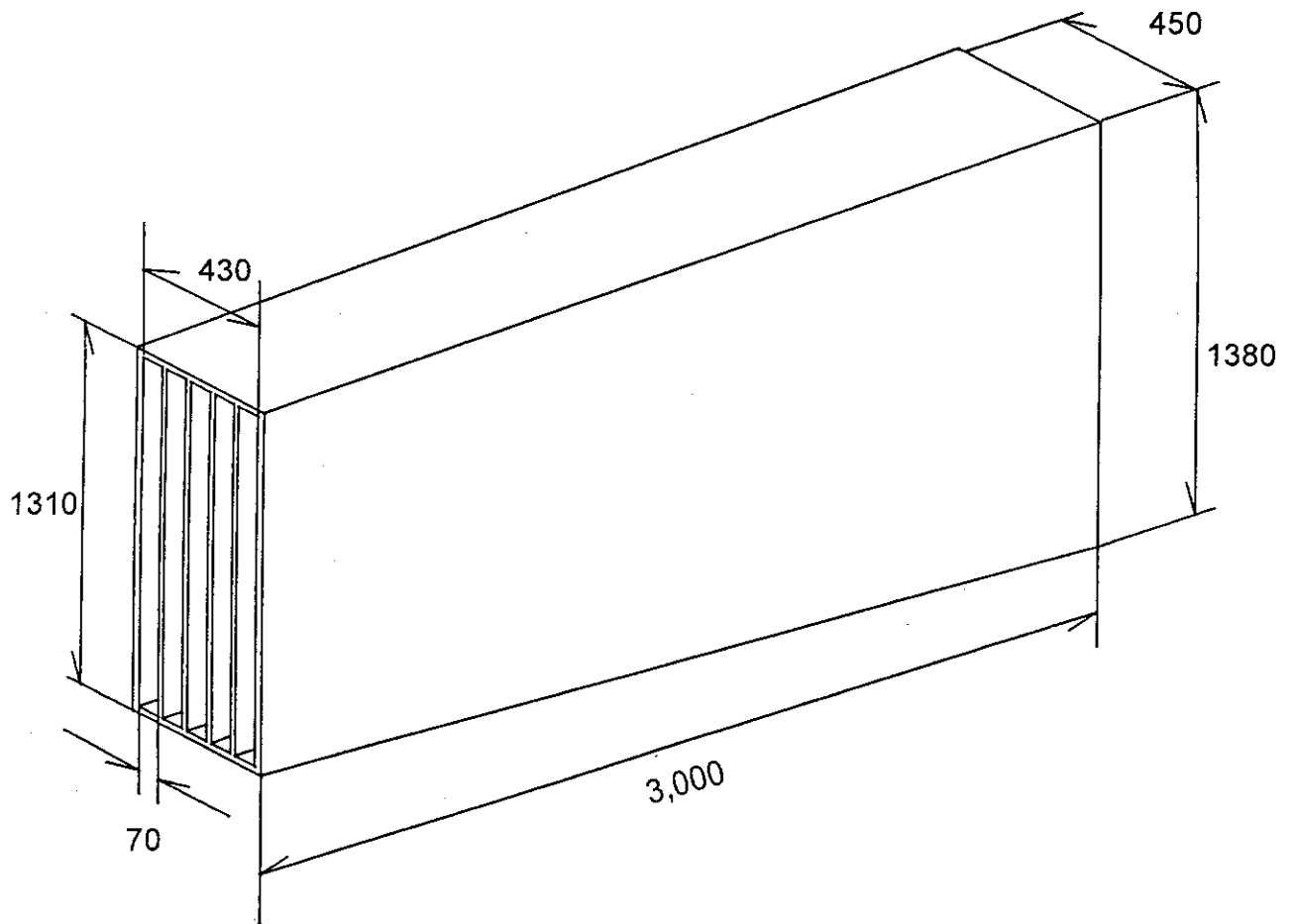


Fig.3-13 A bird's-eye view of the neutralizer  
(Long Beamline Option II)

### 3.8 Magnetic Shield

Stray magnetic field from the ITER tokamak may affect the trajectories of  $D^+$  ion beams, resulting in a power loss and a damage of beamline components. To avoid the distortion of the beam, magnetic shield is needed especially for the ion source/accelerator and the neutralizer.

The stray field from the ITER tokamak was estimated using a 3D magnetic field calculation code, "MAGIC" [1]. Plasma current and PF coil currents change during the burn. The stray fields were estimated at SOB (start of burn), EOB (end of burn) and the middle between SOB and EOB. The stray magnetic field from the ITER is summarized in Table 3-4 for the long beamline option II. The field strength distributions on the axis of beamline are shown in Fig. 3-14 and Fig. 3-15 for the short beamline option and the long beamline option. The results show that the field strength at the neutralizer is about 1200 ~ 1600 Gauss in the short beamline option, 450 ~ 800 Gauss in the long beamline option. It is confirmed that the direction of stray fields is almost vertical in both options.

In the present design, a triple layered passive magnetic shield is proposed. Neutron shield (made of mild steel) and vacuum vessel (made of mild steel) are used as the magnetic shield. This is illustrated in Fig. 3-16 for the long beamline option II. The thickness of the outer magnetifc shield is assumed to be 70 cm and the thickness of the inner shield, i.e. the vacuum vessel, is assumed to be 20 cm.

The residual magnetic field along the beam axis was estimated as the same manner in Ref. [2], where the magnetic shield is regarded as a double cylindrical shell.

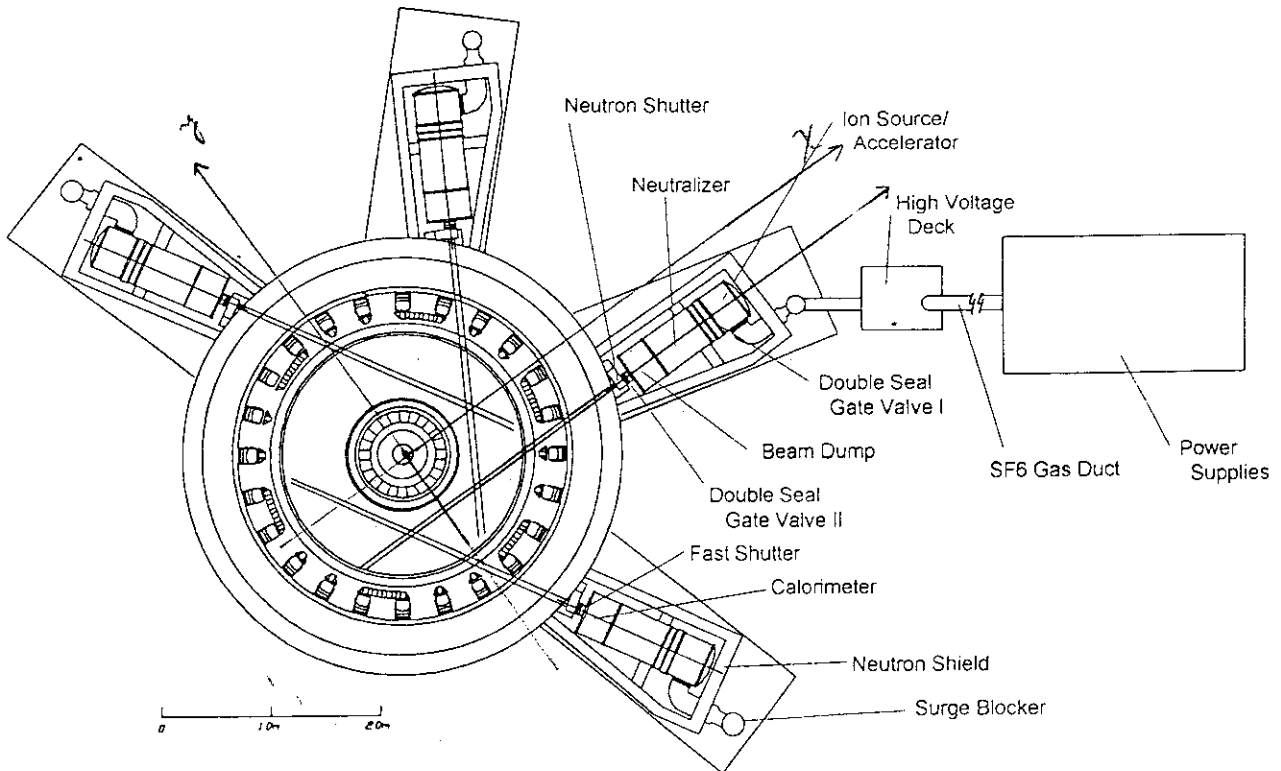
Figure 3-17 shows teh residual magnetic field for the long beamline option II. The field is 0.14-0.24 Gauss in y-direction, and 0.01-0.68 Gauss in z-direction in the neutralizer cell. The field in the ion source/accelerator is 0.04-0.1 Gauss in y-direction, and 0.5-0.9 Gauss in z direction. The beam steering angles due to these residual magnetic fields are 1.25 mrad (z-direction). It was confirmed that triple shell structure is enough for the magnetic shielding.

#### References

- [1] MAGIC: Magnetic field analysis by integral computation, ELF Co.Ltd
- [2] S. Tanaka et al.; JAERI-M 82-140, 1982. (in Japanese)

Table 3-4 Stray magnetic field from the ITER  
(at EDB,  $y = 6.246\text{m}$ ,  $z = 1.325\text{m}$ )

	Distance from the center of the tokamak (m)	x (m)	Stray field (Gauss)		
			Bx	By	Bz
the middle of the ion dump	24.8	24.6	-400	100	900
exit of the neutralizer	25.8	25.0	-320	80	810
the middle of the neutralizer	28.2	27.5	-190	40	630
entrance of the neutralizer	30.7	30.0	-120	20	490
Grounded Grid	32.1	31.5	-90	18	430
Plasma Grid	32.8	32.2	-85	16	400





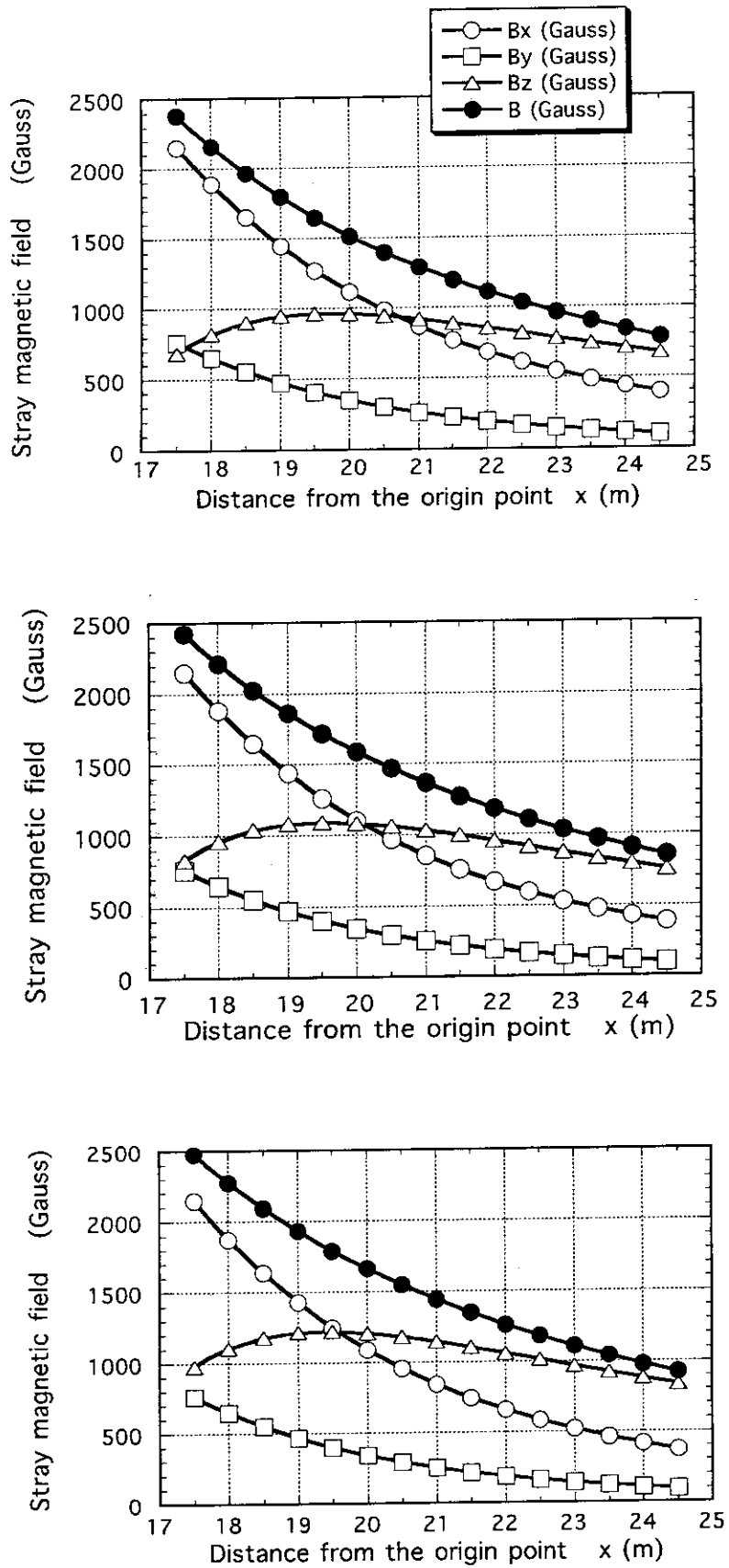


Fig.3-14 Distributions of the magnetic stray field strength along the axis of the beamline (Short Beamline Option)

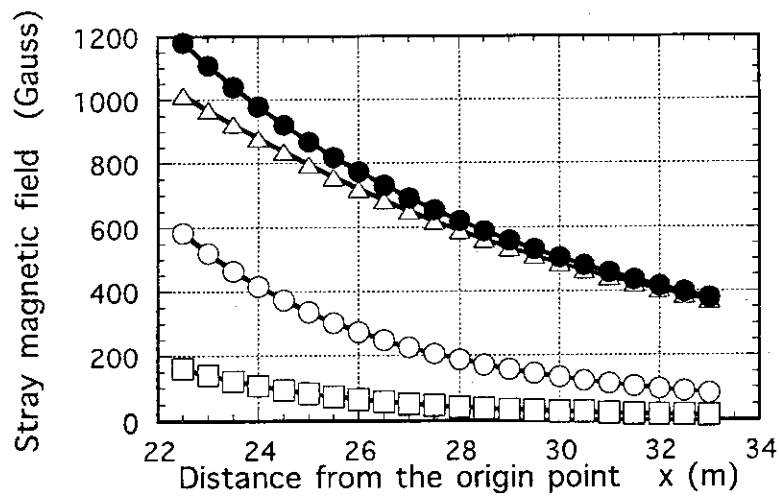
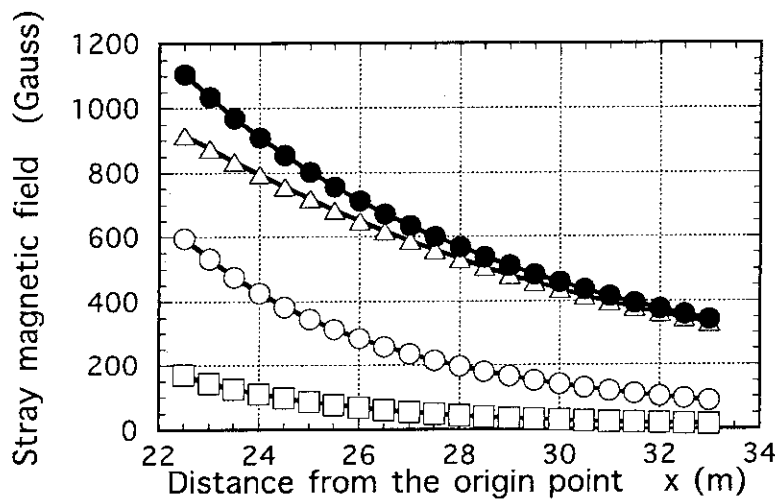
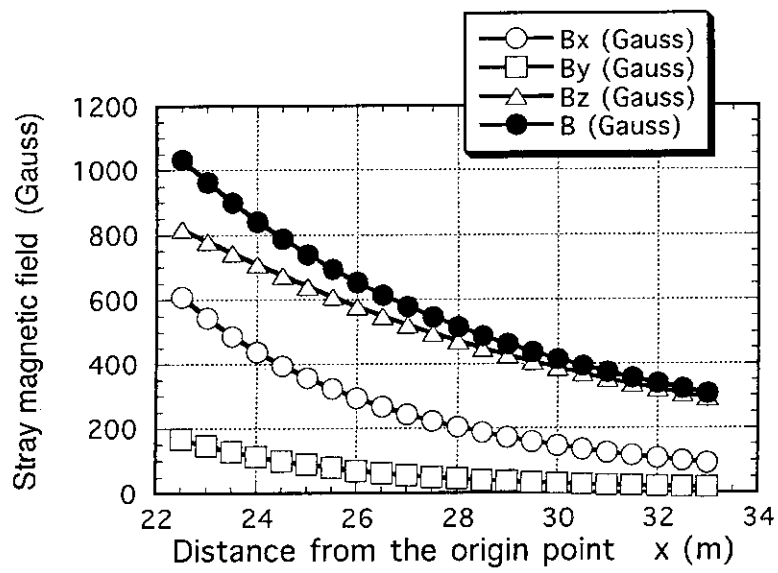


Fig.3-15 Distributions of the magnetic stray field strength along the axis of the beamline (Long Beamline Option)

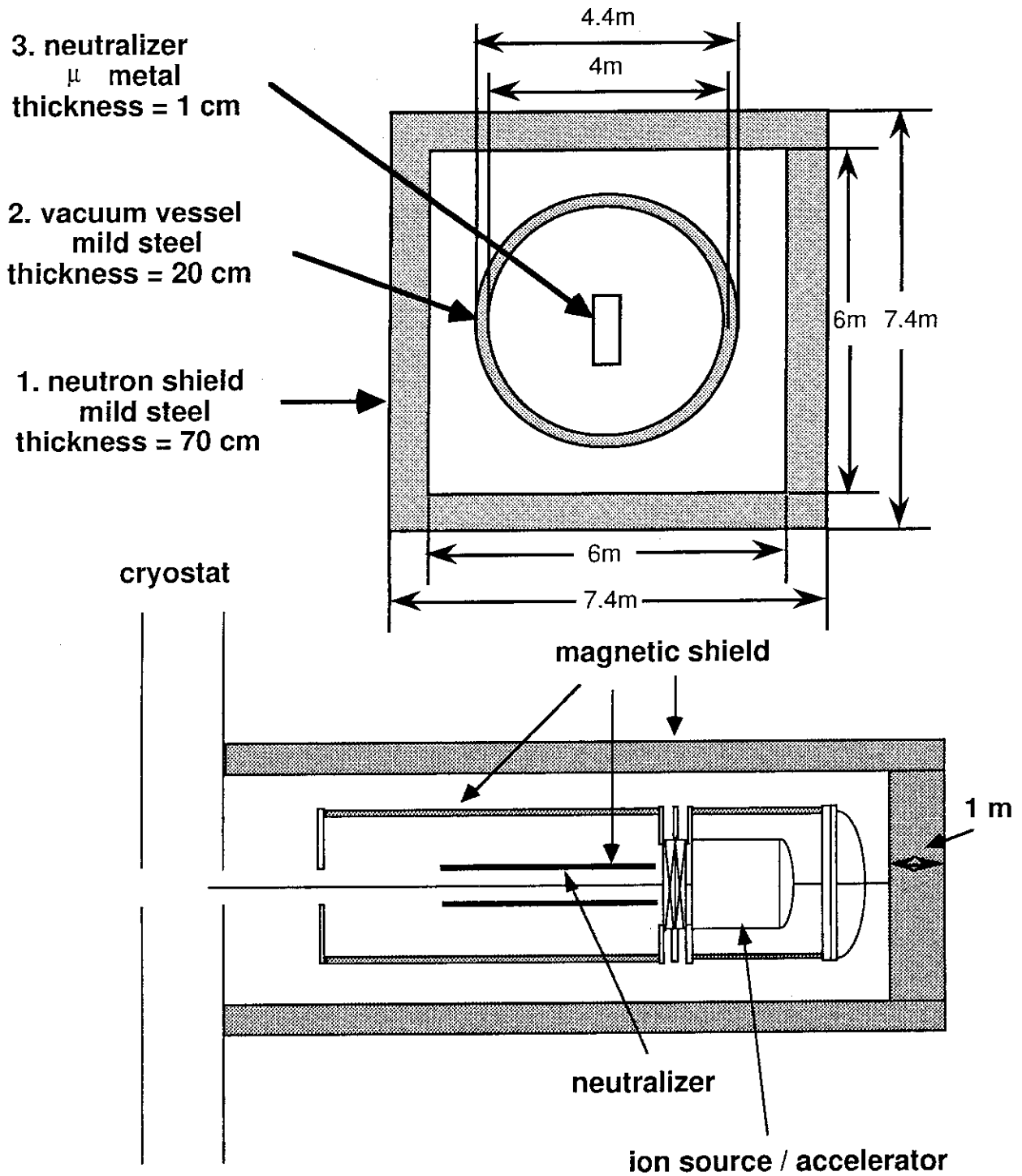


Fig.3-16 Magnetic shield in the Long Beamline Option II)  
 (Triple Shell Model)

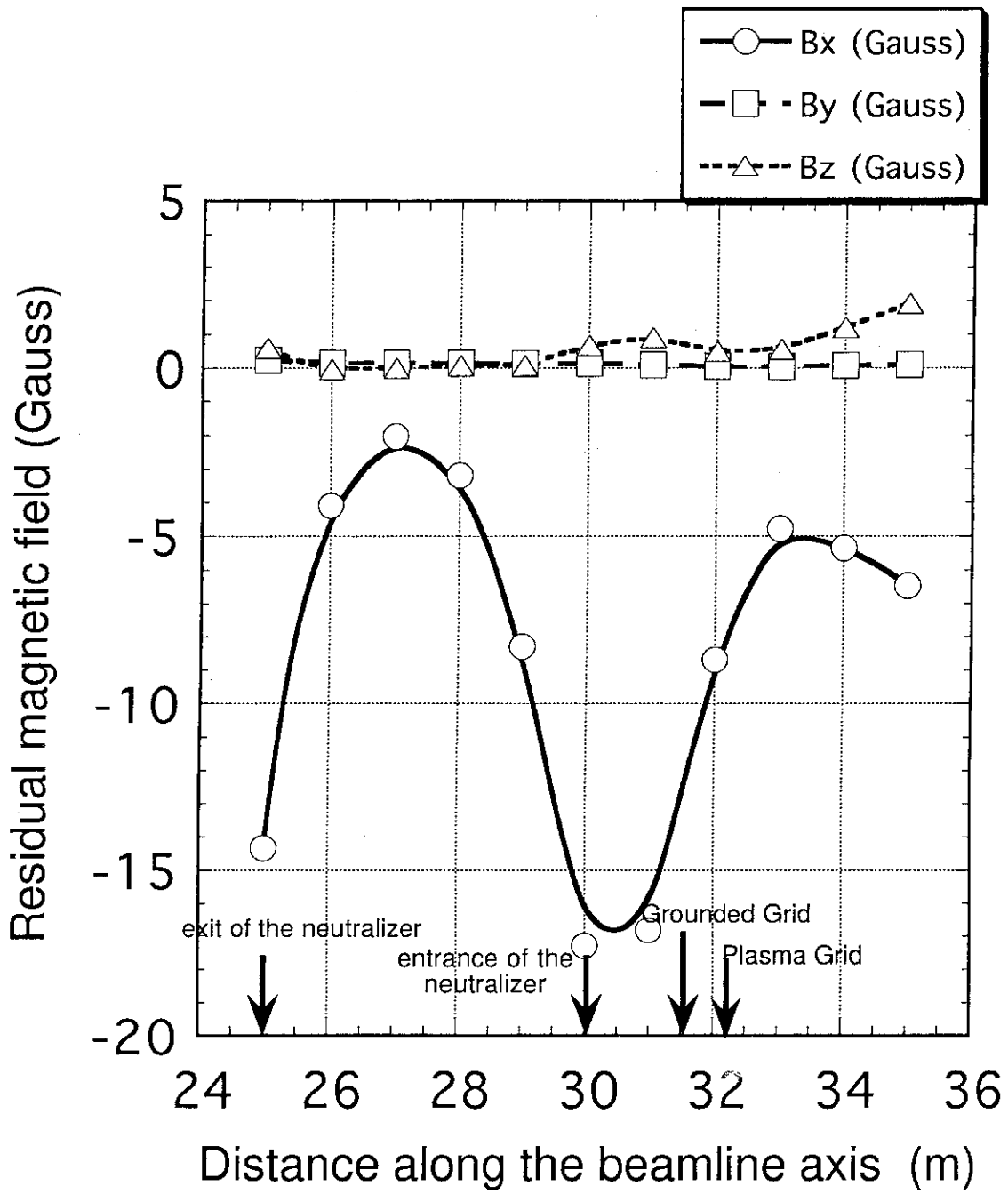


Fig.3-17 Residual Magnetic Field in the beamline  
 (Long Beamline Option II, Triple Shell Model)

### 3.9 Ion Deflector

The  $D^+$  and  $D^-$  ions with an energy of 1MeV, which are not converted to neutrals in the gas neutralizer, are deflected by an ion deflector. The residual beam power of 4.5 MW for each ions is dissipated on the beam dump. In designing the ion deflector, the following conditions are considered.

- (1) Due to the spatial limitation, the beam dump is 1.7 m in length and 1.5 m in height, and the distance between the positive ion dump and the negative ion dump is 0.5 m.
- (2) The stray magnetic field in the ion deflector region is about 1 kGauss.

From these considerations, three types of the ion deflectors, i.e. a magnetic deflector using a large coils, a magnetic deflector using the stray field, and an electrical deflector are considered. Figure 3-18 shows the coordinates used for explanation.

#### Magnetic Deflector Using Large Coils

The residual beams are deflected by a pair of coils placed at the exit of the neutralizer as shown in Fig.3-19(a). The magnetic field of 1.2 kGauss along the Z-axis is needed for guiding the ions to the beam dump. This field can be created by the following coils.

Geometory	:1.7 m x1.5 m
Distance between coils	:1.7 m
Ampere turn	:280 kAT

By the magnetic field created by these coils, the residual ions are deflected and impinged on the area of  $0.35 \text{ m} < X < 1.2 \text{ m}$ ,  $-0.6 \text{ m} < Z < 0.6 \text{ m}$  within the beam dumps. The incident angle is 30 degree.

The required magnetic field is so strong that it seems to be difficult to find a spece for installing these coils in the short beamline option. In the long beamline option, on the other hand, there is enough spece for installing the coils. In addition, the ampere turn can be reduced by designing the beam dump longer than the present design. Hence, this type of the ion deflector is suitable for the long beamline options.

Figure 3-20 shows an example of the calculation of the magnetic deflection for the beamline option II. This field is created by the following condition;

The coil geometry	: 1m x 2.5m
Distance between coils	: 4m
Ampere turn	: 1 MAT
Magnetic field	: about 1 kGauss

### Magnetic Deflector Using the Stray Field

The stray fields are  $B_y=0.5$  kGauss,  $B_z=1.0$  kGauss in the short beamline option, and  $B_y=0.15$  kGauss,  $B_z=0.5$  kGauss in the long beamline options. In the short beamline option, the beams are deflected and impinged on an area of  $0.80 \text{ m} < X < 1.5 \text{ m}$ ,  $-0.53 \text{ m} < Z < 0.83 \text{ m}$  within the beam dumps. Even in the long beamline option, the beams can be sufficiently deflected by using auxiliary coils that can create the magnetic field of 0.5 kGauss in z direction.

### Electrical deflector

Figure 3-19(c) shows the conceptual diagram of the electrical deflector. The residual beams are electrically deflected by the parallel deflection electrodes. Figure 3-21 shows an example of the calculation of the electrical deflection. The conditions are;

Deflection voltage	: $\pm 10$ kV
length of the deflection electrode	: 300mm
Spacing distance	: 90mm

Advantages and disadvantages of the three deflectors are summarized in Table 3-5.

Table 3-5 Comparison of three types of ion deflector

Type of deflector	advantage	disadvantage	comment
Magnetic deflector using a pair of coils	<ul style="list-style-type: none"> <li>- Heating area is small.</li> <li>- Deflector can be controlled independent of the reactor.</li> </ul>	<ul style="list-style-type: none"> <li>- Large coils are necessary.</li> <li>- Magnetic shield is thicker.</li> </ul>	<ul style="list-style-type: none"> <li>- Suitable type of the beamline is long beamline.</li> </ul>
Magnetic deflector using the stray field	<ul style="list-style-type: none"> <li>- Magnetic shield is unnecessary.</li> <li>- Deflector is unnecessary.</li> </ul>	<ul style="list-style-type: none"> <li>- Heating area is large.</li> <li>- Operation of the deflector depends on that of the reactor.</li> </ul>	<ul style="list-style-type: none"> <li>- Suitable type of the beamline is short beamline.</li> </ul>
Electrical deflector	<ul style="list-style-type: none"> <li>- Heating area is small.</li> <li>- Deflector can be controlled independent of the reactor.</li> </ul>	<ul style="list-style-type: none"> <li>- High voltage system is necessary.</li> <li>- Thick magnetic shield is necessary.</li> <li>- Heat load of the ion dump is high.</li> </ul>	<ul style="list-style-type: none"> <li>- Suitable type of the beamline is long beamline.</li> </ul>

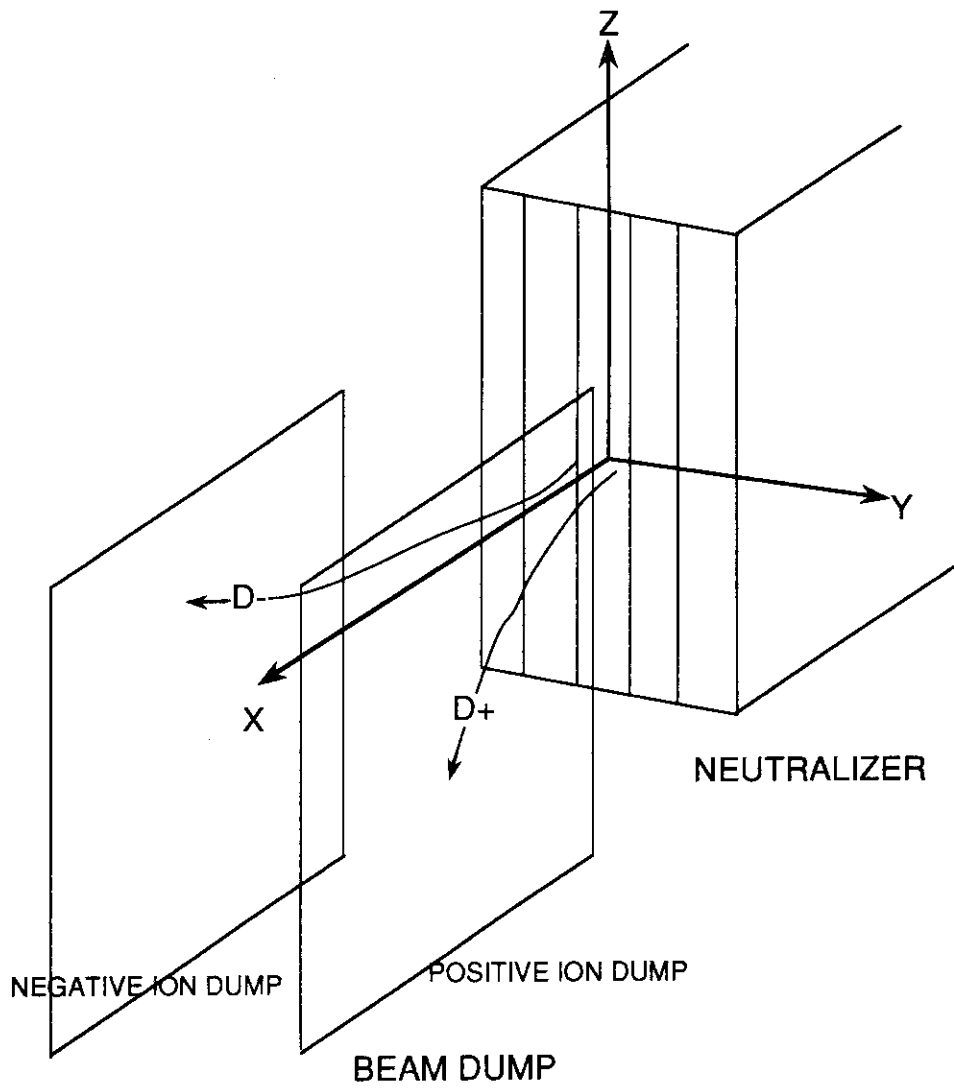
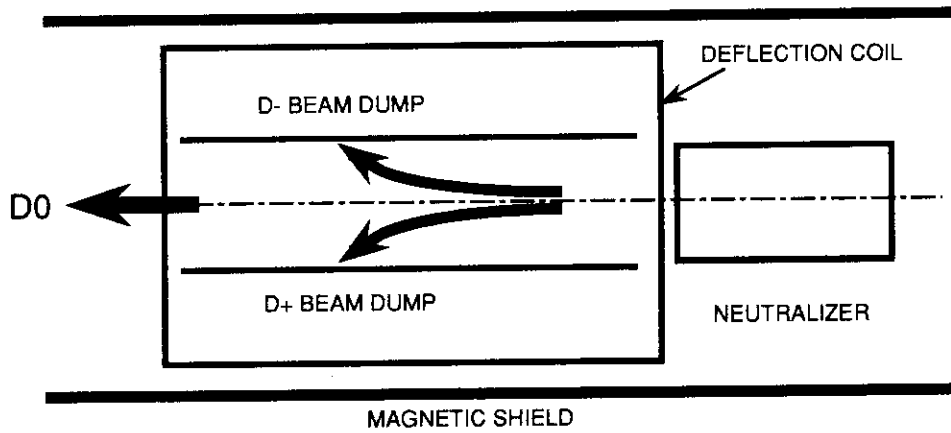
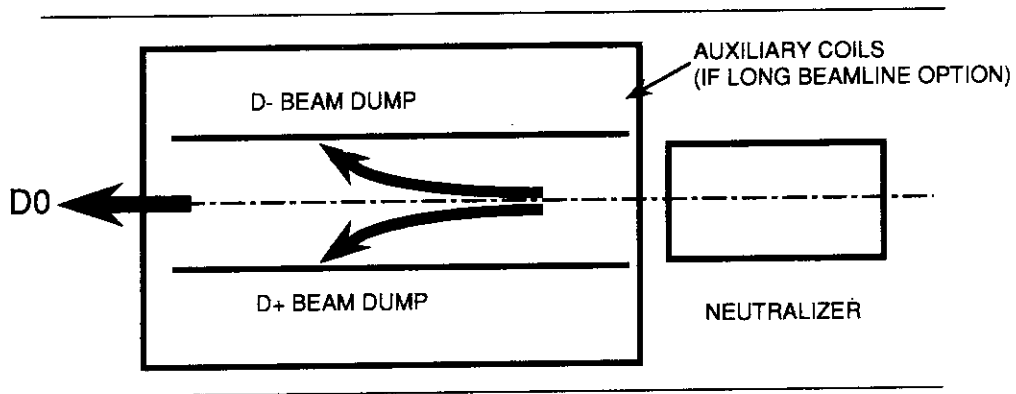


Fig.3-18 Coordinates for explaining the direction of the residual ions

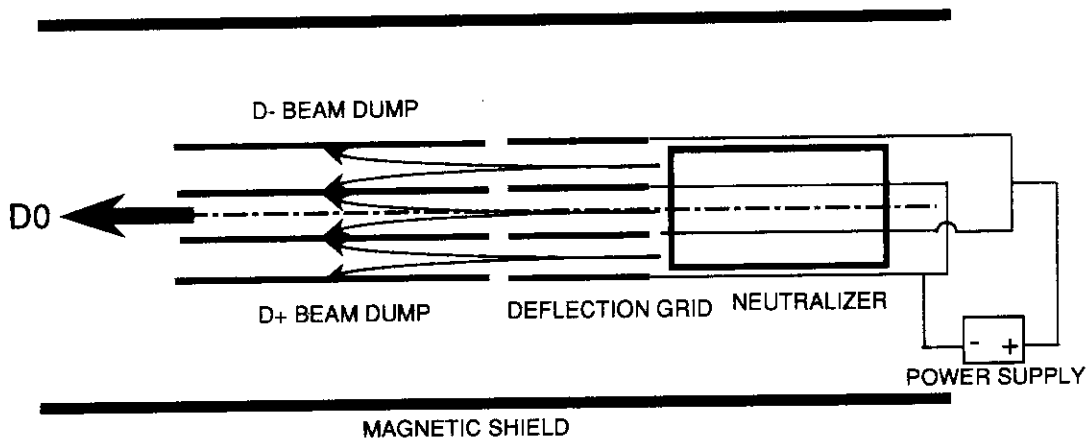




(a) Magnetic deflector using a pair of coils



(b) Magnetic deflector using the stray field



(c) Electrical deflector

Fig.3-19 Conceptual diagram of three ion deflectors

### calculation conditions

- D+/D- residual ion current density :  $5.87 \exp(-r^2/R^2)$  (R; beam divergence 13.5mm)
- initial energy : 1 MeV
- X-Y 2 dimation : 40
- number of beam : 1000mm(wide)x2500(long), spacing 4000mm
- coil geometry : ampere turn 1MAT

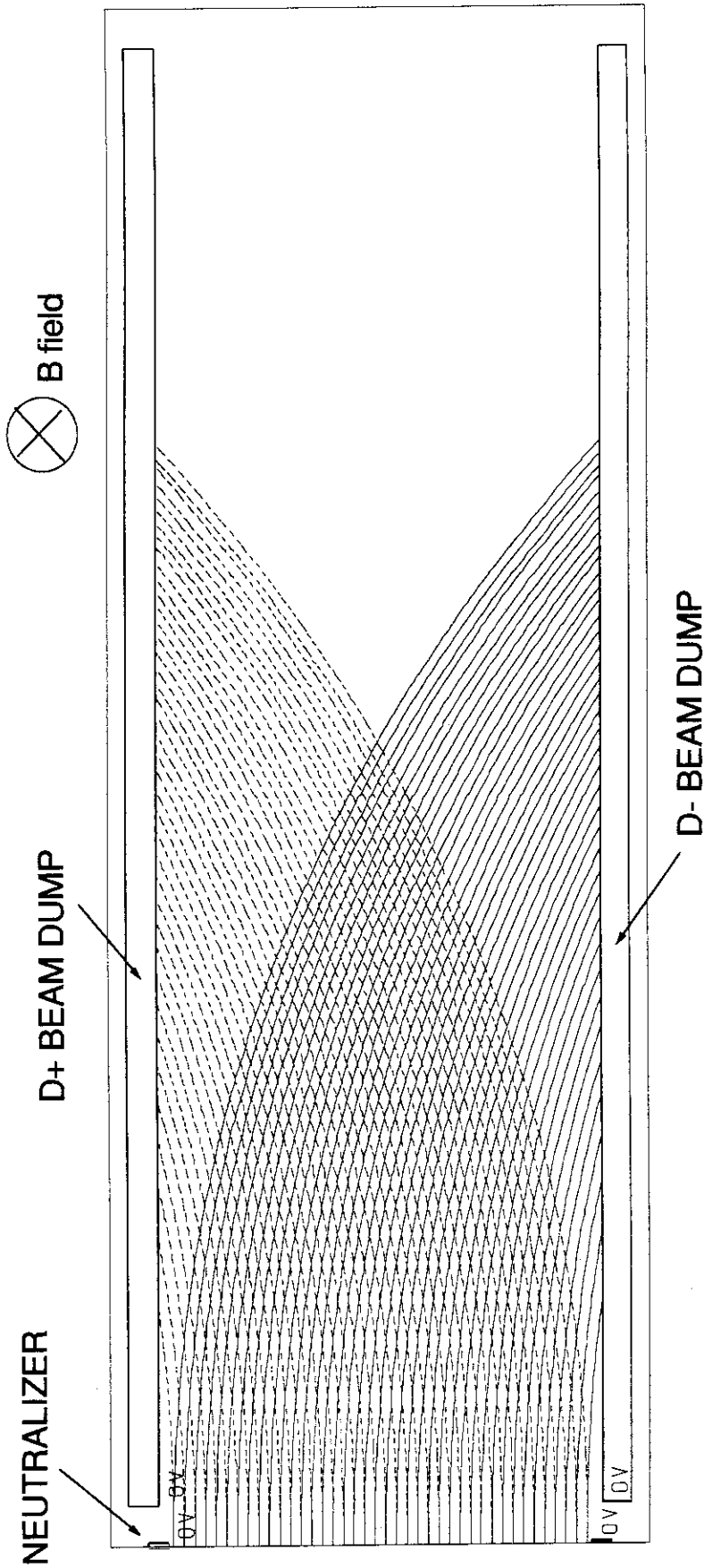


Fig.3-20 An example of the calculation of the magnetic deflection

calculation conditions

- D+/D- residual ion current density :  $5.9 \exp(-r^2/R^2)$  (R; beam divergence 13.5mm)
- initial energy : 1MeV
- X-Y 2dimension : each 30
- number of beam : +10kV
- supplied voltage

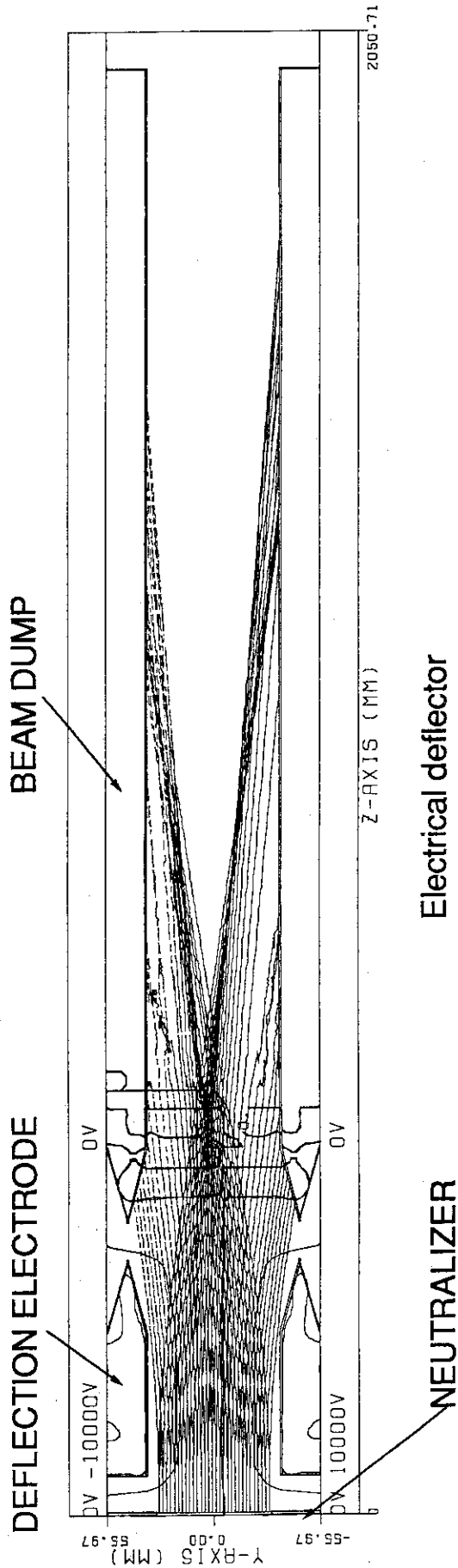


Fig.3-21 An example of the calculation of the electrical deflection

### 3.10 Ion Dump and Calorimeter

In the long beamline option II, the peak heat flux of each residual ion is;

$$28 \times 3 \times 0.2 / (1.35^2 \times 3.14) = 2.94 \text{ kW/m}^2$$

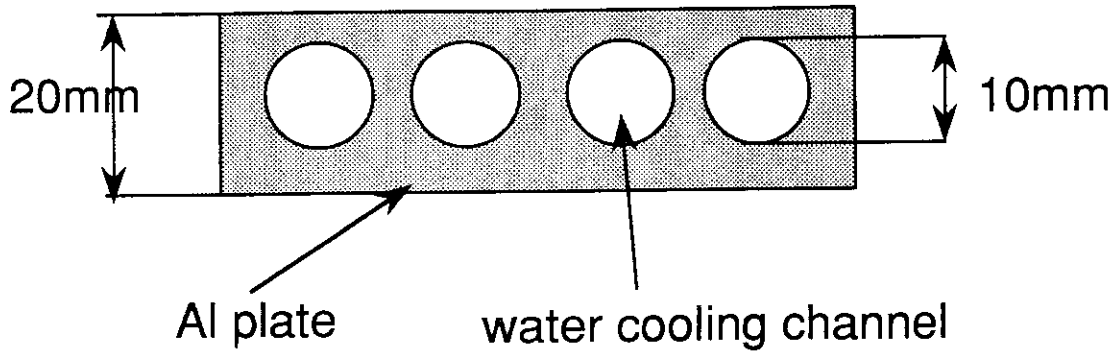
Here, the beam divergence is assumed 3 mrad and three beamlets, each of which has a power of 28kW, is converged.

Figure 3-22 (a) shows the design of the cooling channels of the beam dumps for the electrostatic deflector. The ion dump is sub-divided into 5 channels correspond to the sub-divided neutralizer and ion deflector channels. Since the incident angle of the beam is 40 mrad, the peak heat flux is reduced to 0.12 kW/cm<sup>2</sup> at the beam dump surface. This heat flux can be handled by a thin plate as shown in the figure.

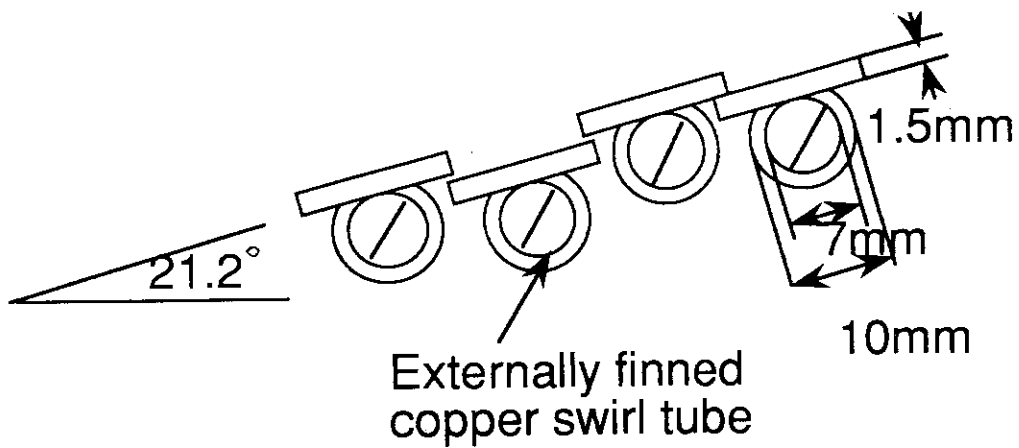
The beam dump for the magnetic deflector is installed with an angle of 21.2 degree against the beam axis. Since the magnetic deflection angle is 30 degree, the incident angle to the beam dump surface is 9.8 degree. It gives the peak heat flux of 1 kW/cm<sup>2</sup>. The beam dump is designed using an externally finned swirl tube, as shown in Fig. 3-22 (b), which has been tested at JAERI to demonstrate the heat loading of 3-4 kW/cm<sup>2</sup> [1].

The calorimeter is also sub-divided in the long beamline option II. Opening of each channels are 8cm in width and 120cm in height. The length is 80cm. Since the Incident angle of the beam is 100 mrad, the peak heat flux at the surface is 0.82 kW/cm<sup>2</sup>. The cooling panels are made of externally finned swirl tubes [1]. The calorimeter moves horizontally when the neutral beam is injected into the plasma.

[1] M. Araki, et al.; Journal of The Japan Society of Mechanical Engineers, vol. B (1991) p.415



(a) using the electrostatic deflector



(b) using the magnetic deflector

Fig.3-22 Cooling channels of the beam dump  
(Long Beamline Option II)

### 3.11 Cryopump

The pumping speed required for the cryopumps and the gas flow rates are;

Source Chamber :137 m<sup>3</sup>/s, 2.75 Pa.m<sup>3</sup>/s (Short BL)  
 :554 m<sup>3</sup>/s, 11.08 Pa.m<sup>3</sup>/s (Long BL)  
 :710 m<sup>3</sup>/s, 14.6 Pa.m<sup>3</sup>/s (Long BL II)

Beam Dump Chamber :685 m<sup>3</sup>/s, 1.31 Pa.m<sup>3</sup>/s (Short BL)  
 :1425 m<sup>3</sup>/s, 2.85 Pa.m<sup>3</sup>/s (Long BL)  
 :2578 m<sup>3</sup>/s, 5.19 Pa.m<sup>3</sup>/s (Long BL II)

To extend the regeneration period of the cryopump, steady state cryopump is installed in the source chamber, where the required pumping speed is not large but a large amount of gas flow rate should be handled. Figure 3-23 shows a conceptual design of the steady state cryopump. The pump has a shutter, by which the pump can be regenerated while other cryopumps are operational. The pumping speed per opening area is designed as 175 m<sup>3</sup>/s m<sup>2</sup>. Therefore, the opening areas of the cryopumps are 0.78 m<sup>2</sup>, 3.17 m<sup>2</sup>, and 4.06 m<sup>2</sup> for the three options, respectively.

The cryopump installed in the beam dump chamber is a conventional panel type. The pumping speed per cryopanel area is 64 m<sup>3</sup>/s m<sup>2</sup>. The required areas are 10.7m<sup>2</sup>, 22.3 m<sup>2</sup>, and 40.3 m<sup>2</sup> for three options.

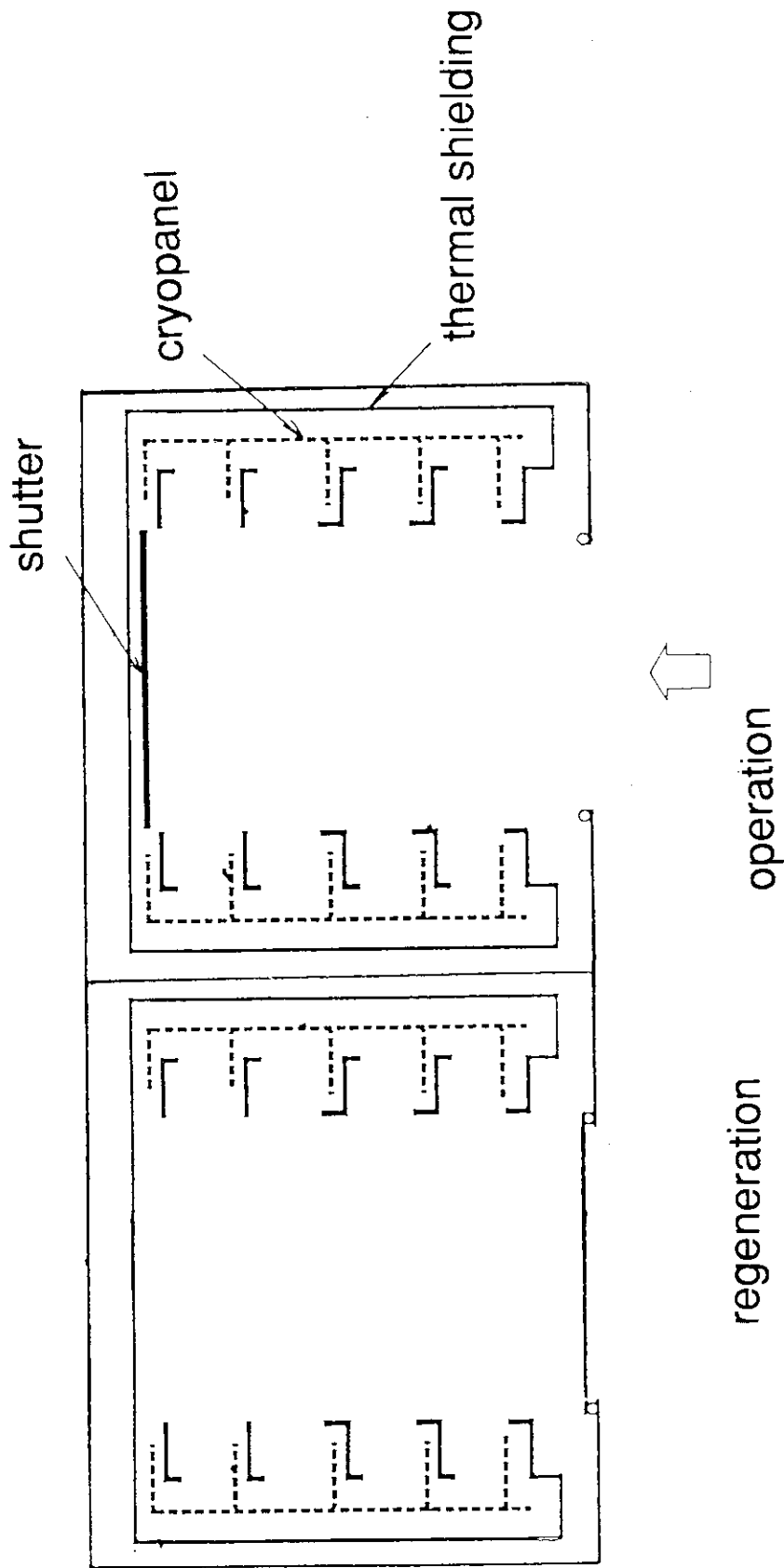


Fig.3-23 Conceptual diagram of the steady state cryopump

### 3.12 Double Seal Gate Valve

#### Functions

The double gate valve is composed of two metal seal valves, and closed to intercept particle flows including tritium gas and activated dust between the beamline and the reactor. They are always open during the reactor operation, and closed in the following events;

1. Vacuum leak in the beamline or in the reactor (water leak, etc.)
2. Vacuum leak test in the beamline
3. Maintenance of the beamline without a vent of the reactor
4. Regeneration of the cryopanel

#### Requirements

Vacuum seal	:metal seal
Leak rate	: $< 1 \times 10^{-8}$ Pa.m <sup>3</sup> /s
Breakout temperature	:200 C
Opening	:1800 mm in height x 600mm in width
Pressure difference	:1 bar( The valve plate is never exposed to the abnormal pressure of 20 bar, since the valve is always open during the reactor operation.)
Open/close time	:< a few seconds
Thickness of the shutter	:Enough to shield $\gamma$ rays from the reactor and the NBI duct ( biological shield $<25 \mu$ Sv/h)

#### Design

The structure of the metal seal is based on the design described in the reference [1], where a couple of rectangular diaphragm rings with a differential pumping system between them are used. In the present design, however, a rectangular thin plate ring is used instead of the diaphragm, so that large rectangular bellows can be eliminated. An outline drawing is shown in Fig. 3-24.

One of the gate valves on the reactor side has a capability to shield  $\gamma$  rays from the NBI port and the reactor. The thickness will be  $\sim 1$ m for the biological shield. The gate valve



on the NBI side has a capability to shield  $\gamma$  rays from the beamline. The thickness required will be  $\sim 0.5$ m. The total thickness will be about 1.5 m, but accurate evaluations is required.

[1] H. Ishikawa, et al., "All aluminum alloy, 800-mm-inner diameter gate valve using dual flat-face seals together with differential pumping", J. Vac. Sci. Technol. A3(3), (1985) p.1703.

### 3.13 Fast Shutter

#### Functions

1. To reduce the gas load on the beamline cryopump due to the outflow of the reactor gas filled before the plasma ramp-up and after the plasma ramp-down and also the plasma disruption. As a result, tritium accumulation in the beamline can be reduced.
2. To reduce the gas flow from the beamline to the reactor during the conditioning.
3. To intercept sputtered particles from the reactor to the source

#### Requirements

Opening	:600 mm x 1800mm
Open/close time	:<1 s
Gas conductance	:<<opening; e.g. 0.01 m <sup>3</sup> /s
Life	:10 <sup>5</sup> ( > 1000 shots x 10 times x 10 years )

#### Design

The fast shutter of the JT-60 NBI is 600 mm in opening diameter, and the thickness is 220 mm. The open/close time is less than 1s. The fast shutter for the ITER NBI is same as that of the JT-60 NBI, but the thickness will be about 300 mm.

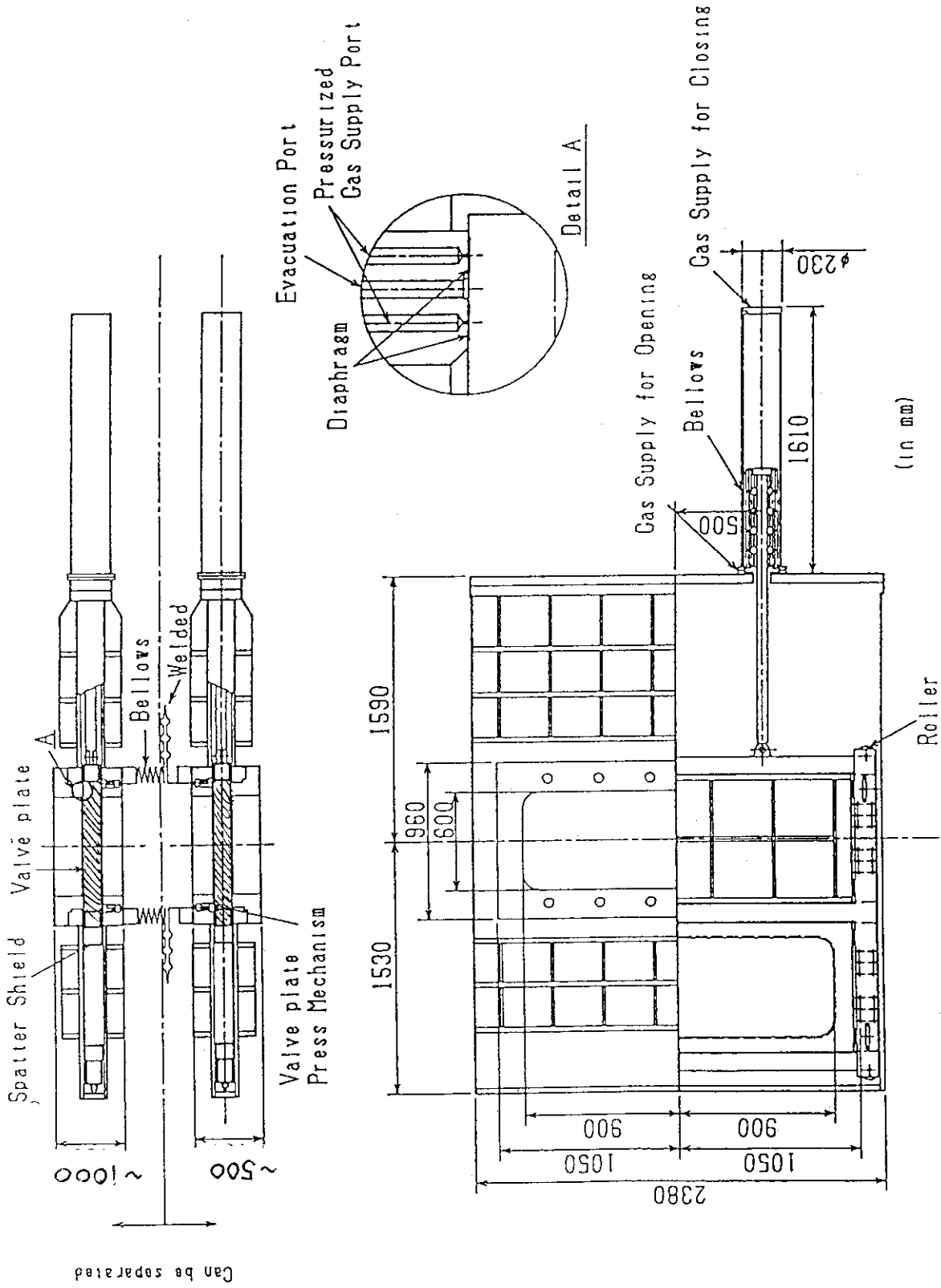


Fig.3-24 Large metal seal gate valve.

### 3.14 Bellows

A formed circular bellows is mounted in the NBI port. The bellows has to be designed so as to absorb a lateral movement of  $\pm 25\text{mm}$ , which occurs in the cool down phase of the SC coils. In addition, the bellows has to withstand against 20 bars in case of the accident.

Figure 3-25 shows a design of the bellows that satisfies these requirements. There is an external cylindrical limiter around the bellows. The buckling will occur above 7.5 bar, but the bellows will not be broken by the over pressure of 20 bar owing to the limiter. After the over pressure accident, the bellow need to be replaced.

#### Design

Type	: Formed Bellows
Movement	
Axial	: $\pm 5\text{mm}$
Lateral	: $\pm 25\text{mm}$
Angle	: $\sim 0$
Temp.	: 100 C
Material	: sus 304
Thickness of bellows	: 1.5 mm
Buckling pressure	: 7.5 bar
Life	: 17,000 cycles

These numbers are estimated by Uno Kogyo Co. Ltd., using Standards of the Expansion Joint Manufactureres Association, Inc.

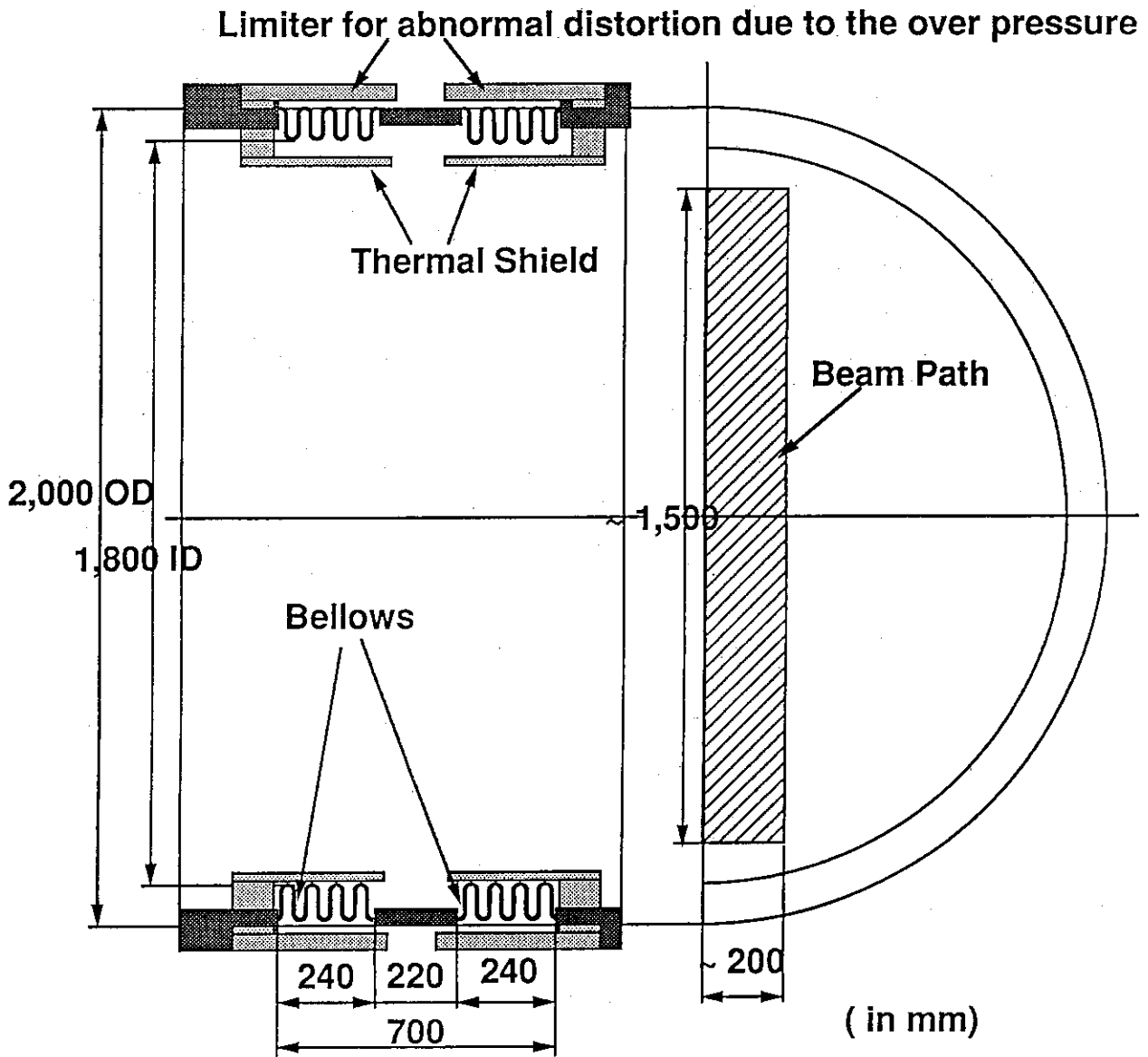


Fig.3-25 A conceptual design on the bellows which withstand 20 bar inner pressure.

### 3.15 High Voltage Power Supply

A schematic diagram of a power supply system is shown in Fig. 3-26. The power supply system consists of a source power supply and an acceleration power supply. A high frequency inverter system[1] is utilized in the 1MV acceleration power supply. Out put of the inverters are rectified and connected in series to obtain a DC high voltage of -1MV. High speed switching is performed by the inverters at AC side instead of DC switches. Out put voltage is also controlled by the inverters. Such system were already adopted in the acceleration power supplies of JEBIS[2] and JT-60 N-NBI[3]. In the JT-60 N-NBI system, three stages of inverters were adopted to produce -500 kV. Adding two stages of the inverters is required for the 1 MV system.

### 3.16 Surge Blocker

A surge blocker is one of the most important elements in the power supply to make a stable beam acceleration system. Newly developed magnetic cores whose name is FINEMET[4,5] (Fe Based Soft Magnetic Alloys Composed of Ultrafine Grain Structure) can be adopted. The core consists of rolled magnetic tape with insulation layer of  $\text{SiO}_2$ . The core has a saturation magnetic flux density of 1.35 T that is about 4 times higher value than that of a former ferrite core.

An insulating transformer of the source power supply has a big stray capacitance. Therefore, a surge suppression L-R is adopted to reduce a size of the surge blocker. The surge blocker is utilized to absorb the surge that comes from stray capacitance between the high voltage part and the ground of the insulated cable duct and the high voltage platform. The capacitance was roughly estimated to be 2600 pF. A resistor of 500 ohm is connected in a secondary circuit of the surge blocker to dissipate the surge energy. A twice higher value of the  $V \cdot s$  can be utilized with biasing current. The peak of the current can be suppressed to lower than 2 kA by the surge blocker whose capacity is 0.9 T ( $V \cdot s$ ). The required cores are 76 pieces. The dimensions of the core are 0.9 m in diameter and 3 m in length with insulators between the cores. An input energy to the accelerator was estimated to be smaller than 0.2 J by assuming that an arcing voltage is 100 V. Specifications of the surge blocker is shown in Table 3-6. Table 3-7 shows a comparison of surge blocker in three high voltage systems.

Table 3-6 Specifications of the surge blocker

Dimensions	:0.9 m in diameter , 3 m in length
Weight	:8 t
V.s	:0.9 V.s with biasing current
Surge Current	:< 2 kA
Surge Energy	:< 0.2 J

#### References

- [1] W.Praeg, Proc. 13th Symp. on Fusion Technology, Varese, Italy(1984)p.859.
- [2] M.Mizuno et al., Proc. 13th Symp. on Fusion Engineering, Knoxville, (1989)p.574.
- [3] NBI Facility Division and NBI Heating Lab., JAERI-M 94-072(1994) (in Japanese).
- [4] Y.Yoshizawa et al., "Fe-Based Soft Magnetic Alloys Composed of Ultrafine Grain Structure", Materials Transaction, JIM, vol.31, No.4(1990), pp.307-314.
- [5] S.Nakajima et. al., "Development of a surge blocker core using a material of Fe-Based Soft Magnetic Alloys Composed of Ultrafine Grain Structure", National Convention Record IEE Japan 14-58 (1991)(in Japanese).

Table 3-7 Comparison of surge blocker in high voltage systems

(FINEMET core)

	ITER NBI	MeV Stand	JT-60N-NBI
Voltage Current	1MV,35A	1MV,1A	500kV,64A
Stray C	* 2600pF	450pF	* 1000pF
Stored Energy	1300J	225J	125J
Surge Current	< 2kA	< 2kA	< 1kA
Input Energy	< 10J	(< 0.1J)	< 6J
Core Size (mm)	$\phi$ 900- $\phi$ 400x 25.4x76pcs	$\phi$ 900- $\phi$ 400x 25.4x13pcs	$\phi$ 900- $\phi$ 500x 25.4x30pcs
V.s with bias	0.9	0.14	0.3
Weight of SB	8 t	1.5 t	3.5 t

\*Stray C of the HV platform and cable duct. Stored energy at other parts should be dissipated by surge suppression L-Rs.

(Stray C at each accelerator gap and stored energy are estimated to be about 1050 pF and 21J, respectively.)

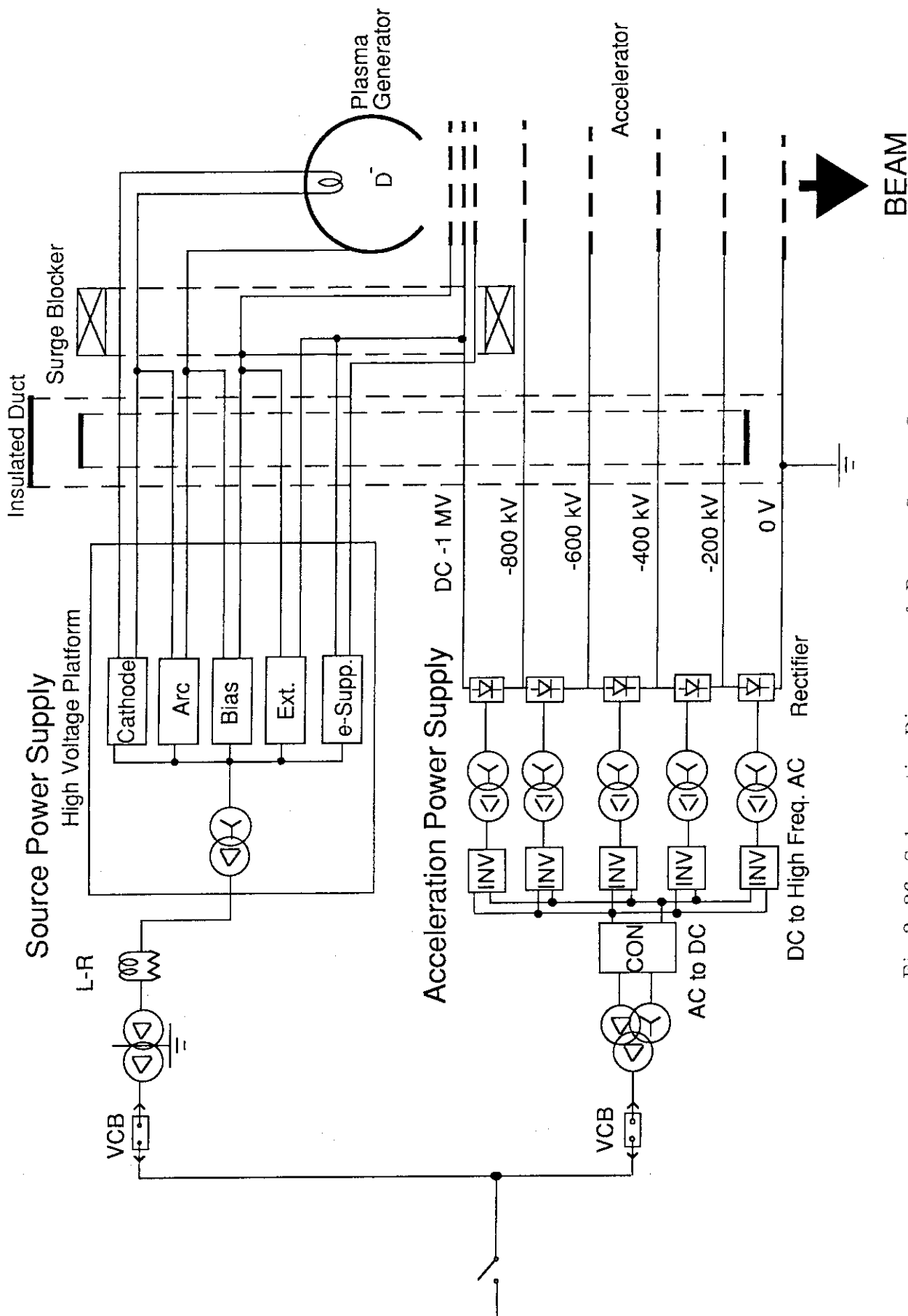


Fig.3-26 Schematic Diagram of Power Supply System



### 3.17 Maintenance

Regular maintenance is required for the ion source and accelerator possibly once or twice per year depending on the cathode life, replenishment of cesium to the source and removal of cesium from the accelerator. On the other hand, the beamline components require no regular maintenance, since they are designed and manufactured based on the sophisticated technology and thought to be reliable. However, maintenance procedures of the beamline unit (B/L) are also studied together with the ion source unit including the accelerator (I/S) for two options; the short beamline option and the long beamline option. The maintenance procedures are based on the following principles;

1. In-situ repair of the components should not be considered in principle. Every component in the units is repaired in the hot cell.
2. At the time of transportation of the unit, the activated dust and tritium should be confined within the unit.
3. Every unit is removed or installed by remote handling.
4. To minimize the termination period of the reactor due to the maintenance, the unit is replaced with a spare one.

In the short beamline option, a double gate valve is mounted between I/S and B/L. Hence, I/S can be replaced without the vent of the reactor vacuum vessel. However, no gate valve can be installed between the reactor vessel and B/L because of the limited area for B/L. Every component in B/L is regarded as one of the in-vessel components, and its replacement needs the vent of the reactor vessel, which may interfere with the reactor operation considerably. Additionally, a large cask with a double door system [1] will be required to remove B/L. Fortunately, the replacement of B/L will be possible only from the beamline side and not from the reactor vessel, and hence will be easier compared to the replacement of the in-vessel components like the RF antenna and the divertor plate. The maintenance procedures of I/S and B/L are shown schematically in Fig.3-27 and 3-28, respectively.

In the long beamline option, the entire beamline including the ion source and accelerator is located outside the cryostat and connected to the injection port of the reactor via a double gate valve. Therefore, they can be separated from the reactor without the vent of the reactor vessel. The maintenance procedures of I/S and B/L are shown schematically in Fig. 3-29 and 3-30, respectively.

In summary, the ion source unit can be replaced easily without the vent of the reactor in

either option. The beamline unit in the short option can not be replaced easily since it needs a large containment cask with a double door system and the vent of the reactor vessel. However, the beamline unit in the long option can be exchanged as easily as the ion source unit. From the maintenance point of view, the long beamline option is superior to the short beamline option.

#### References

- [1] T. Honda et al.; ITER Documentation Series No.34, IAEA/ITER/DS/34, IAEA, Vienna (1991).

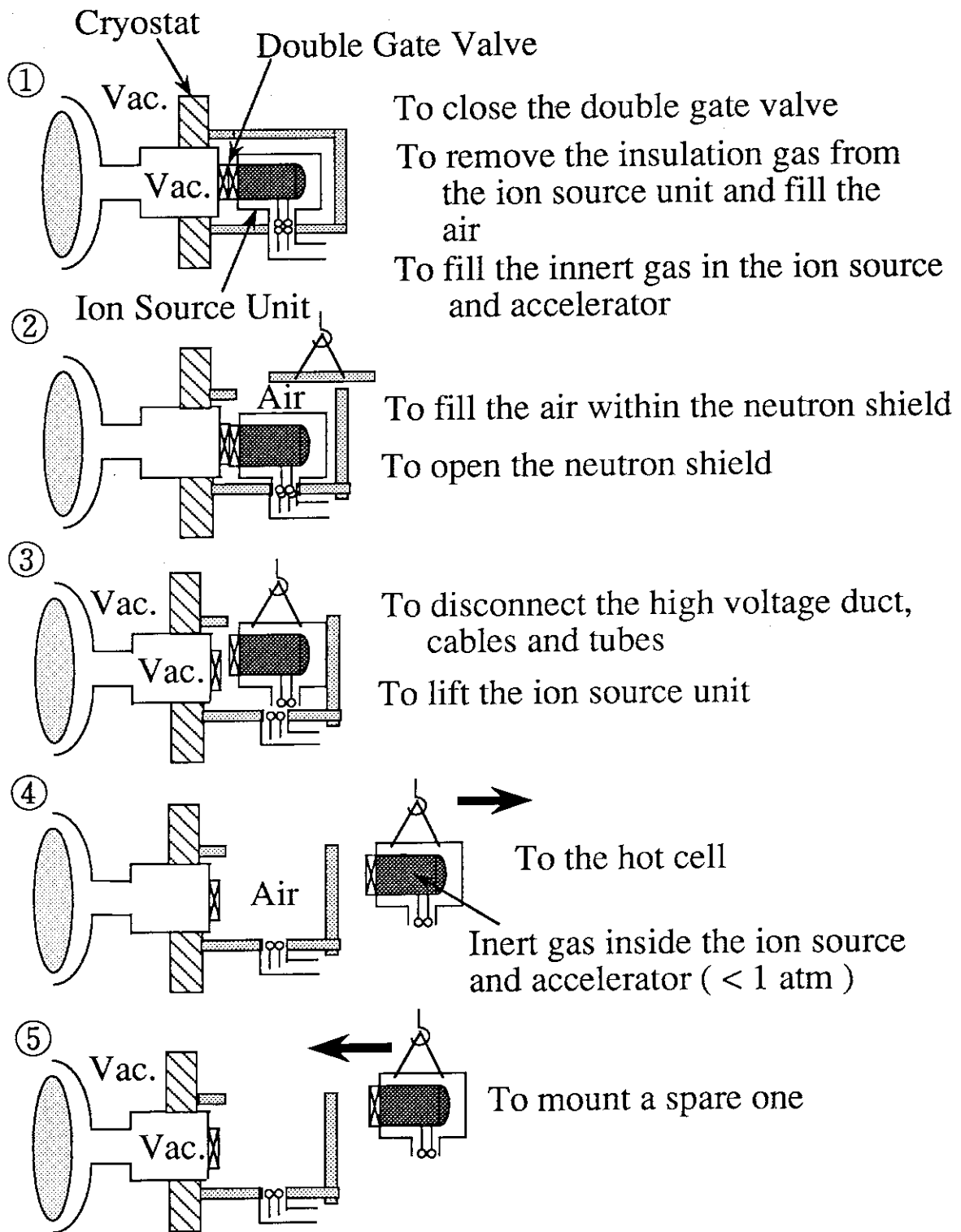
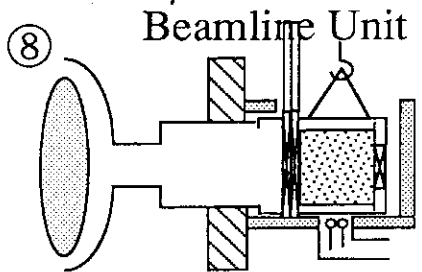
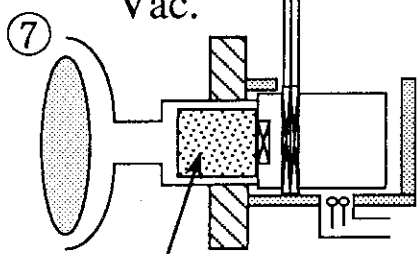
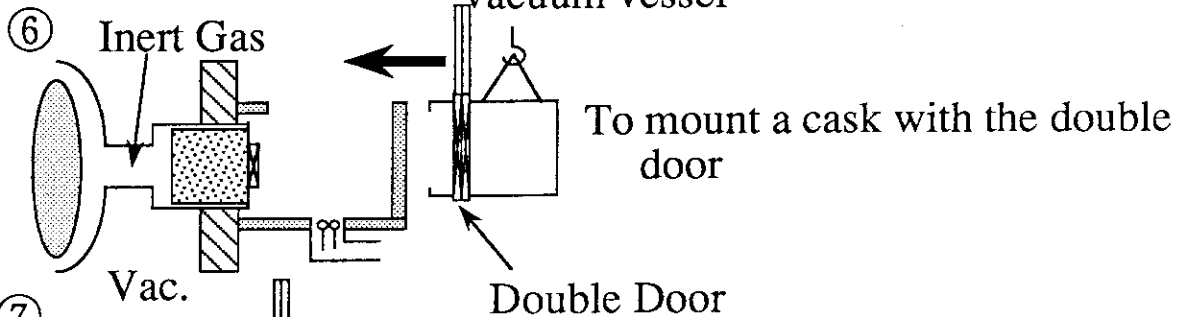


Fig.3-27 Maintenance procedures of the ion source unit for the short beamline option. Regular maintenance will be required once or twice per year.

Same procedures as the ion source maintenance

①②③④⑤

To ventilate the reactor  
To disconnect cables and tubes for the beamline unit without the vacuum vessel

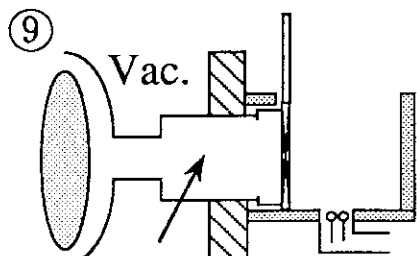


To open the beamline

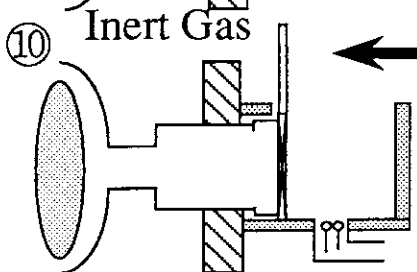
To pull out the beamline unit to the cask

To close the double door

To disconnect the double door



To bring to the hot cell



To mount a spare one

Fig.3-28 Maintenance procedures of the beamline unit for the short beamline option.

Regular maintenance of the beamline unit is not

required but only at the time of an accident in the beamline components.

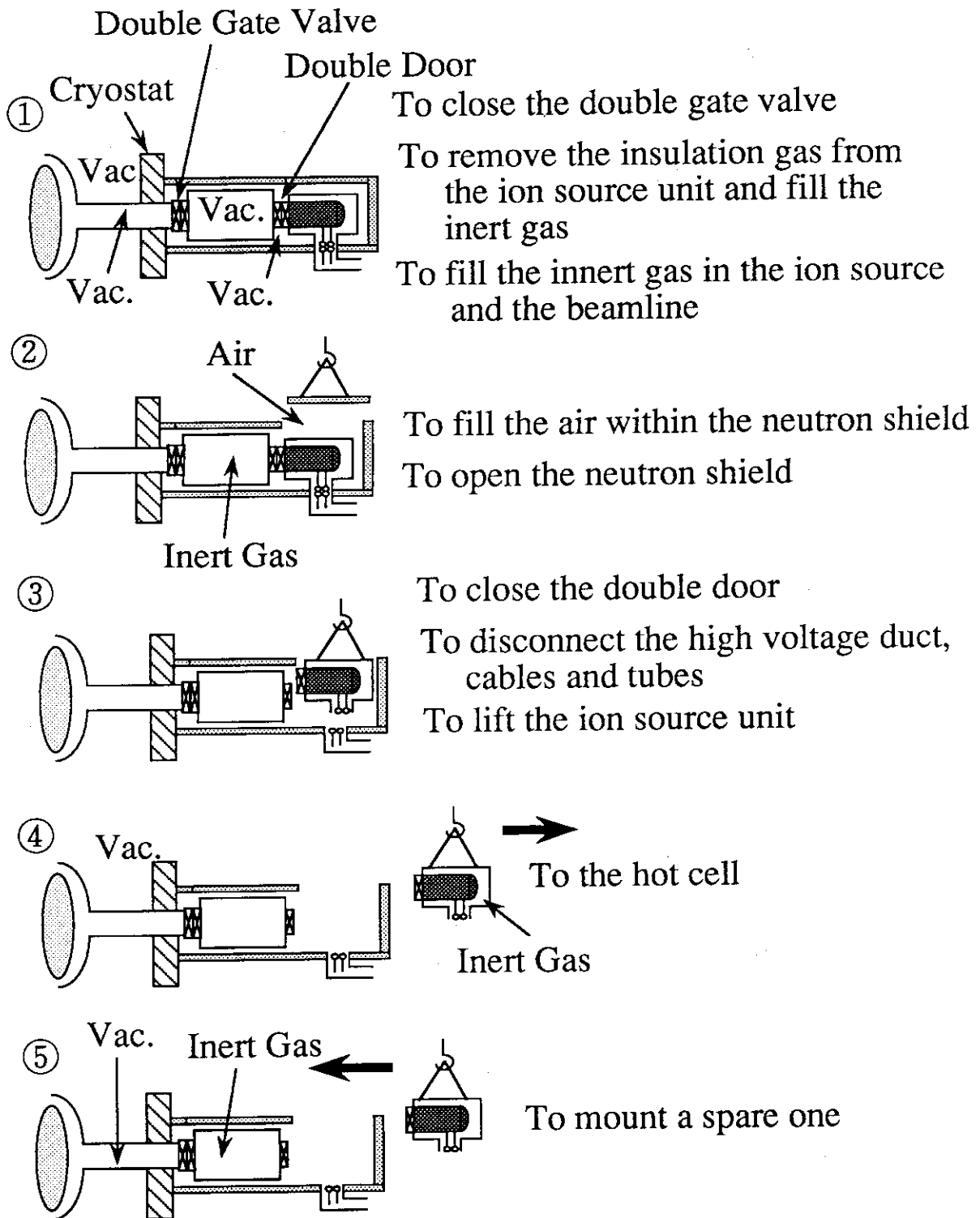
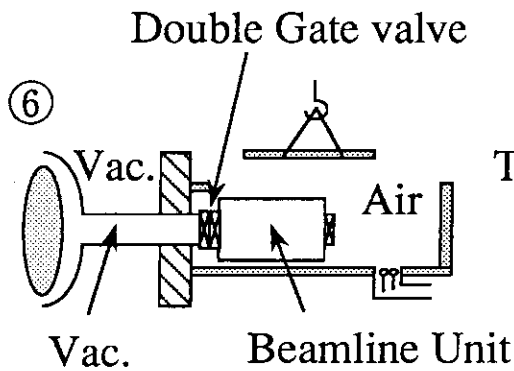


Fig.3-29 Maintenance procedures of the ion source unit for the Long beamline option. Regular maintenance will be required once or twice per year.

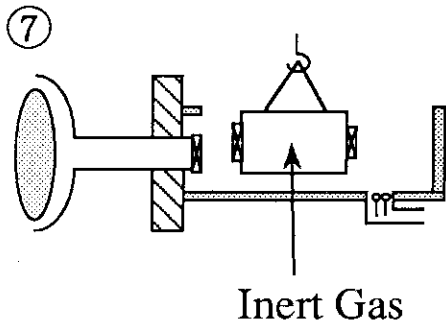
① ② ③ ④ ⑤

Same procedures as the ion source maintenance

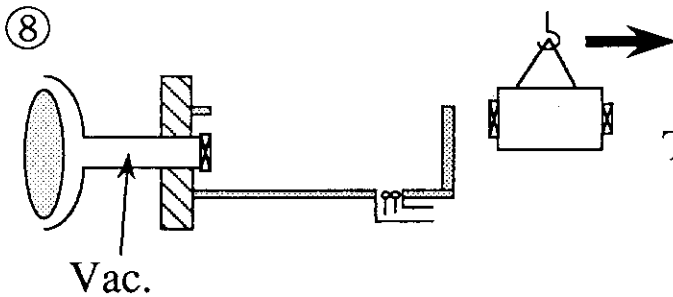
To disconnect cables and tubes for the beamline unit with the vacuum vessel



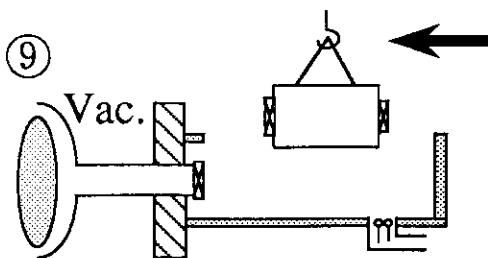
To enlarge the opening of the neutron shield



To lift the beamline unit  
To disconnect the double gate valve



To bring to the hot cell



To mount a spare one

Fig.3-30 Maintenance procedures of the beamline unit for the Long beamline option.

Regular maintenance of the beamline unit is not required but only at the time of an accident in the beamline components.

### 3.18 Gas Handling System

A conceptual diagram of the gas handling system is shown in Fig. 3-31. The  $D_2$  gas fed to the ion source and to the neutralizer is evacuated by the cryo-condensation pumps placed at the entrance and exit of the neutralizer. The accumulated  $D_2$  gas on the cryopanel is periodically exhausted by the roughing pumping system, and then is supplied to the reactor fueling system. The period is determined by the adsorption limitation of the cryopumps. Especially, the period is determined by the cryopump placed at the entrance of the neutralizer, since the gas flow rate per a square meter is higher. In case of the normal cryopump using the liquid helium of 4.2 K, the critical adsorption amount per a square meter is around  $2 \times 10^5 \text{ Pam}^3/\text{m}^2$ . Dividing the critical adsorption amount by the gas flow rate ( $0.18 \text{ Pam}^3/\text{m}^2\text{s}$ ), the regeneration period is 28 hours, which corresponds to 100 shots with a duration of 1000s. Namely, the cryopump needs to be regenerated every 2 or 3 days.

The  $T_2$  gas through the NBI port is also accumulated on the cryo-pump. The tritium amount in the cryopump can be evaluated from the conductance of the beamline and the pumping speed of the cryopump. The result shows the following relations;

[short beamline option]

$$\begin{aligned} \text{Cryopump at the entrance of the neutralizer} & : 0.59 P_T (\text{Pam}^3/\text{s}) \\ \text{Cryopump at the exit of the neutralizer} & : 243 P_T (\text{Pam}^3/\text{s}) \end{aligned}$$

[long beamline option]

$$\begin{aligned} \text{Cryopump at the entrance of the neutralizer} & : 3.57 P_T (\text{Pam}^3/\text{s}) \\ \text{Cryopump at the exit of the neutralizer} & : 312 P_T (\text{Pam}^3/\text{s}) \end{aligned}$$

where,  $P_T$ (Pa) is the partial pressure of the tritium at the scrape off region of the torus NBI port. These relations are shown in Fig.3-32. After 28 hours, the accumulated tritium amounts to the order of gram if the  $P_T$  is in order of  $10^{-4}$  Pa.

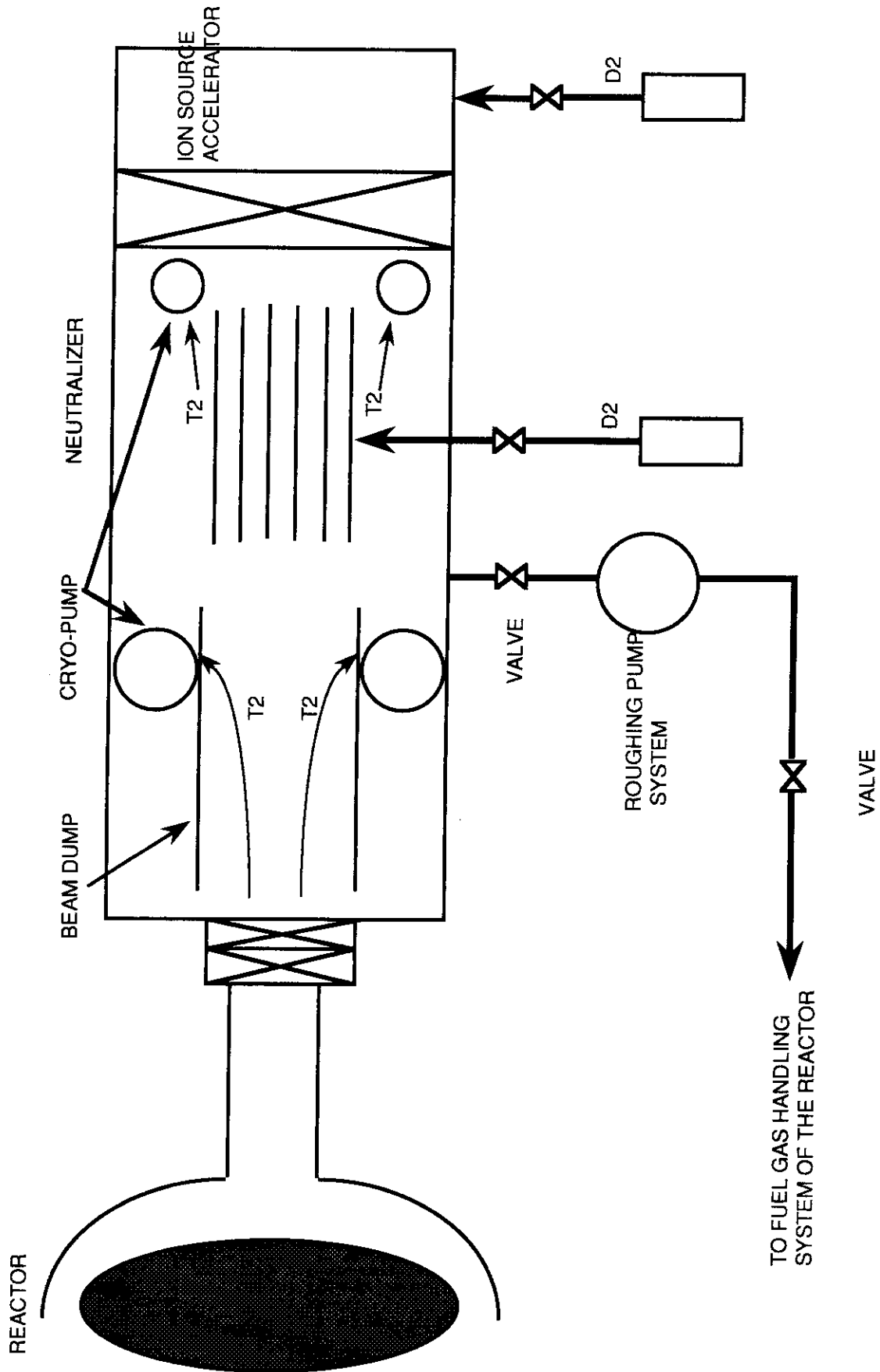


Fig.3-31 conceptual diagram of gas handling system in the NB system



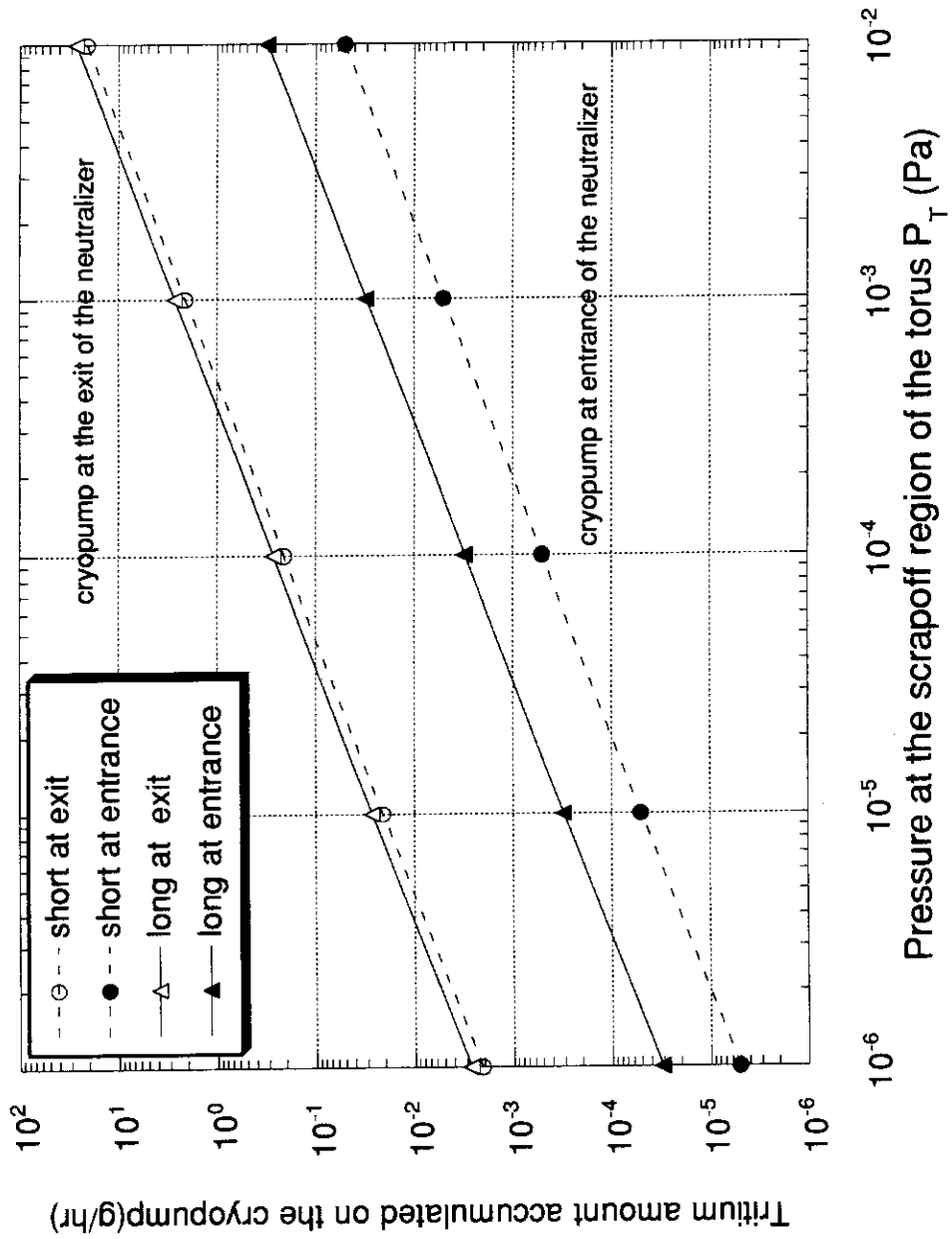


Fig.3-32 Relation of the tritium amount to the pressure at the scrapoff region of the torus  $P_T$  (Pa)

## 4. Neutronics

### 4.1 Modeling of Computation

A computational analysis was carried out to make clear the neutronics environment of the NB system[1]. Two independent models of the system were introduced; one for tokamak with NB duct, and the other for the NB beamline with the ion source/accelerator.

The model of the tokamak and the NB duct is a two dimensional (X-Y) model as shown in Fig. 4-1. From an identical analysis conducted in ITER CDA phase[2], a radiation shield of 46.6 cm thick, made of 80 % stainless steel and 20 % water, was adopted along the NB duct. This model was used in an evaluation of neutronics response in TFC.

An illustration of the NB beamline is shown in Fig. 4-2. A major change of the NB system from that in CDA is an adoption of ion extractor/accelerator of "multi-single" type with beam merging system in the short beamline option. By the merging beam total area of the beam cross-section is considerably reduced in comparison with a conventional "multi-multi" type system. This enables to reduce a transparency of beamline to prevent backstreaming of neutron from the reactor plasma. In the present design the neutralizer is designed to be an iron plug, i.e. the neutralizer consists of 22 cells for the beam neutralization, while outside of the cells is filled with an iron block for attenuation of neutron streaming.

The NB beamline was modeled in two dimensional R-Z symmetry structure as shown in Fig.4-3. The neutralizer was modeled as an iron block of reduced density for the void of beam path in the short beamline option. The length of the beam duct was varied in a range from 5.5 m to 11.5 m to examine a merit of short and long beamlines. From results of the computation with this model, neutronics environment in the main component of the NB system were estimated.

The two dimensional discrete ordinates transport code, "DOT 3.5" has been used with the multi-group (neutron: 42,  $\gamma$ -ray: 21) nuclear constants "FUSION-40" library. For a accurate calculation of the streaming neutrons in the narrow NB duct/beamline, an angular quadrature set of 166 division (highly forward bias) was applied in the computation.

All calculational results were normalized to an average neutron wall load on the first wall of  $1 \text{ MW/m}^2$ . The dose are calculated for an operational fluence of  $3 \text{ MW a/m}^2$ .

## 4.2 Results of Neutronics Calculation

The contour maps of neutron fluxes at 14 MeV,  $>0.1$  MeV and total energy are shown in Fig. 4-4 ~ 4-6 for the model of NB duct. The  $\gamma$ -ray flux contour map is also shown in Fig. 4-7. The contour maps of NB model (short beamline option) is shown in Fig. 4-8 ~ 4-11 for the neutron and  $\gamma$ -ray fluxes.

## 4.3 Nuclear Heating in TFC and Cryopump

Neutronics responses at points A and B (shown in Fig. 4-1) in the TFC is summarized in Table 4-1. The design limits taken from CDA design are also listed in the table. Since the computation is done for the infinite NBduct, the results give conservative evaluation. However, the results are below the design limits by the factor of three.

In the model of the cryopump in the ion dump room of the NB beamline, the distance between the beam axis and the inner surface of the pump and the volume was preserved to be the same as the present design (the distance: 1m). The nuclear heating in the cryopump was evaluated to be several watt for the long beamline option. While the nuclear heating in the cryopump reached to a few hundreds watt in the short beamline option. Since the neutron and  $\gamma$ -ray fluxes are strongly dependent on the distance from the beamline axis, the nuclear heating of the cryopump will be reduced by replacing the cryopump far from the high flux region in the beamline.

Although liquid nitrogen was used in the present calculation for a coolant of thermal shield, gas helium is more realistic for the purpose from a viewpoint of activation.

## 4.4 Radiation in the Accelerator Insulator

An alumina ceramics is used as an insulator of the accelerator column. Mechanical and electrical characteristics of an alumina ceramics deteriorate under a high neutron and  $\gamma$ -ray fluence. These radiation damages are described in the Appendix in this chapter.

Contour maps of total neutron and  $\gamma$ -ray fluxes obtained in the present computation[1] are shown in Fig. 4-8 ~ 11 (short beamline option). The fluxes are drastically decreased in the neutralizer structure. Both total neutron and  $\gamma$ -ray fluxes are attenuated by an order of 6 - 7 in the neutralizer with the reduced density. The fluxes at the ion source/accelerator position is estimated to be of the order of  $10^4$  n/cm<sup>2</sup>s and  $10^6$  photon/cm<sup>2</sup>s for total neutron and  $\gamma$ -ray, respectively.

In the actual neutralizer, the neutron streaming may be enhanced through the channels as the beam path. A brief estimation of the streaming through the cells indicates that the fluxes increase as an order of three at the maximum than the present analysis. For detailed calculation, 3-D Monte-Carlo neutron streaming simulation should be conducted.

Taking this enhancement factor into account, the fluxes at the accelerator insulator is estimated to be at most of the order of  $10^7$  n/cm<sup>2</sup>s (=  $10^{-5}$  Gy/s) and  $10^9$  photons/cm<sup>2</sup>s for total neutrons and  $\gamma$ -rays, respectively. Assuming the irradiation duration to be  $10^6$  s/year, the neutron fluence in the insulator is  $10^{17}$  n/m<sup>2</sup>year. As described in the Appendix, no degradation of the mechanical properties of the insulators is expected below the neutron fluence of  $10^{25}$  n/m<sup>2</sup>. Therefore, the mechanical properties are not disturbed at all during the life of ITER. Additionally, the Radiation Induced Conductivity (RIC) does not occur since the dose rate is far below  $\sim 1$  Gy/s, and the Radiation Induced Electrical Degradation (RIED) is not anticipated because the insulator is operated at room temperature, as described in the Appendix.

#### 4.5 Radiation Effect of the Permanent Magnet in the Ion Source

For an application to the accelerators, many irradiation tests of the permanent magnets have been carried out in laboratories of high energy physics. An example of the threshold dose for the degradation of the magnetic property is as follows for the Sm<sub>2</sub>Co<sub>17</sub> permanent magnet.

Neutron Irradiation[4-7] :  $\sim 10^{19}$  n/cm<sup>2</sup>.

<sup>60</sup>Co  $\gamma$ -ray Irradiation[8,9] : No degradation observed up to 500 kGy.

The threshold of SmCo<sub>5</sub> magnet is reported to be slightly lower than that of Sm<sub>2</sub>Co<sub>17</sub>, and Nd-Fe magnet shows the magnetic degradation at one order of magnitude lower fluence/dose.

The fluence/dose at the ion source position is evaluated to be low enough with respect to the above thresholds. Hence replacement of magnets in the ion source may not be necessary in the NB system.

#### 4.6 Activation of the Insulation Gas

SF<sub>6</sub> gas has been widely utilized for DC high voltage insulation in the existing NB system. However Seki[10] pointed out that the concentration of activated nuclei transmuted by the reaction  $^{32}\text{S}(n, p)^{32}\text{P}$  in the SF<sub>6</sub> gas duct exceeded a permissible level. The insulation by air was also evaluated, showing that unnegligible amount of  $^{14}\text{C}$ , as a long life radio isotope, is transmuted in the system.

Two alternatives, C<sub>2</sub>F<sub>6</sub> and CO<sub>2</sub> gases, are examined for the insulation gas of the ITER NB system in the present design. The insulation capability of C<sub>2</sub>F<sub>6</sub> is also twice as high as that of air. Though that of CO<sub>2</sub> is a slightly lower than the air, 1 MeV dc high voltage is sustainable by pressurizing the gas pressure up to 2 MPa.

Assuming that the flux of 14 MeV neutron at the position is  $10^9 \text{ n/cm}^2\text{s}$ , which corresponds to the long beamline option with a safety factor of one order, the activation of the gases were roughly estimated. It was found that the following activation reactions and radio isotopes should be paid attention:

- 1)  $^{12}\text{C}(n, 2n)^{11}\text{C}$ :  $3 \times 10^3 \text{ Bq/cm}^3$
- 2)  $^{17}\text{O}(n, a)^{14}\text{C}$ :  $3 \times 10^{-4} \text{ Bq/cm}^3$
- 3)  $^{19}\text{F}(n, 2n)^{18}\text{F}$ :  $2 \times 10^5 \text{ Bq/cm}^3$

A half life of  $^{11}\text{C}$  and  $^{18}\text{F}$  are 20.38 min. and 109.8 min., respectively. They are attenuated below a negligible level within two days.

The present estimation was made assuming that the gases were irradiated uniformly at the fluence of  $10^9 \text{ n/cm}^2\text{s} \times 10^6 \text{ s}$ . However, as shown in Fig.4-8 ~ 10, the flux was taken from the maximum value near the beamline axis. Also gas circulation system will be equipped in the actual system, which results in substantial reduction of the activated gas concentration. The concentration of  $^{14}\text{C}$  in the actual NB system will be below a permissible level.

## References

- [1] S. Zimin, K. Maki, H. Takatsu, S. Sato, T. Tsunematsu, T. Inoue, and Y. Ohara, "Shielding Analysis of the ITER NBI Duct", to be published in JAERI-M 94-015 (1994).
- [2] K. Maki et al., Fusion Eng. Design., Technical Note 22, 427 (1993).
- [3] T. Shikama, and G. P. Pells, "Radiation Effects in Ceramics", Report of Research Institute of Tohoku University, RITU (1994).
- [4] H. Spitzer, A. Weller, "Magnetisierungverlust von Samarium-Kobalt Permanentmagneten in hohen Neutronenfeldern", KFA Julich GmbH SNQIN./BH2205 84.
- [5] J. R. Cost, R. D. Brown, A. L. Giorgi, and J. T. Stanley, "Radiation Effects in Rare-Earth Permanent Magnets", LA-UR 87-1455.
- [6] R. D. Brown, E. D. Bush Jr., and W. T. Hunter, "Radiation Effects on Samarium-Cobalt Permanent Magnets", LA-9437-MS.
- [7] J. R. Cost, R. D. Brown, A. L. Giorgi, and J. T. Stanley, "Effects of Neutron Irradiation on Nd-Fe-B Magnetic Properties", IEEE Trans. on Magnets 24/3 (1988).
- [8] K. Boockmann, M. Liehr, W. Rodenald, E. Salzborn, M. Schlapp, and B. Wall, "Effect of g-radiation on Sm-Co- and Nd-Dy-Fe-B-Magnets", J. Magnetism and Magnetic Materials 101 345-346 (1991).
- [9] A. F. Zeller and J. A. Nolen, "Radiation and Temperature Effects on Sm-Co and NdFeB Magnets in Low Permeance Configurations", Paper No. Wp3.2 at 9th Int. Workshop on REM and their Applications, Bad Soden, FRG, Aug. 31- Sep. 2 (1987).
- [10] Y. Seki, private communication.

Table 4-1 Neutronics responses in the Troidal Field Coll  
(neighbor of NB duct)

	Computational Result	Design Limit
Fast Neutron to Nb3Sn	$< 1.5 \times 10^{18} \text{ n/cm}^2$	$1 \times 10^{19}$
Dose to Insulator	$< 1.6 \times 10^9 \text{ rad}$	$5 \times 10^9$
Displacement in Cu Stabilizer	$< 1.2 \times 10^{-4} \text{ dpa}$	$6 \times 10^{-3}$

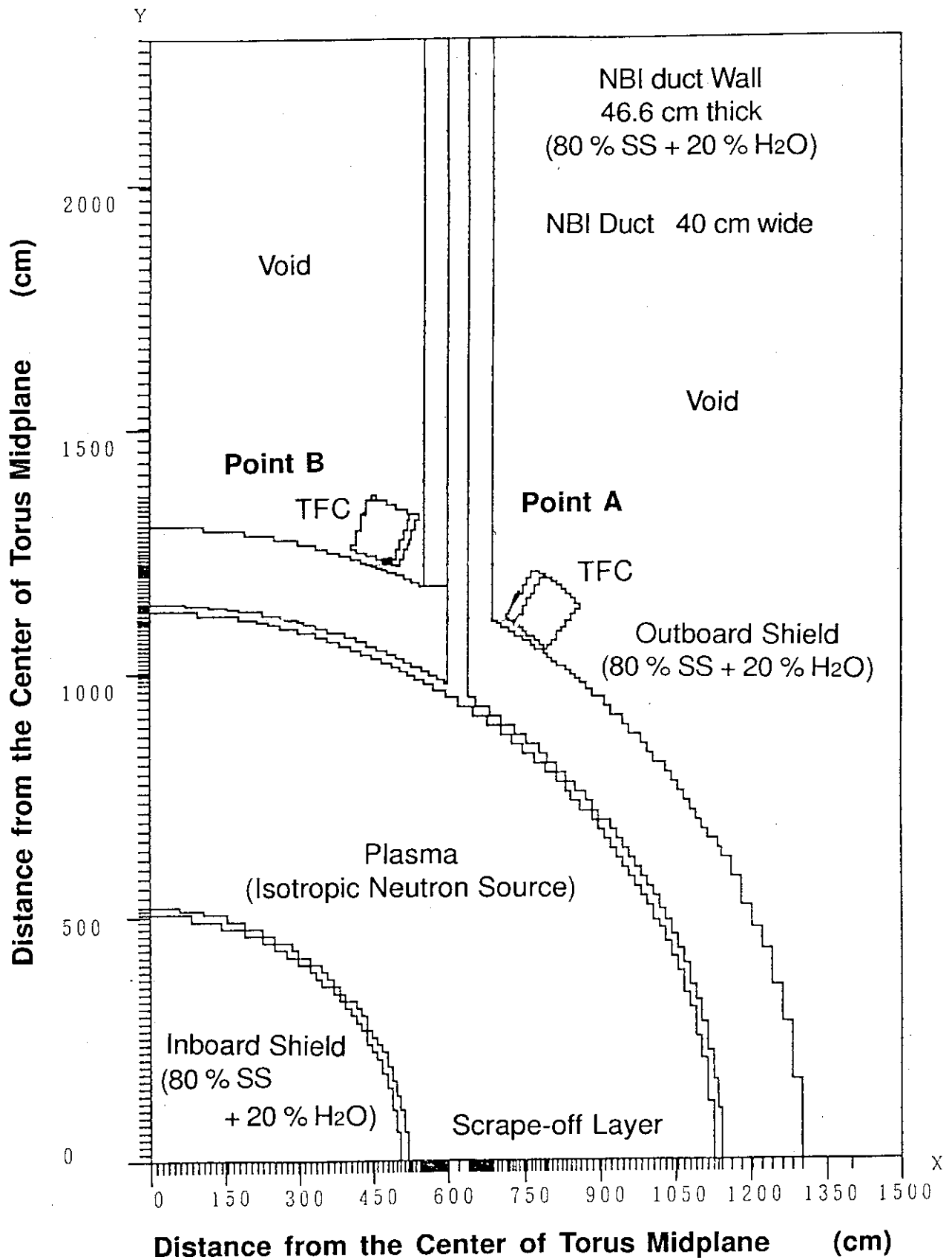


Fig.4-1 The X-Y two dimensional model of the tokamak and the NB duct.

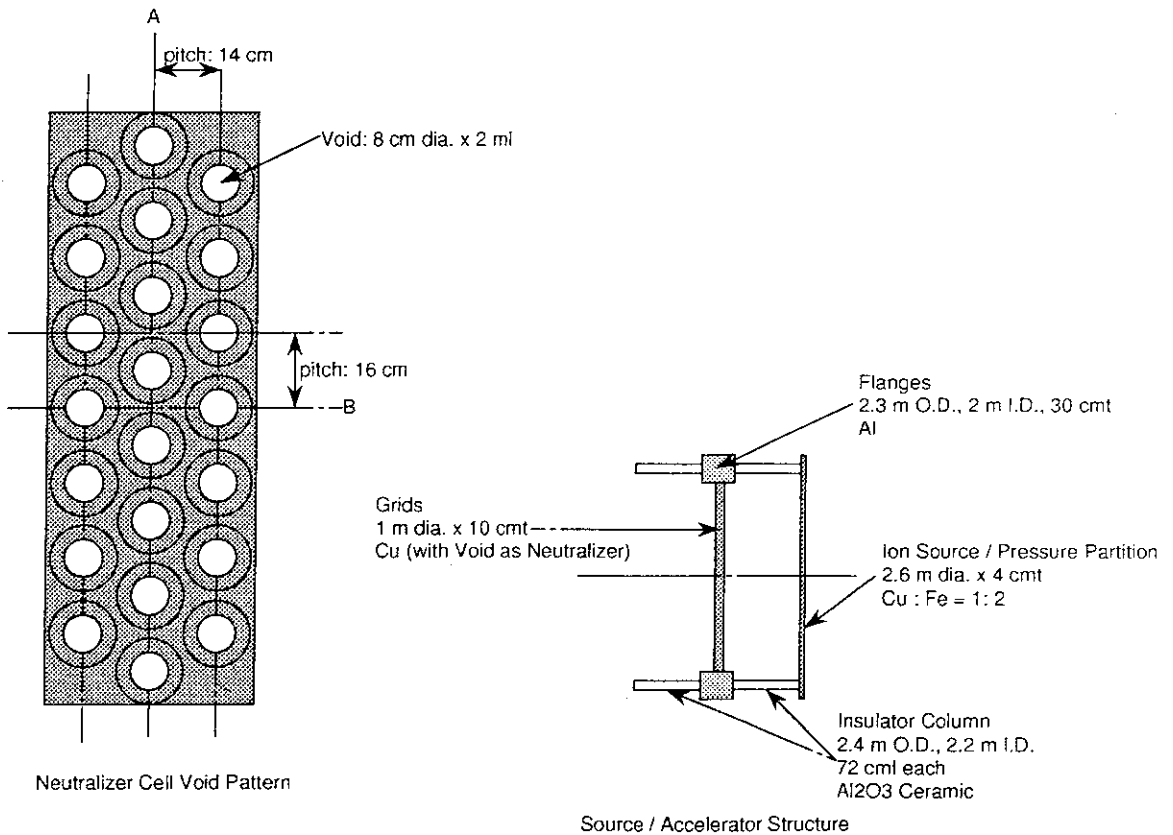
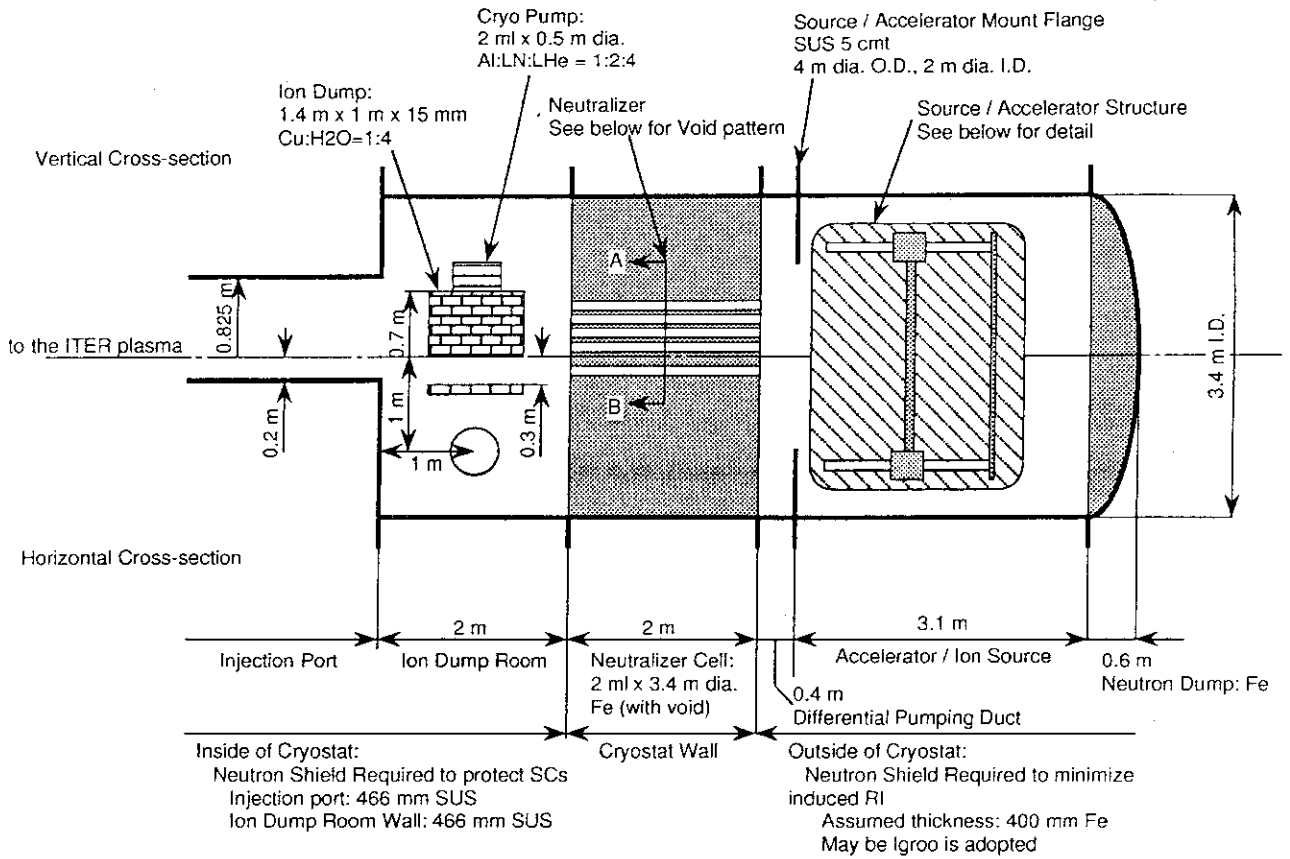


Fig.4-2 An illustration of the NB beamline.



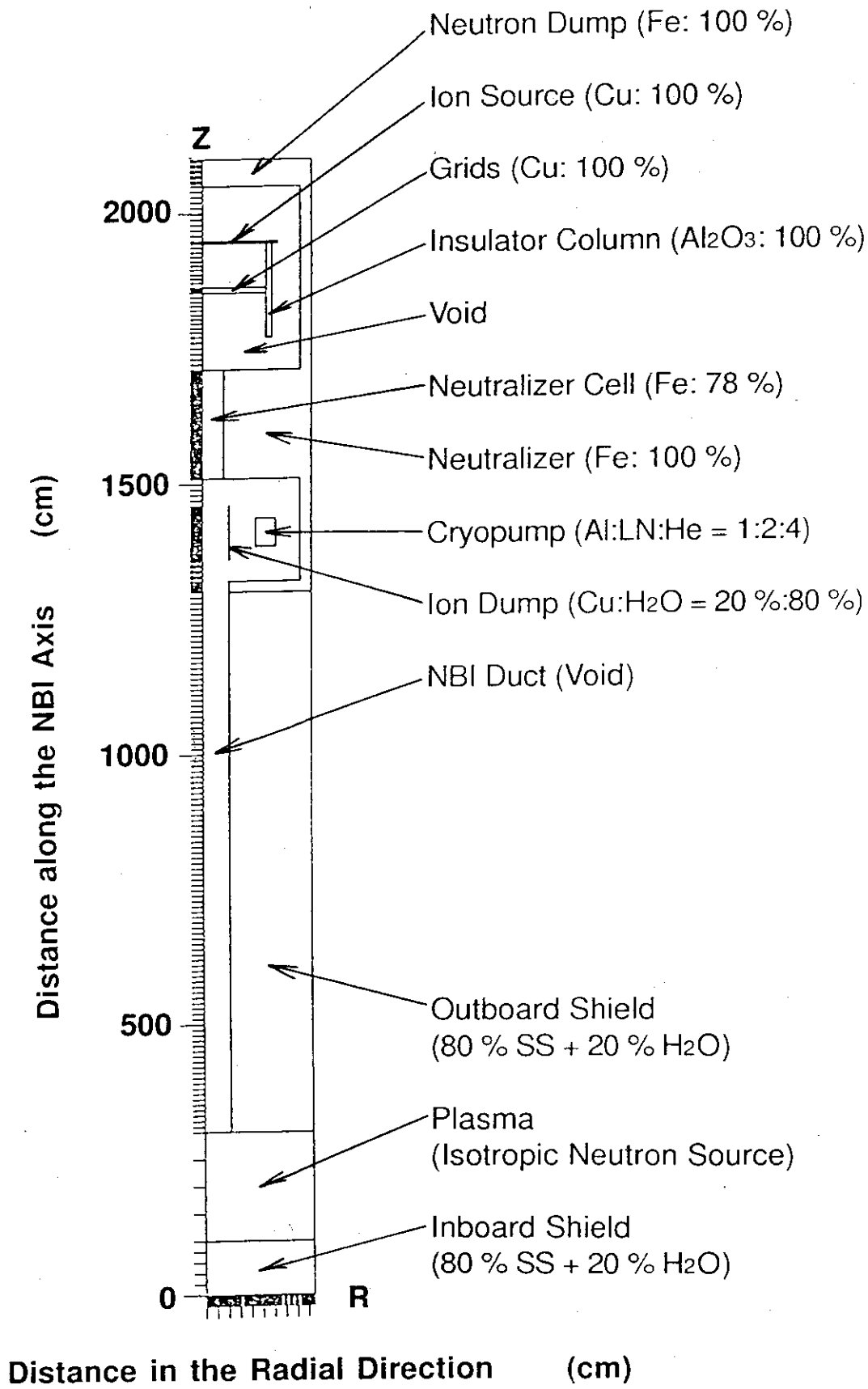


Fig.4-3 The R-Z two dimensional model of the NB beamline with the ion source and the accelerator.

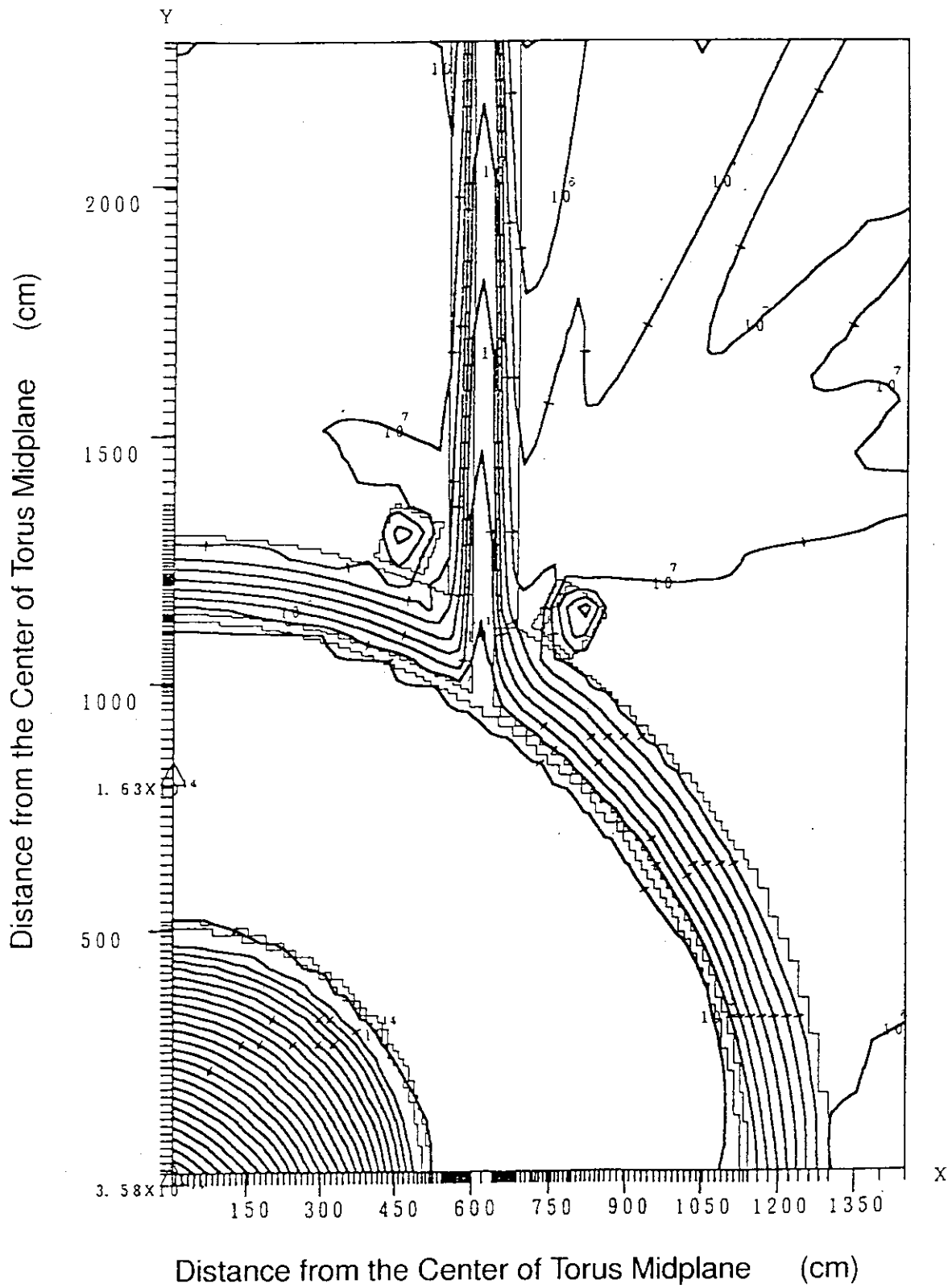


Fig.4-4 Contour map of 14MeV neutron flux in the NB beamline (tokamak and the NB duct).

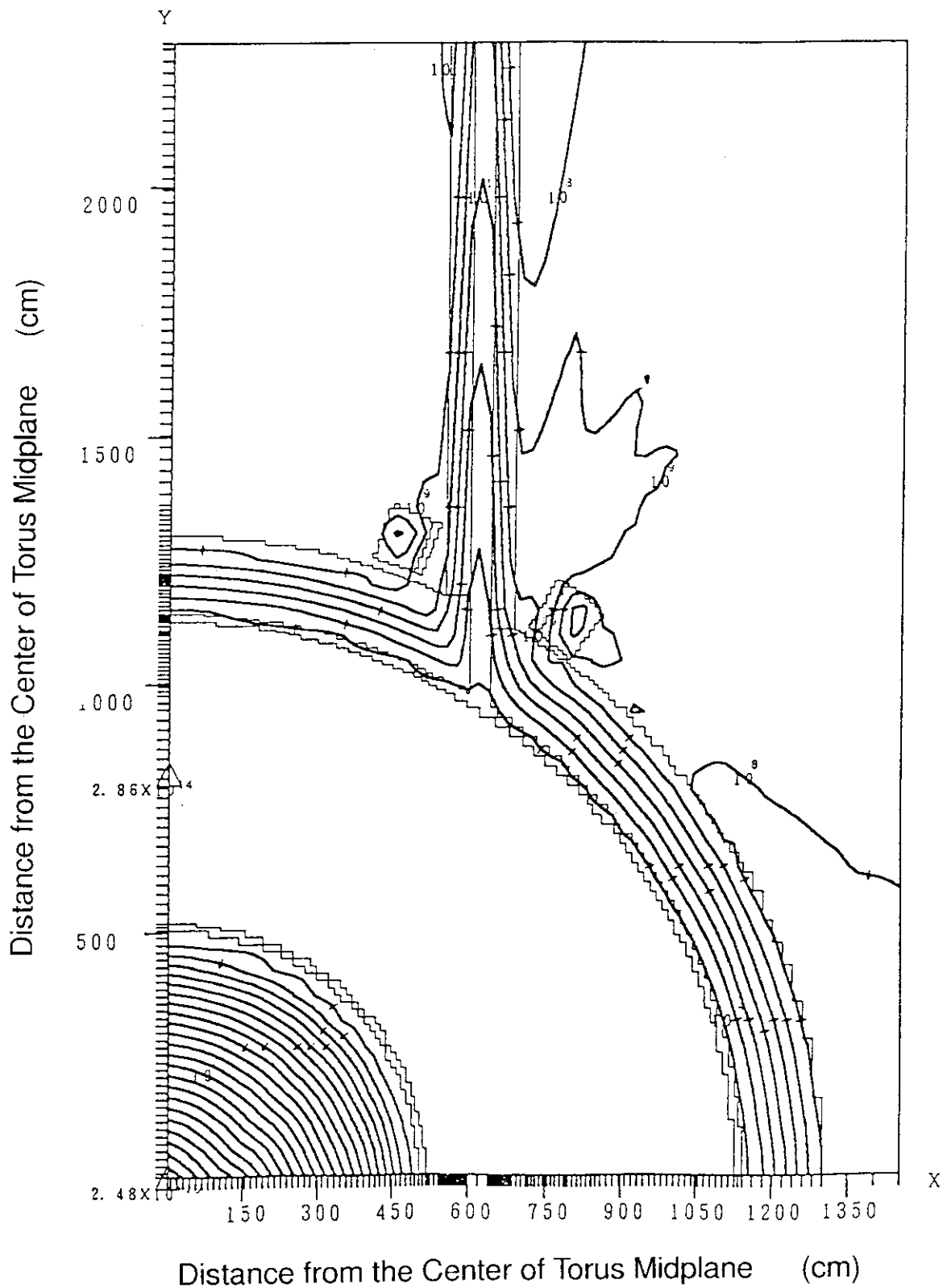


Fig.4-5 Contour map of  $>0.1\text{MeV}$  neutron flux in the NB beamline (tokamak and the NB duct).

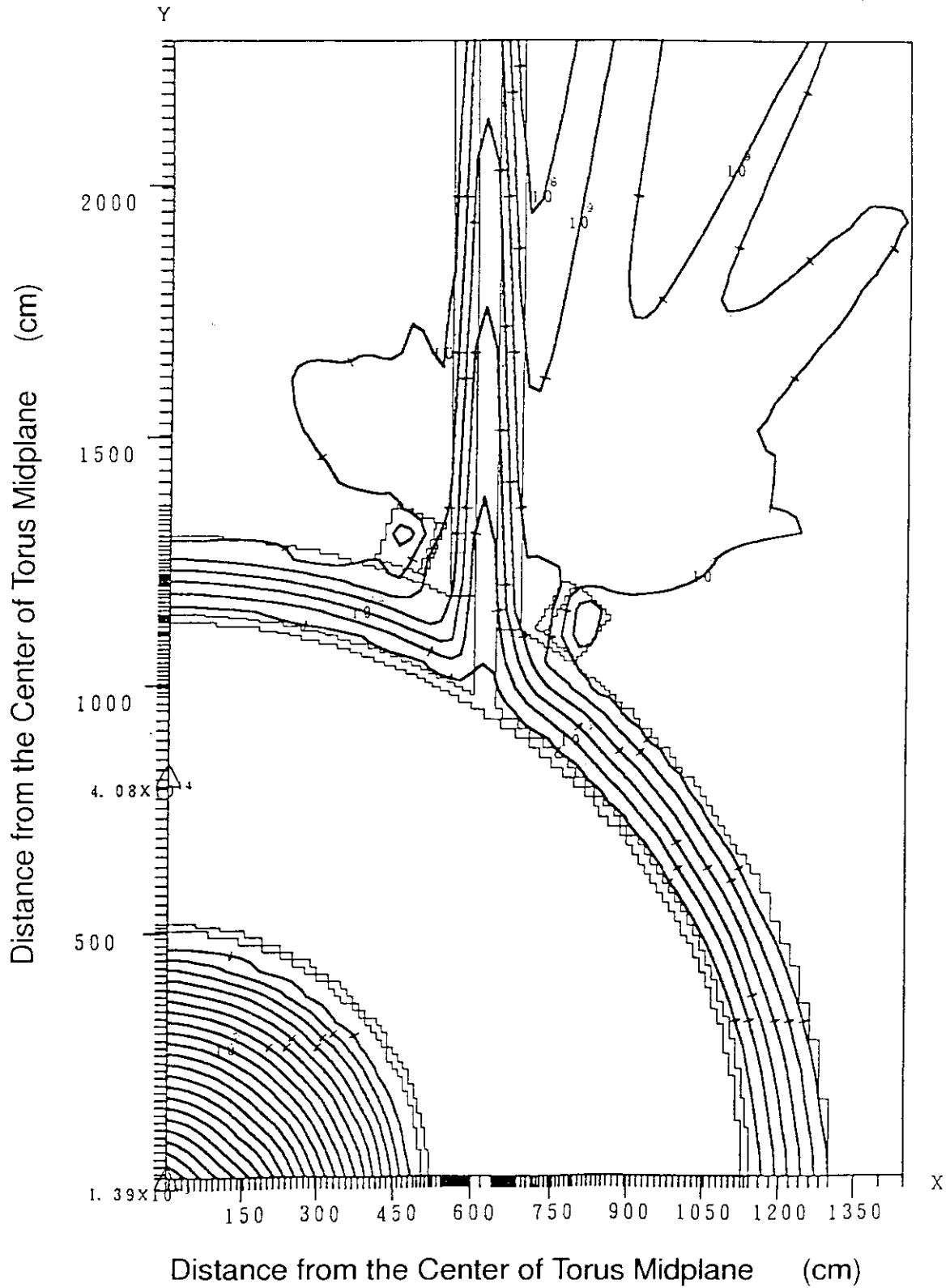


Fig.4-6 Contour map of the total neutron flux in the NB beamline (tokamak and the NB duct).

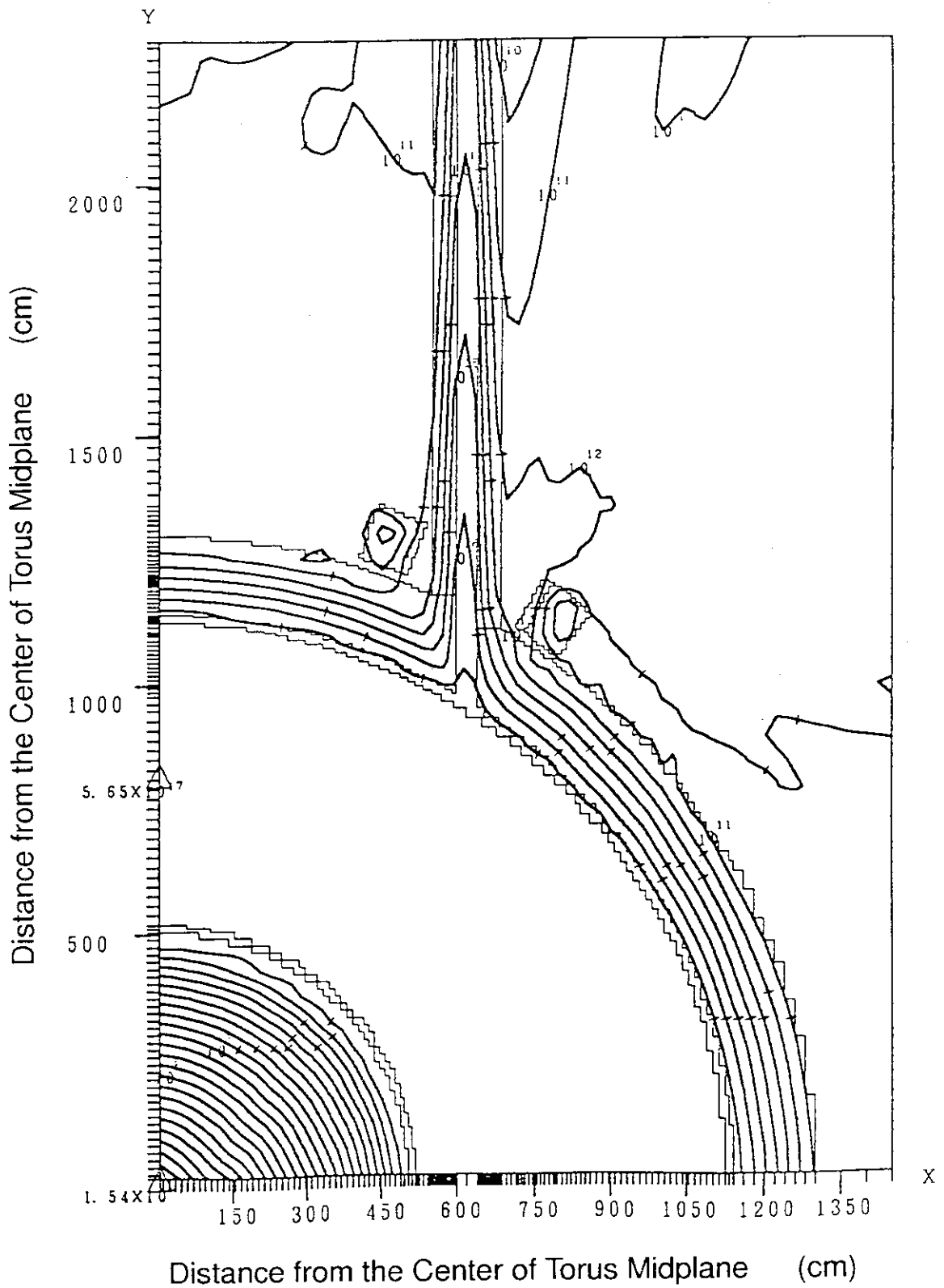


Fig.4-7 Contour map of the  $\gamma$ -ray flux in the NB beamline (tokamak and the NB duct).

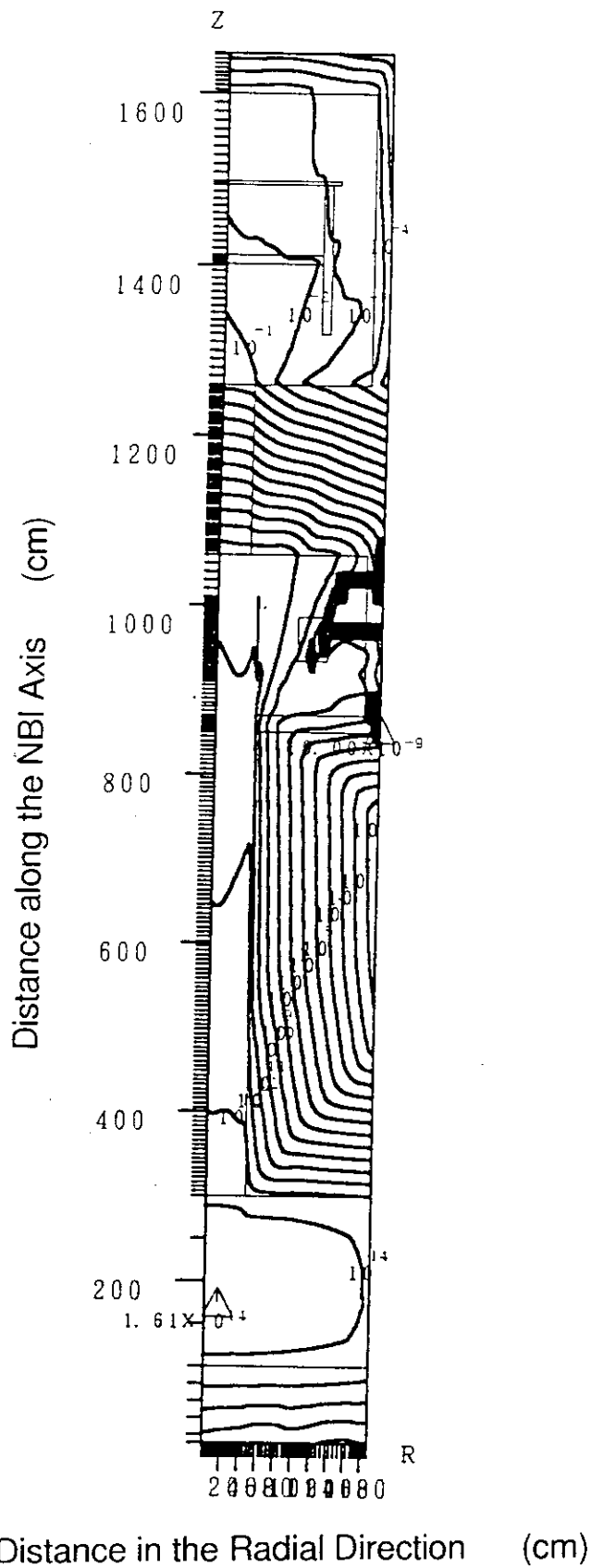


Fig.4-8 Contour map of 14MeV neutron flux in the NB beamline (short beamline option).

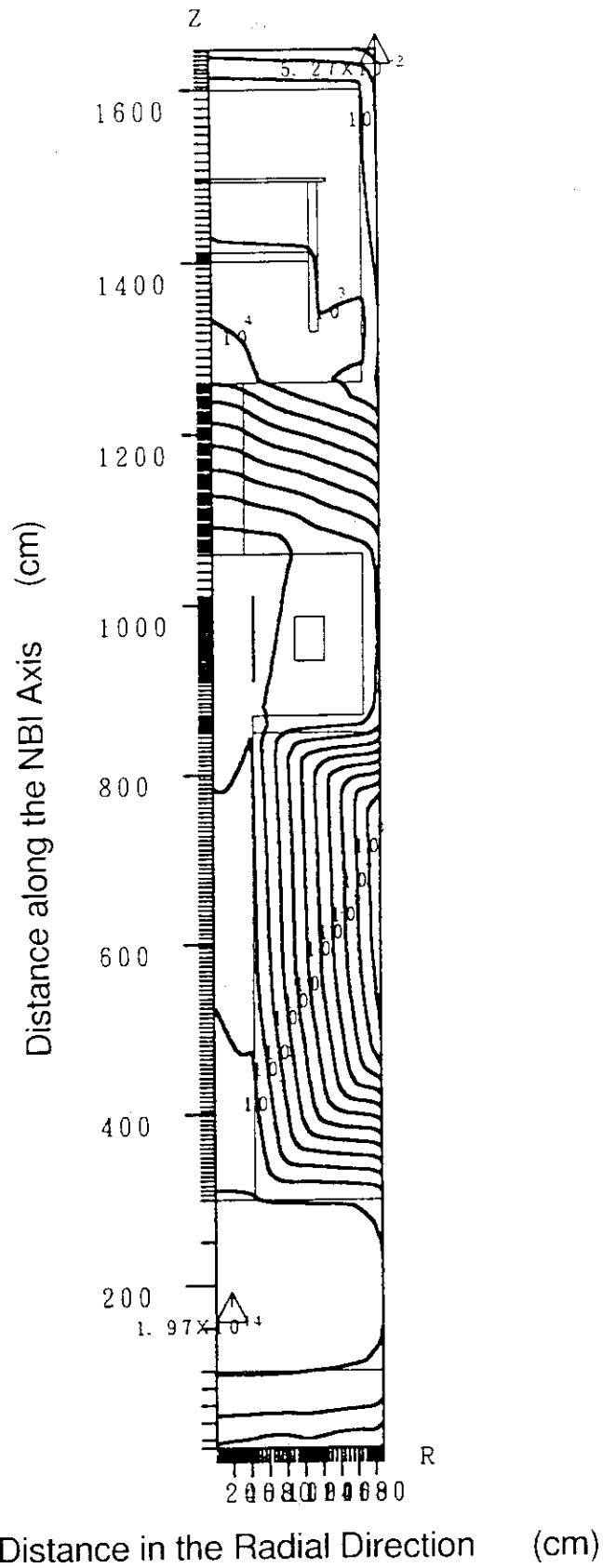


Fig.4-9 Contour map of  $>0.1\text{MeV}$  neutron flux in the NB beamline (short beamline option).

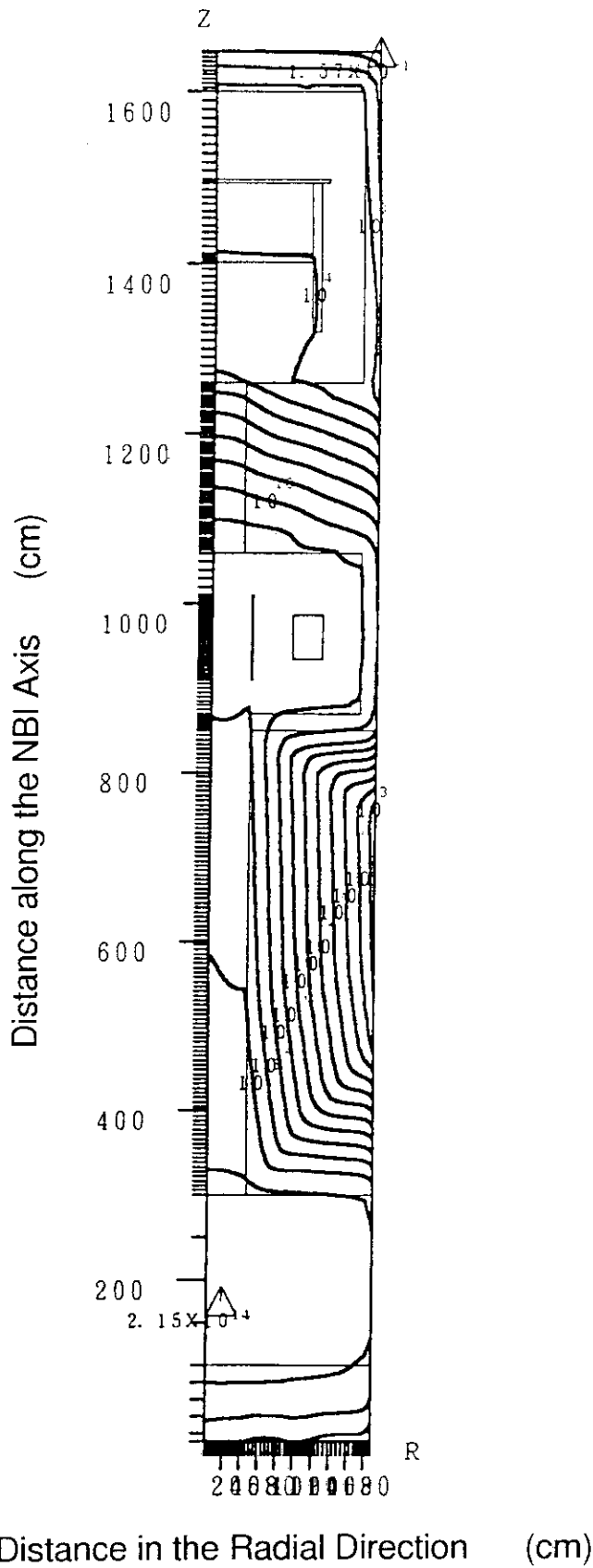


Fig.4-10 Contour map of the total neutron flux in the NB beamline (short beamline option).



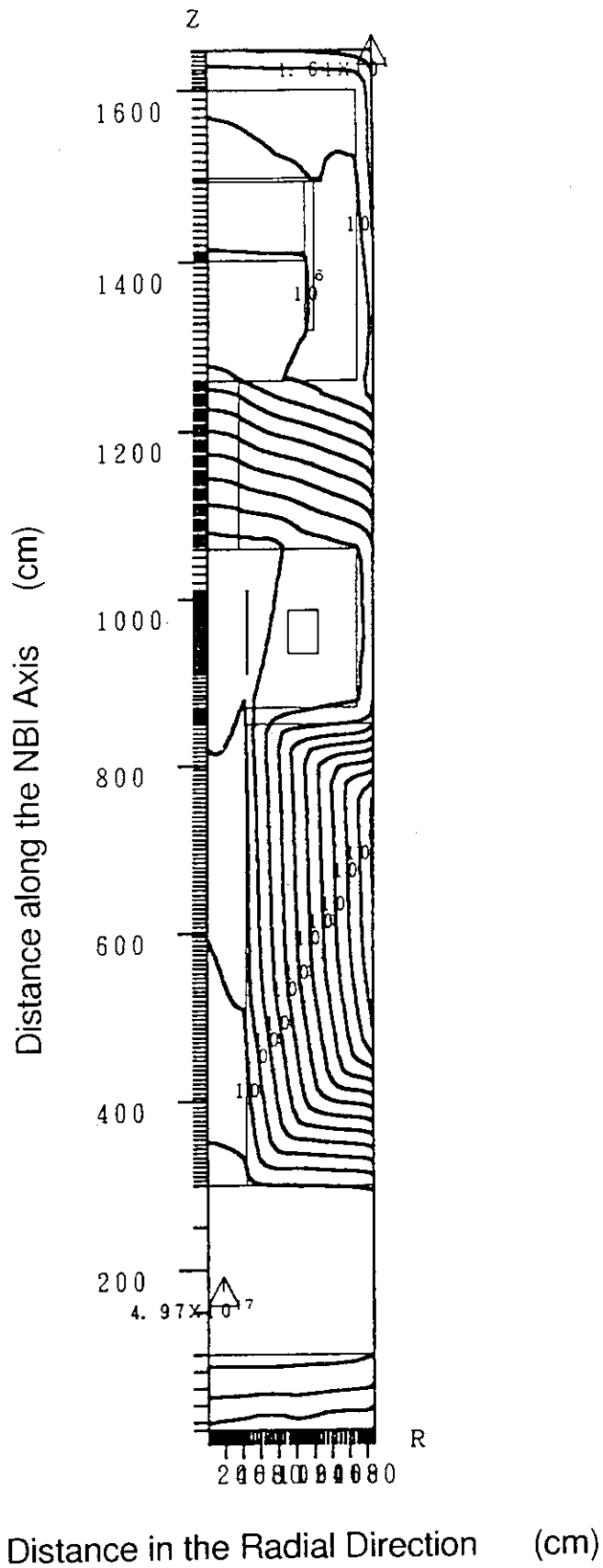


Fig.4-11 Contour map of the  $\gamma$ -ray flux in the NB beamline (short beamline option).

## Appendix: Radiation Effect of an Alumina Ceramic

### Mechanical Properties

The mechanical strength is closely related to the swelling, which increases almost linearly with neutron fluence as shown in Fig.4-12. It is well understood that the degradation of mechanical properties of alumina is observed above 1 dpa (displacement per atom) or the swelling of 1 volume %, which corresponds to the neutron fluence of about  $5 \times 10^{25} \text{ n/m}^2$ . So long as the neutron fluence is far below  $10^{25} \text{ n/m}^2$ , no degradation of the mechanical properties of the insulators is expected.

### Electrical Properties

There are two major irradiation effects in ceramic materials. One is Radiation Induced Conductivity (RIC) and the other is Radiation Induced Electrical Degradation (RIED). The RIC is a dynamic irradiation effect that the electrical conductivity increases only during the irradiation. Once the irradiation is terminated, the conductivity is recovered immediately, namely, the RIC is a reversible phenomenon. It is generally agreed that the RIC is caused by free electrons excited by ionizing irradiations. The observed increase of electrical conductivity,  $\sigma_{\text{RIC}} [\Omega \cdot \text{m}]^{-1}$ , is shown in Fig. 4-13 as a function of the dose rate in Gy/s. In designing the accelerator insulators, electrical conductivity should be kept below  $10^{-10} \sim 10^{-8} [\Omega \cdot \text{m}]^{-1}$  to suppress the joule heating of the insulator due to the leakage current below a reasonable level, i.e., less than 1 mA. From this view point, it is essential to reduce the dose rate in the insulator below  $\sim 1 \text{ Gy/s}$ .

On the other hand, the RIED is a permanent degradation of electrical insulating ability of ceramic insulators. The RIED depends on dose or dpa, and increases drastically above a critical dose as shown in Figures 4-14 and 4-15. The critical dose decreases at a lower dpa rate. Fortunately, the RIED does not occur at a room temperature. It occurs only in the temperature range of  $400 \sim 800^\circ\text{C}$ . The RIED is thought to be caused by two effects, i.e., volume effects and surface effects. The volume effect is due to the displacement damage caused primarily by neutron irradiation. The surface effect is due to the formation of aluminum rich surface by surface desorption mechanisms of oxygen, and also surface contamination by carbon, and caused primarily by electrons or ions rather than by neutrons or  $\gamma$ -rays.

Almost all the data on irradiation effects in alumina ceramics have been obtained using a high purity alumina. Since the large accelerator insulator can be manufactured using a

high purity alumina (99%) according to Kyocera Co. Ltd., these data can be available for evaluating the radiation effects in the accelerator insulator.

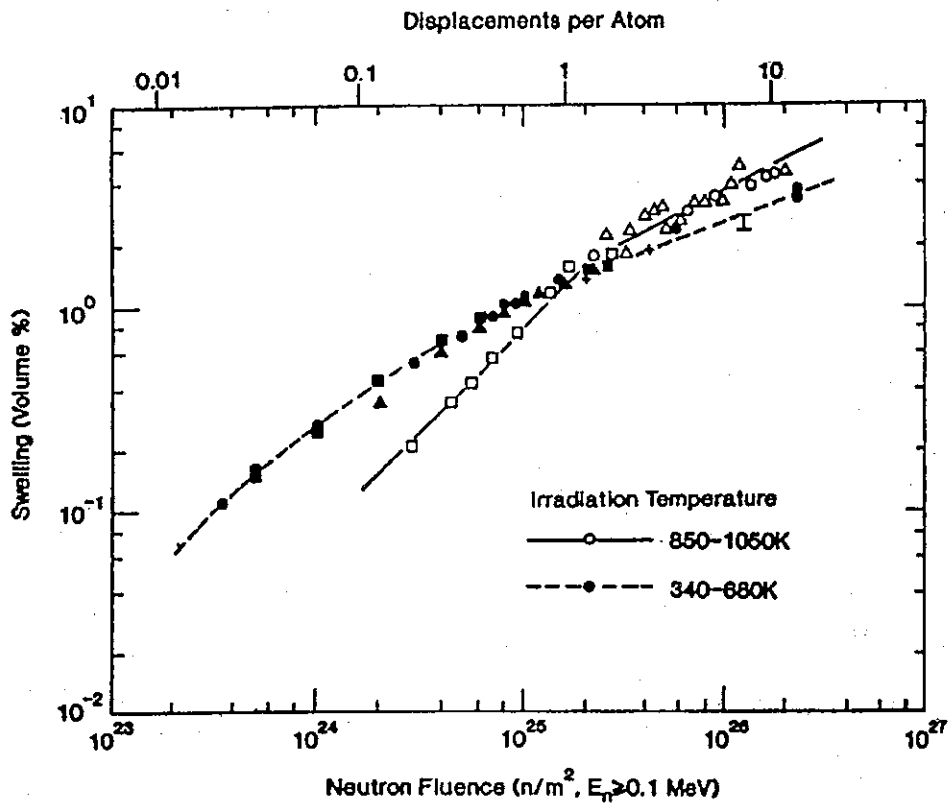


Fig.4-12 Swelling of alumina as a function of neutron fluence [1]

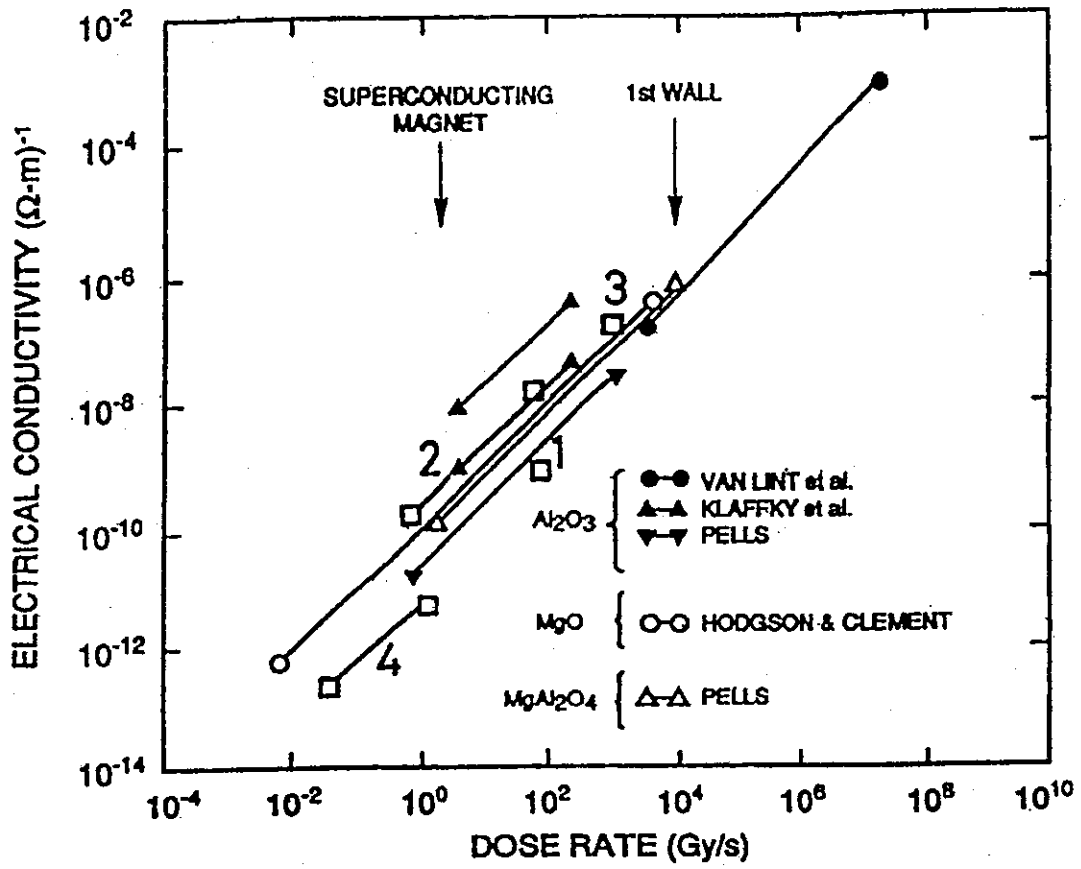


Fig.4-13 Observed RIC with different irradiation sources as a function of ionizing dose rate [1] 1.Farnum et al., 2. Neverov and Revyakin, 3 Shikama et al.

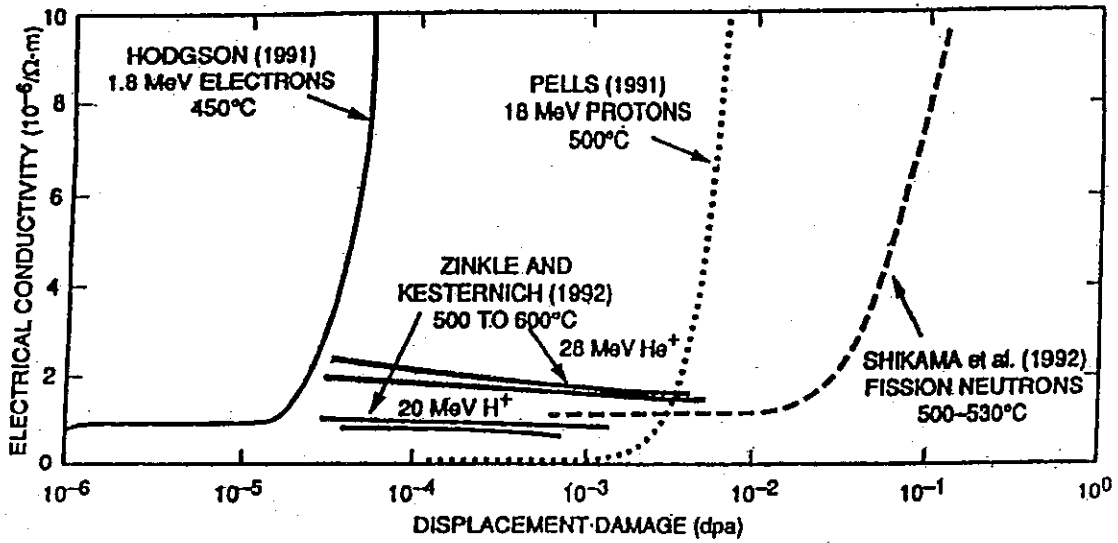


Fig.4-14 RIED of alumina observed with different irradiation sources.(compiled by Zinkle)

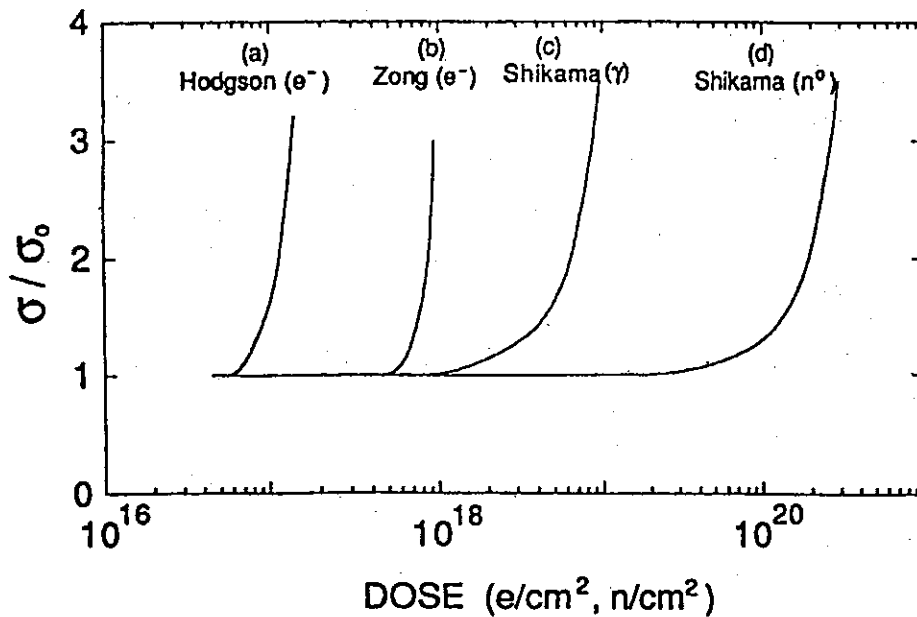


Fig.4-15 Comparison of RIED observed with different irradiation sources. (by Chen et al.)

## 5. Conclusion and Necessary Future R&Ds

Based on the recent progress on the negative ion beam development, design studies on NB system have been made for ITER-EDA. Two types of designs are proposed; one is characterized by a very short neutralizer, which makes it possible to integrate the beamlines within the cryostat. The other has a conventional layout, but is more compact than the ITER-CDA design. In both designs, four beamlines having one ion source per beamline are installed on four tangential ports, and 50 MW neutral beam power is injected into a plasma at the beam energy of 1 MeV.

The irradiation dose rate in the accelerator insulator can be suppressed to a moderate value by applying a neutralizer with multiple narrow channels which serves as an efficient neutron shield. Judging from the results of the neutronics calculation conducted so far, the mechanical and electrical properties of the insulator would not change during the life of ITER.

The most urgent and critical R&D in developing the NB system for ITER is;

- to demonstrate negative ion acceleration up to an energy of 1 MeV with a good beam optics and an enough current density. For a proof-of-principle demonstration, negative ion current of the order of 1 A is desirable.

In addition, following R&Ds are necessary to evaluate the feasibility of the NB system prior to the choice of the Heating and Current Drive System for ITER.

- to develop a negative ion source producing a high current negative ion beams of more than 10 A at a low operating gas pressure. Reduction of the operating gas pressure is essential to make the beamline compact and to enhance the system efficiency
- to develop the beam merging technology for the short beamline option

For the engineering design of the NB system for ITER, additional R&Ds should be conducted;

- to develop a long life cathode or a RF plasma generator for the negative ion source
- to develop a large bore insulator made of alumina ceramic
- to develop a plasma neutralizer cell for a future upgrade
- to demonstrate the neutralization of negative ion beam at an energy of 400-500 keV/nucleon using the gas and the plasma neutralizer
- to develop a beam dump that can endure a high heat flux of 30-40 MW/m<sup>2</sup>

- to demonstrate high voltage insulation using the proposed insulation gas
- to evaluate chemical effect of the insulating gas by radiation

## **ACKNOWLEDGMENT**

The authors would like to thank S. Shimamoto, the director of Department of Fusion Engineering Research at JAERI and S. Matsuda, the Home Team Leader of Japan for their continuous encouragement and supports. They are also grateful to H. Takatsu, S. Sato, T. Tsunematsu for their cooperation in the neutronics calculation.

- to demonstrate high voltage insulation using the proposed insulation gas
- to evaluate chemical effect of the insulating gas by radiation

## **ACKNOWLEDGMENT**

The authors would like to thank S. Shimamoto, the director of Department of Fusion Engineering Research at JAERI and S. Matsuda, the Home Team Leader of Japan for their continuous encouragement and supports. They are also grateful to H. Takatsu, S. Sato, T. Tsunematsu for their cooperation in the neutronics calculation.